QUANTIFYING HYDROLOGICAL FLUXES OF CONTRIBUTING HILLSLOPES IN THE WEATHERLEY CATCHMENT, N E CAPE, SOUTH AFRICA

Kevin George Bursey
B.Sc (Hons)

Submitted in partial fulfilment of the
Requirements for the degree of

MASTER OF SCIENCE

School of Bioresources Engineering and Environmental Hydrology
University of KwaZulu-Natal
Pietermaritzburg

July 2008

DECLARATION

I hereby certify that the research reported in this dissertation is my own original and unaided work except where specific acknowledgement is made.

K G BURSEY

Date:

S LORENTZ

(Supervisor)

Date:

ACKNOWLEDGEMENTS

The author wishes to express his sincere appreciation for the assistance given by the following people and institutes:

- **Prof. S. Lorentz,** Associate Research Professor, School of Bioresources Engineering and Environmental Hydrology, University of KwaZulu-Natal, for his invaluable assistance, time and support while supervising this research;

- **Prof. G. Jewitt,** Associate Research Professor, School of Bioresources Engineering and Environmental Hydrology, University of KwaZulu-Natal, for his co-supervision;

- **Prof. J. Smithers,** Head of School, School of Bioresources Engineering and Environmental Hydrology, University of KwaZulu-Natal, for all his administrative support;

- **Prof. R. E. Schulze,** Head of Hydrology, School of Bioresources Engineering and Environmental Hydrology, University of KwaZulu-Natal, for his invaluable assistance, time and advice with my thesis;

- **Mr S. Thornton-Dibb,** Computer Programmer, School of Bioresources Engineering and Environmental Hydrology, University of KwaZulu-Natal, for his invaluable assistance with data acquisition and help with the Weatherley Research catchment database;

- **Mr J. Pretorius,** Senior Technician, School of Bioresources Engineering and Environmental Hydrology, University of KwaZulu-Natal, for his advice and invaluable assistance on numerous field trips and maintenance of field equipment;

- **The Water Research Commission,** for partial funding of this project;

- **Mondi Forests,** for partial funding of this project;

- **Mr P. Goba,** Laboratory technician, School of Bioresources Engineering and Environmental Hydrology, University of KwaZulu-Natal, for determining soil physical properties in the past which were useful in my research at Weatherley;

- **Mr M. Horan,** GIS programmer, School of Bioresources Engineering and Environmental Hydrology, University of KwaZulu-Natal, for his patient assistance and much advice on using the GIS;

- **Mrs Kunz, Mrs Maney and Mrs Hoosen,** Secretaries and Assistants, School of Bioresources Engineering and Environmental Hydrology, University of KwaZulu-Natal, for their constant help with financial queries and day to day assistance;

- **Messrs M. Jili and K. Ngeleka,** Technical Staff, School of Bioresources Engineering and Environmental Hydrology, University of KwaZulu-Natal, for their much appreciated assistance and advice required on countless field trips;

- my **Friends and girlfriend** for their support and patience in day to day university life;

- my **Parents and family** for their continual support and encouragement through university.

ABSTRACT

Hillslope mechanisms and processes are a complex and dynamic set of interactions, but are nevertheless vital components of hydrology due to their critical interactions with surface and groundwater (Lorentz, 2001a). In order to observe and quantify these flow generating mechanisms, the Weatherley subcatchment was selected where the components of streamflow generation have been studied and can be quantified separately. Surface, shallow subsurface and the deeper groundwater interactions are particularly important when quantifying runoff generation from within hillslope, riparian and wetland zones as they are the dominant runoff generating zones within the Weatherley catchment. These components of flow are important to quantify for the further study of flow generation mechanisms, their dynamics and fluxes at the hillslope and small catchment scale, low flow contributions, climate change as well as the consequences of land use change (Lorentz, 2001b).

Transfer functions were found to be the best adaptation of hydrograph separation for distributed hydrological modelling purposes when attempting to quantify the various streamflow hydrograph components. In this study, the runoff components were simulated along transects using the HYDRUS-2D model, where the simulated soil water dynamics are compared with the observed tensions and water contents at different depths within the soil profile in order to quantify the contributing hillslope fluxes to streamflow generation. The 2001 data set was used with the rainfall and potential evapotranspiration data being converted into rates according to the breakpoint rainfall data. The HYDRUS-2D modelling exercise is performed to calculate the variety of flux rates (timing and quantities) within the subcatchment, so that the overall stream hydrograph can be properly deduced when modelling this catchment with transfer functions in the future. An understanding of the driving forces as well as the behaviour of sources and flow paths was extracted from this thesis, along with gaining some knowledge about the mechanisms and behaviour of streamflow generating mechanisms at the hillslope and small catchment scale.

Troch *et al* (2003) clearly encapsulates the essence of modern day catchment hydrology in stating that hillslope response to rainfall remains one of the most central problems of catchment hydrology in order to quantify catchment responses. The processes whereby rainfall becomes runoff continue to be difficult to quantify and conceptualise (Uhlenbrook *et al*., 2003) and this is because the characterisation of subsurface water flow components is one of the most complex and challenging tasks in the study of the hydrologic cycle (Achet *et al*., 2002). Since trying to understand the temporal and spatial variability of moisture content and the subsurface flow mechanisms is a complicated problem (Achet *et al*., 2002), an attempt is made in this thesis to gain insights into the temporal and spatial variability of soil tensions and soil moisture content at various depths on hillslope transects by combining modelling exercises with field observations. From this modelling, the hillslope water balance and contributing fluxes are derived in effort to augment, at a later stage, the hillslope response functions.

LIST OF FIGURES

LIST OF TABLES

LIST OF APPENDICES

LIST OF ACRONYMS

Δ SS	Change in Soil Storage
˚C	Degrees Celsius
α	Inverse of Air Entry Value or Bubbling Pressure
$\alpha(h)$	Plant Water Stress Response Function
θ	Volumetric Water Content
θ_r	Residual Water Content
θ_s	Saturated Water Content
$g(t)$	Unit Response Function
q_{out}	Surface Runoff
$d(t)$	Excitation Factor
τ	Mean ResidenceTime
%	Percetage
A	Constant or Cross-Sectional Area
ABF	Atmospheric Boundary Condition
ACRU	Agrohydrological Modelling System
ADM	Advection Dispersion Model
a(h)	Water Stress Response Function
ATMOSP.IN	Atmospheric Input File for HYDRUS-2D
CAY	Average Monthly Crop Coeffecient
CDE	Convection-Dispersion Equation
CDM	Convection-Dispersion Model
CTF	Composite Transfer Function
CumQAP	Cumulative Total Potential Surface Flux across the Atmospheric Boundary
CumQRP	Cumulative Total Potential Transpiration Rate
CumQA	Cumulative Total Actual Surface Flux across the Atmospheric Boundary
CumQR	Cumulative Total Actual Transpiration Rate
Cum_Q.out	Output File from HYDRUS-2D
D	Dispersion Coeffecient
DEM	Digital Elevation Model
EMMA	End-Member Mixing Analysis
EPM	Exponential-Piston Flow Model
Eqn	Equation
Es	Input Soil Evaporation
Es_{act}	Actual Soil Evaporation Cumulative Flux Rate
ET	Evapotranspiration
Et	Input Transpiration Cumulative Flux Rate
Et_{act}	Actual Transpiration Cumulative Flux Rate
Evap	Evaporation
F_t	Fraction of the Total Plant Available Transpiration

FAO	Food and Agriculture Organisation
GIS	Geographic Information Systems
h	Pressure Head
hr	Hour
I	Input across the Atmospheric Boundary
IRF	Instantaneous Response Function
ISCW	Institute for Soil, Climate and Water
IUH	Instantaneous Unit Hydrograph
K	Unsaturated Hydraulic Conductivity
K_d	Monthly Crop Factor
KI	Known Input
Kr	Relative Hydraulic Conductivity
Ks/K_{sat}	Saturated Hydraulic Conductivity
km^2	Square kilometeres
l	Pore Connectivity Parameter
L	Length of the Atmospheric Boundary
LC	Lower Catchment
m	Metres
MAE	Mean Annual Evaporation
MAP	Mean Annual Precipitation
MIM	Mobile-Immobile-Water-Model
mm	Millimetres
n	Pore Size Distribution
NTF	Nonparametric Transfer Function
PPT_{act}	Actual Precipitation
P_3	Value of the pressure head below which root water uptake ceases
P_2L	Pressure head value for a potential transpiration rate
P_2H	Pressure head value below which roots can't extract water at max rate
PO	Pressure head value below which roots start to extract water from soil
RF	Response Function
rRoot	Potential Transpiration
rSoil	Potential Soil Evaporation
S	Seepage
S	Sink Term
SFDM	Single-Fissure-Dispersion Model
Sp	Potential Water Uptake Rate
SWRC	Soil Water Retention Characteristic
t/T	Time
TDR	Time Domain Relectometry
TFM	Transfer Function Model
T_{min}	Maximum Temperature
T_{max}	Minimum Temperature
TPLR	Two Parallel Linear Reservoirs

TRANSEP	Transfer Function Hydrograph Separation Model
UC	Upper Catchment
UH	Unit Hydrograph
UKZN	University of Kwa-Zulu Natal
V	Volume

TABLE OF CONTENTS

1. INTRODUCTION

Hillslope hydrology mechanisms and processes are a complex and dynamic set of interactions, but are nevertheless vital components of hydrology due to their critical interactions with surface and groundwater. These hillslope processes describe the streamflow generation mechanisms that may vary in time, magnitude and space are well defined in the Weatherley Catchment; located in the north Eastern Cape (Lorentz, 2001a). Lorentz (2001b) said that "the study of flow generation mechanisms at the hillslope and small catchment scale is important in quantifying runoff generation dynamics, low flow contributions as well as the consequences of land use change" and followed that "this is important because mechanisms of water storage during wet periods and subsequent release from hillslopes during dry periods affect the sustainability of small catchment practices and can have significant control on the low-flow rates at the large catchment scale". It was deemed valuable to define flow generation and its' subsequent storage as components of the hydrograph within the hillslopes of the Weatherley catchment. These processes were studied and it was decided from reviewing literature that these mechanisms should be considered in terms of hydrograph separation and transfer function modelling. From this review, it was found that transfer functions were the best adaptation of hydrograph separation for distributed hydrological modelling purposes when attempting to quantify the various streamflow hydrograph components. They are particularly attractive because they use readily available hydrological inputs. Transfer functions also embrace the temporal and spatial variability of rainfall (both in depth and intensity) and can aptly simulate the long "tail" phenomenon often encountered on the receding limb of the hydrograph, which is especially important in times of low flow. Normally, different transfer functions are associated with different source areas within the catchment and there can theoretically be any number of combinations of the streamflow sources contributing to the total streamflow hydrograph. A further complication is that hillslopes are dynamically different, with local factors being known to have a

greater control in the spatial distribution of soil moisture than the distinguishable topographic attributes (Puigdefabregas *et al*., 1998).

The objective of this study was therefore to provide the hillslope flux responses for translation into transfer functions, at a later stage, for simulating the hillslopes soil water component of catchment responses. In order to do this, the aims of this study are to stimulate the need for hillslope response function modelling; observe hillslope responses; simulate vertical and lateral fluxes at the hillslope scale and to provide a guide to transfer function development for hillslope reponse mechanisms.

Surface, shallow groundwater and the deeper groundwater interactions are particularly important when quantifying runoff generation from hillslope, riparian and wetland zones as they are generally the dominant runoff generating zones within the Weatherley catchment. These zones are all well represented in the Weatherley catchment. These source area flow components are therefore grouped in this thesis according to the contributing hillslope transects that they represent, as the overland flow component, the macropore flow component, the seepage flow component, the perched groundwater and the deep groundwater flow component within the upslope, wetland and the riparian streamflow generating zones, because they have been recognized as the first-order qualitative controls on hydrological behaviour of the Weatherley catchment. Following this, Troch *et al.,* (2003) clearly encapsulates the essence of modern day catchment hydrology in stating that hillslope response to rainfall remains one of the most central problems of catchment hydrology in order to quantify catchment responses. Troch *et al.,* (2003) holds that hillslopes are indeed the basic landscape elements of catchments, therefore understanding the interactions and feedbacks between hillslope forms and the processes responsible for the transportation of water, sediments, and pollutants is of great importance for catchment scale water and land management. The processes whereby rainfall becomes runoff continue to be difficult to quantify and conceptualise (Uhlenbrook *et al*., 2003) and this is because the characterisation of subsurface water flow components is one of the most complex and

challenging tasks in the study of the hydrologic cycle (Achet *et al*., 2006). The various mechanisms of soil moisture accumulation at the base of the slope under unsaturated semi-arid conditions are not well understood (Achet *et al*., 2002).

In fact, following Achet *et al.,* (2002), there is a unique and typical control on soil moisture content and thus according to Bogaart and Troch (2003), streamflow generating mechanisms are therefore subject to a complex interplay of several factors including antecedent moisture conditions, snowmelt or precipitation input, soil depth, soil hydraulic properties, slope angle, vegetation characteristics, depth to water table, surface and bedrock topography as well as other ecological properties of the catchment. In order to observe and quantify these flow generating mechanisms, the Weatherley catchment was selected. The Weatherley catchment is situated near the town of Maclear in the Mooi river catchment that contributes to the Umzimvubu basin, which supplies water to the people of the old rural Transkei “homeland” area where there is a demand for potable and agricultural water. This basin is sensitive to many anthropogenic influences, where commercial agriculture, irrigation, domestic and rural settlements and forestry all compete for water use (Lorentz, 2001b).

Since trying to understand the temporal and spatial variability of moisture content and the subsurface flow mechanisms is a complicated problem (Achet *et al*., 2006), an attempt is made in this thesis to gain insights into the temporal and spatial variability of soil tensions and soil moisture content at various depths on hillslope transects by combining modelling exercises with field observations from the Weatherley catchment. From these simulations of the Weatherley catchment, conclusions can be drawn as to the source of low flows either being sustained by accumulations of localized upslope water contributions at the subcatchment scale or from contributions from deep regional groundwater bodies.

Nevertheless, in order to use the transfer functions at the hillslope scale, the runoff components need to be quantified along the transects that run through

the Weatherley research catchment. This is done with the HYDRUS-2D model, where the simulated soil water dynamics at different depths are compared to the measurements that were observed in the Weatherley catchment in 2001 from detailed hydrometric data such as tensiometers (automatically logged at twelve minute intervals), perched groundwater observation holes (physically measured monthly) and neutron meter probes in order to quantify the different contributions from the various source areas. The 2001 data set was used, with the rainfall and potential evapotranspiration data being converted into rates according to the breakpoint rainfall data. The HYDRUS-2D modelling exercise is performed to calculate the variation of flux rates (timing and quantities) within the catchment, so that the overall stream hydrograph can be properly separated into components of flow when modelling the catchment with transfer functions in the future. The fluxes are quantified at different depths within the soil profile and also for the various source areas in order to develop transfer functions for surface flow, perched groundwater and deep groundwater type flows along the hillslope, wetland and riparian zones.

From quantifying these source area fluxes, the correct transfer function for application in a convolution integral can be selected for the various contributing areas apparent within the Weatherley catchment. In order to accurately differentiate between the various source areas, Geographic information systems (GIS) are used as a tool to delineate the various source areas for distributed modelling purposes within the Weatherley catchment. The areas of streamflow generating mechanisms are then identified and delineated. The soils, land use and the digital elevation model (DEM) grids are used for this distributed type delineated modelling. McGlynn and McDonnell (2003) adopted a new approach, which identifies the most basic units of the watershed, and examines how they store, receive, and deliver water during and between rainfall events. These basic units can be identified because the topographic, hydrologic and pedologic variability that exists between hillslope and riparian areas offer a clear, unambiguous differentiation and thus allow mapping based on solute signatures, soils, landform (toposequence) and observed responses to storm precipitation.

These same transfer functions that are to be developed for the specified source areas within the small Weatherley catchment (1.5 km^2) can then be applied to guide the modelling of the much larger Mooi river catchment (about 360 km^2) in a similar way with distributed hydrological modelling. Once this is achieved, the effects of climate change, forestry and pollution as well as sediment studies can be applied to various catchments without intensive data collection surveys being necessary.

2. HYDROGRAPH SEPERATION AS A TOOL FOR DISTRIBUTED HYDROLOGICAL MODELLING

The catchment landscape systems controlling storm runoff generation, it's timing, and the runoff mixing dynamics are inadequately tacit (McGlynn and McDonnell, 2003). While much work continues on watershed-scale models of runoff formation, pioneering tools for clear, unambiguous separation and simplification of the runoff hydrograph is still being sought after by researchers (Weiler *et al*., 2003). According to McGlynn and McDonnell (2003), while the geographic source areas (Hooper and Shoemaker, 1986; McDonnell *et al.,* 1991; Noguchi *et* al., 1999; Lorentz *et al.,* 2003; Lorentz and Hickson, 2001; Scanlon *et al.*, 2000) and temporal sources (Sklash *et* al., 1986; McDonnell, 1990; Asano *et al*., 2002) of stormflow have been extensively studied, a generalizable perception of which landscape units contribute to which parts of the stormflow hydrograph remains elusive. This is important because, "until we can relate the catchment hydrologic mechanisms to the stream response, models of landuse change, non-point source pollution, and low flow estimation will be poorly understood" (McGlynn and McDonnell, 2003). This frequently researched subject on disaggregating the land surface into sub-areas of similar behaviour such as hydrological response units or dynamic contributing areas is well covered by a plethora of literature over the last few decades. Most studies, however, focus rather on the qualitative investigation of these flowpaths with little quantitative understanding of the individual processes within the catchment or their integration. Thus, the amalgamation of techniques using various extensive methodologies from subsurface resistivity to time domain reflectometry (TDR) surveys, hydrometric, isotopic and solute tracer data in a landscape discretization context are necessary to acquire an undeniable understanding and quantification of both spatial and temporal runoff sources (McGlynn and McDonnell, 2003).

Confusion and mishandling follow the utilization of tracer studies alone for hydrograph separation, with multiple combinations of tracer concentrations and volumes occurring with similar outflow tracer dynamics. Also, only

external information is used and the outcomes are routinely accepted as the unequivocal results by the majority of model users, resulting with the processes often being somewhat misunderstood. Within the plethora of hydrograph separation knowledge there are a number of techniques that can be used as tools for expressing the components of streamflow qualitatively and quantitatively. Throughout the world, many chemical and natural isoptope tracer experiments have been used to identify hillslope flowpaths with varying precision, but are indeed useful in the process of quantifying the components of streamflow from different contributions within catchments. The component hydrograph separations are useful, but end-member mixing analysis (EMMA) portrays the streamflow components graphically ("mixing diagrams") as well as quantitatively and gives some information as to the residence times on an event basis based on a subscribed statistical approach. These experiments have helped considerably in the building up of methodologies for two, three and five component hydrograph separation. EMMA has also been used to assess the involvement of a particular component in catchments where the dominant hydrological flowpaths are known (Katsuyama *et al.*, 2001). More recently these tracer experiments have been used in union with the application of transfer functions in unfolding the travel times of event and pre-event water as well as the overall water flux response (Weiler *et al.*, 2003). Despite the many studies that have been done this past decade by combining tracer and hydrometric rainfall-runoff data, we still do not identify with the timing, flow path, and source behaviour of catchments (Burns, 2002).

Hydrograph separation models allow the simulation of catchment runoff response to storm events, but do not divulge how the catchment system actually works (Kendall *et al.*, 2001). It has become clear that the real restriction on predicting catchment runoff is not the detail involved in the model configuration but in defining the features of the individual areas being modelled (Alila *et* al., 2001; Beven, 2001). This includes identifying those areas where high saturated hydraulic conductivities, high antecedent moisture conditions, lateral flows, macropore flows and preferential pathways dominate the landscape features (Ballantine and Dunne, 2001; Elsenbeer, 2001). Also, according to McGlynn and McDonnell (2003), we have known for some time

that hillslope and near-stream riparian zones perform and respond in different ways to storm precipitation. Therefore, there is no quick and easy way of accomplishing a hydrograph separation and according to Flühler and Hagedorn (2001), the problem common to all hillslope modelling from plot to catchment scale is the fact that we should “parameterise the topology of the travel paths through the hydrological system, or simply employ hillslope segments to quantify catchment runoff”. In order to do this effectively, a comprehensive appreciation of the assortment of hillslope flowpaths of water is needed (Bishop *et al*., 2001). Therefore the value of tracer techniques used in conjunction with hydrometric measurements have been widely adopted in order to quantify sources of stormflow, identify flow pathways and define catchment runoff mechanisms (Buttle, 1994; Newman *et al.*, 1998; Brown *et al.*, 1999; Weiler *et al.*, 1999; Brassard *et al.*, 2000; Collins *et al.*, 2000; Ladouche *et al.*, 2001; Lorentz *et al.*, 2003; Wenninger *et al.*, 2004). Once these mechanisms have been identified, the complicated process of quantifying them begins. Transfer functions were reviewed and discovered to be an advantageous way of quantifying these runoff generation processes. A discussion of this technique follows.

2.1 Transfer Functions

Of the hydrograph separation techniques, rainfall-runoff models contrived from the convolution integral, linking rainfall rates, system transfer functions and system responses have an significant role in the future (Denic-Jukic and Jukic, 2003). Transfer function source area modelling uses easily obtainable hydrological data with rainfall being the excitation factor that produces each component of runoff from a particular source area by means of a particular transfer function. This process can be seen in Figure 2.1 below, where the excitation factor is translated into a response through a transfer function which describes a unit response for the system. Linear and non-linear forms of the convolution integral can be applied in quantifying runoff, but the linear variety is more popularly used (Moussa, 1997). The result of the convolution integral is the response of the system that corresponds to that particular source areas’ observed data. The transfer functions that were used by Stewart and Loague

(2000) were generalised impulse-response functions, which defined not only the response of a particular system that is characterised by a particular soil profile and surface water flux, but also give a representative response for sufficiently similar systems.

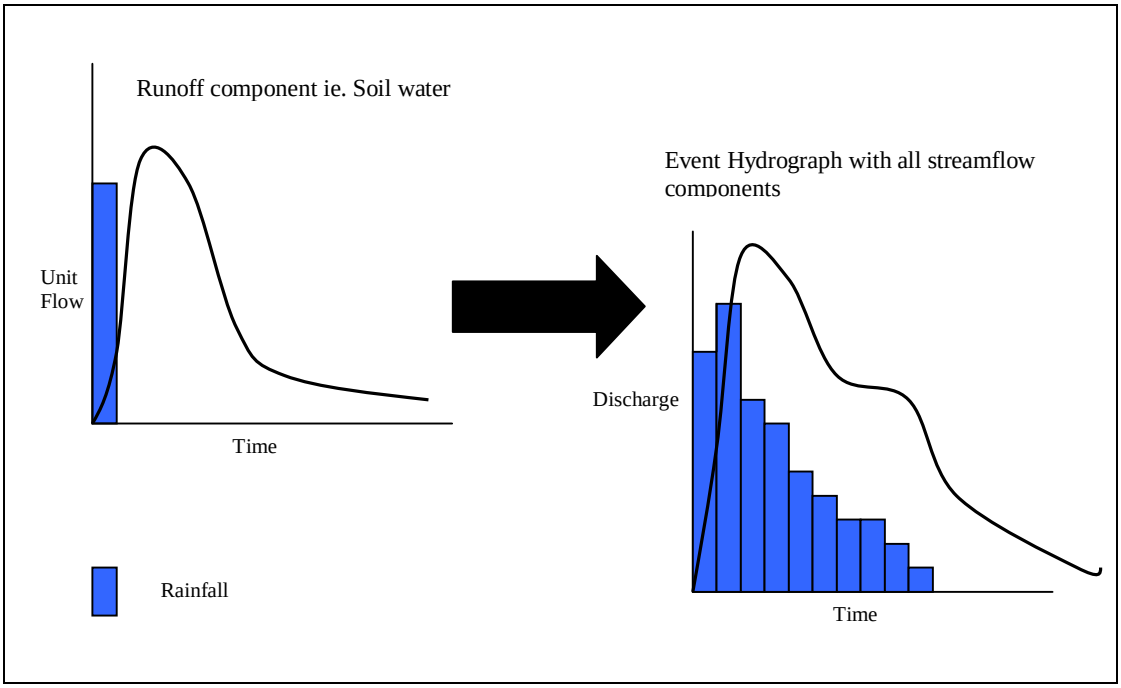

Figure 2.1 Diagram showing a unit transfer function being converted into a hydrological response by an excitation factor (rainfall).

There are basically **two groups of transfer functions**. The first group consists of identification methods that establish a parametric transfer function; e.g. one that has the structure of an instantaneous unit hydrograph (IUH) derived from a conceptual model. Examples of these parametric transfer functions given by Denic-Jukic and Jukic (2003) are the Nash linear reservoirs model (Labat *et al.*, 1999), the Zoch model (Singh, 1988) and the polynomial transfer function identification method (Labat *et al.*, 1999). The second group documented by Denic-Jukic and Jukic's (2003) comprise numerous methods for the determination of nonparametric transfer functions (NTF). Denic-Jukic and Jukic (2003) suggests a fresh structure for a transfer function, namely the composite transfer function (CTF). Results of the CTF application are presented in Figure 2.2, where the CTF is determined as the superposition of two transfer functions adapted for quick and slow flow hydrograph component

modelling. By using the CTF, the irregular nature of the rainfall responses and their tailing off can be modelled as it utilises a quick and a slow flow contributing hydrograph component. Thus, the simulation of the recession period as well as the simulation of the complete hydrograph becomes more accurate as the finer details of the slow flow component provides more accuracy to the “long tails” often seen in low flow analyses (Denic-Jukic and Jukic, 2003). The slow flow component is modelled using four types of the IUH, two of which are represented in Figure 2.2, that are derived from linear conceptual models.

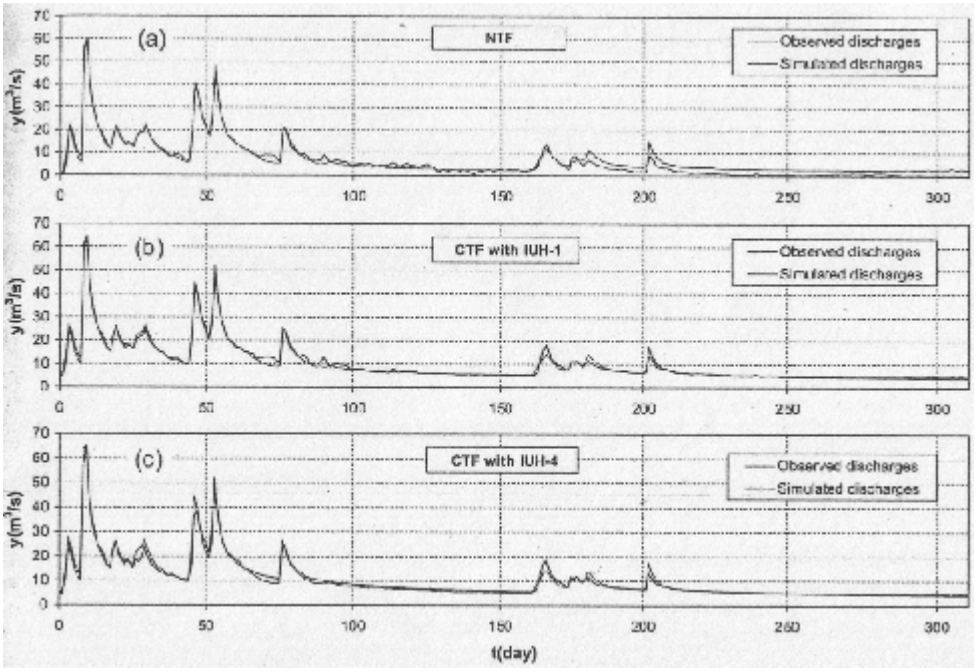

Figure 2.2 Simulated and observed discharges from using different transfer functions. Simulations were performed with NTF (a), CTF with Nash’s linear reservoir model or IUH-1 (b) and CTF with a time variant linear reservoir coefficient function or IUH-4 (c), (Denic-Jukic and Jukic, 2003).

These four **IUH**’s are (1) the linear Nash reservoirs model, (2) the Zoch model (concept of a linear channel and a linear reservoir), (3) the use of the notion of two parallel disparate linear reservoirs with recession coefficients and (4) from the perception of a time variant linear reservoir, whose recession curve is expressed by a coefficient which is a function of time (Denic-Jukic and Jukic,

2003). The conclusion in this particular case is that the NTF cannot sufficiently describe the discharges of long recession periods and also that there is considerable abnormality of the tail of the identified transfer function and low-quality simulations during low flow periods (Denic-Jukic and Jukic, 2003). The fourth IUH that was used to model the slow flow component gave quite a good simulation, and it can be seen that this type of IUH eliminates all irregularities in the tail of the transfer function, as can be seen in Figure 2.2. At the same time the simulation becomes smooth for the entire recession part of the hydrograph; the agreement between observed and simulated discharges is good (Denic-Jukic and Jukic, 2003).

Moussa (1997) uses the **Hayami approximation solution of the diffusive wave equation** which has been specifically adapted for routing hydrograph separation through the channel network. Moussa (1997) stated that “each subcatchment produces, at its outlet, an impulse response which is routed to the outlet of the whole catchment using the diffusive wave model described by two parameters: celerity and diffusivity which are functions of the geometrical characteristics of the channel network obtained from digital elevation models”. The distributed routing model was used to incorporate the spatial variability of rainfall and effective rainfall within the catchment to enhance the distributed nature of the transfer function procedure. It enables the identification of various parts of transfer function responses for each hydrological unit present and the simulation of the contributions of each individual hydrograph to the system hydrograph at the outlet (Moussa, 1997). The effective precipitation is then routed to the outlet through a transfer function. The parameters of both functions (production and transfer) are said to be time invariant. The method executes a concurrent identification of both the excess precipitation and the transfer function, dissimilar from most UH based approaches, which only recognizes the transfer function (Moussa, 1997). The main assumption is that the UH model structure corresponds to the catchment behaviour reasonably well. Accuracy of the method depends on the quality of the DEM, the procedure used to extract the channel network, subcatchment data and the data used to compute slopes, particularly on flat areas. This transfer function is well adapted for distributed hydrological modelling (Moussa, 1997).

Weiler, *et al.,* (1998) used a variety of solute transport models in addition to the linear models of hydrograph separation. The Convection-Dispersion-Model (CDM), Transfer-Function-Model (TFM), non-equilibrium models, Single-Fissure-Dispersion-Model (SFDM) and the Mobile-Immobile-Water-Model (MIM) were fitted to tracer breakthrough curves acquired from surface and subsurface runoff components. One model was then chosen for each breakthrough curve based on goodness-of-fit and physical credibility of the transport parameter. The conversion of solute transport parameters into flow parameters is vital if the structure of the fitted solute transport model does not account for real physical flow mechanisms. To reduce these complications, future research should then focus on developing transport and flow models that are related to each other (Weiler *et al.*, 1998).

An diagnostic solution for the **instantaneous response function** (IRF), which is a simplification of the IUH, was derived and straightforward expressions were developed to compare the peak and the time of peak of the IRF by Agnese, *et al.,* (2001). The IRF conveys the non-linearity and time variation of the hydrological response in a straightforward manner.

Yue and Hashino (2000) derived the **unit pulse response function for quick and slow runoff components of streamflow**. The proposed method has the following advantages: (1) it can be used to separate quick and slow streamflow components; (2) it is suitable for forecasting streamflow hydrographs produced by a variety of storms such as single-peak and multi-peak storms without resorting to altering the model's parameters; and (3) it does not necessitate either a prior calculation of rainfall excess or baseflow separation for deriving the UH. The response function (RF) for the total, quick and slow runoff components are derived using the model of three successively coupled tanks with a parallel tank (Yue and Hashino, 2000). Therefore, in this case there is no need to identify rainfall and split the direct runoff from streamflow beforehand. The control of the antecedent soil moisture conditions on runoff generating mechanisms is also considered. This

model can be used to develop streamflow hydrographs fashioned by various storm events without resorting to altering the models parameters for a given basin or catchment (Yue and Hashino, 2000).

Asano *et al.,* (2002) created **a transfer function that specifies the transfer time distribution of water within the system**. A shared exponential-piston flow model (EPM) connects in series both the exponential and piston flow model theory into a RF. Then from the combined RF, mean residence times were evaluated (Asano *et al.*, 2002).

According to Weiler *et al.*, (2003), "hydrographs are an enticing focus for hydrologic research: they use readily available hydrological data that integrate the variety of terrestrial runoff generation processes and upstream routing." Weiler *et al.,* (2003a) produce a new method for hydrograph separation that incorporates the IUH and employs the temporal unpredictability of rainfall isotopic composition. The model computes the transfer function for pre-event and event water designed from a time variable event water fraction. The **Transfer function hydrograph separation model (TRANSEP)** "provides coupled but constrained representations of transport and hydraulic transfer function, overcoming the limitations of other models" (Weiler *et al*., 2003a). Weiler *et al.,* (2003a) stated that "stable isotope mass balance mixing model methodologies are limited to some extent in the light of their acknowledged assumptions and limitations inherent in the technique" and that "TRANSEP embraces the temporal variability of rainfall isotopic composition, but also includes new transfer functions for pre-event and event water determined from the time variable event water fraction". A transfer function expressive of the runoff response (IUH) is used to limit the event residence time distribution and the hydrograph components (Weiler *et al.*, 2003a). Whilst other models have been developed that employ the UH techniques to represent tracer transport time, they comprise only a combined transport and hydraulic transfer function or use uncomplicated triangular weighting functions (Joerin *et al.*, 2002). Weiler *et al.,* (2003a) believe it obligatory to include both types of

responses to appreciate catchment behaviour, given that one response (e.g. residence time) represents actual conventional solute travel time (i.e. along flowpaths) and the other embodiess hydraulic dynamics (e.g. rainfall-runoff behaviour). A diagram describing the processes that are involved in obtaining the desired TRANSEP runoff hydrographs is presented in Figure 2.3.

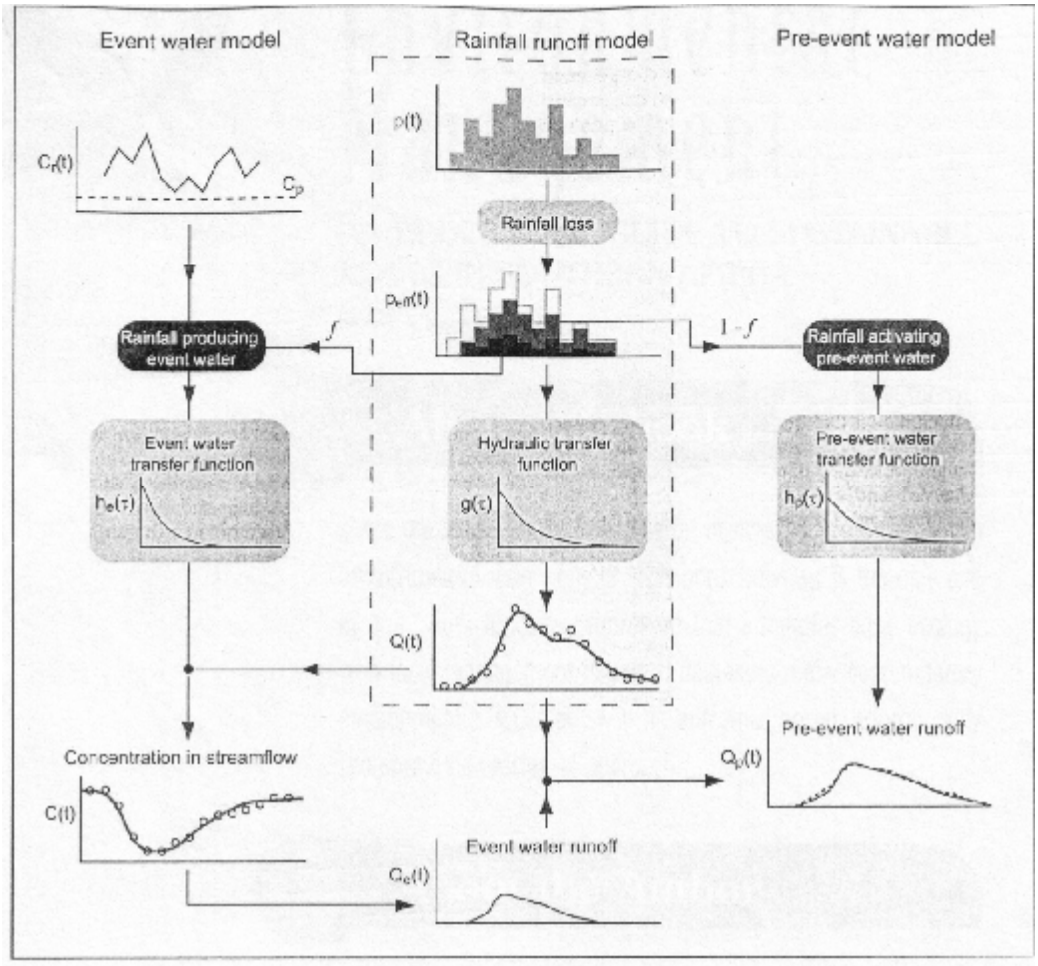

Figure 2.3 Flowchart of TRANSEP, showing the conventional part of an IUH rainfall-runoff model in the dashed line box and the new modules describing the transfer of event and pre-event water (Weiler *et al.*, 2003)

Weiler *et* al., (2003a) highlighted that there are many potential transfer functions for hydrological applications such as in IUH literature there are probability distributions with two to three parameter models (e.g. gamma, lognormal) and linear reservoir approaches are also used. However, within

tracer and solute transport literature, the convection dispersion equation (CDE), the lognormal probability distribution, the exponential and piston flow model, and the gamma distribution have been widely used as well. In order "to make TRANSEP flexible and test multiple transfer function approaches", Weiler *et al.,* (2003a) implemented "three different models for defining the runoff, pre-event and event water transfer functions: Exponential-Piston flow (EPM), Gamma distribution or linear reservoirs in series and two parallel linear reservoirs (TPLR)". When comparing solely the EPM and Gamma distribution transfer functions, the performance of the EPM is generally better for predicting the concentration and the Gamma distribution is better for predicting the streamflow (Weiler *et al.*, 2003a). The second improvement is "directly related to the sequential parameter optimisation (first rainfall-runoff, then concentration) where a better fit for the runoff data increases the performance of the tracer concentration optimisation". However, a visual control of the simulation results exposed a inferior performance of the EPM and Gamma transfer functions for the recession part of the hydrograph and isotope concentration. Thus signifying that the simpler two-parameter transfer functions cannot adequately capture the complex runoff generation processes in the studied catchments, where obviously a fast and slow component are accountable for generating the runoff (Weiler *et al.*, 2003a). Therefore, the TPLR approach was preferred not only because of the enhanced model performance but also in terms of encapsulating the runoff generation processes in the catchment (Weiler *et al.*, 2003a). According to Iorgulescu and Beven (2003), parallel transfer functions for fast and slow linear responses have the benefit of easy parameter recognition from the data.

Weiler *et al.,* (2003a) indicated that "the information available in the rainfall and stream ^{18}O concentration time series are sufficient to characterize a transfer function for the event water and furthermore that the sequential parameter optimisation (first rainfall-runoff, then concentration) increases the identifiability of the six parameters defining the separation and transfer of the event water". In effect, Weiler *et al.,* (2003a) "attemted to **combine the process merits of tracer based hydrograph separation with the hydraulic**

function approach of the unit hydrograph in an effort to increase the information gained from the storm hydrograph using a quantitative approach to describe the residence time of solute transport and transmittance of hydraulic behaviour". In conclusion Weiler *et al.,* (2003a) stated that the tools required to extract the process-level information from these innovative combined tracer-hydrometric data sets that include event-based isotope and discharge data were still lacking.

One real **restraint on transfer functions** was highlighted in Hjerdt *et al.,* (2001), concluding that dynamic thresholds in catchment response and subsurface stormflow commencement are poorly understood. "This remains a predicament for the generalisation and transferability of hydrologic models, as well as for the simulation of catchment response under variable antecedent and input conditions". Threshold processes appear to function both spatially and temporally within a catchment and initiate non-linearity to the system response function (Hjerdt *et al*., 2001). Another drawback of transfer function modelling is that the rainfall inputs are seen as spatially homogenous (Buttle 1994).

2.2 Linking Transfer Functions to Distributed Hydrological modelling

The current emphasis of many hydrological investigations is to firstly **identify and then to quantify the key hydrological processes** in order to define and model the dynamics of the hydrological cycle at the hillslope scale under specific land uses. This is of importance in order to comprehend "the movement of different water reserves and bodies in and on hillslopes" (Lorentz *et al*, 2003). The recognition of the sources and the quantification of the response dynamics of components of streamflow have been the focus of extensive research in the recent past (McDonnell, 1990; McDonnell *et al.,* 1991; McCartney and Neal, 1999; McGlynn *et al.*, 2001a; McGlynn *et al.*, 2001b; Seibert, *et al*., 2001; Sidle *et al*., 2001). While there has been significant effort from researchers in using environmental isotopes and other natural tracers in order to construe flow mechanisms by means of end member mixing models (Stewart and McDonnell, 1991; McDonnell *et al*.,

1991a; McCartney an Neal, 1999), there has been some doubt as to their reliability, given that there are many variabilities in the source signals and mixing flowpaths (Lorentz *et al*., 2003). Clearly these methods have need of a more comprehensive incorporation with hydrometric methods in order to derive dependable definitions of flow pathways, residence times and fluxes (Buttle, 1994). The long record of hydrometric measurements at the Weatherley catchment contributes to the evaluation of these streamflow components by using physically based estimation techniques (Lorentz, *et al.,* 2003). Once these streamflow generation mechanisms have been quantified using the physical measurements, a unit response function is derived for each and combined in a convolution integral with an excitation function to simulate the observed responses from the various contributing source areas (Stewart and McDonnell, 1991; Lorentz and Kienzle, 1994; Yue and Hashino, 2000). A sizeable amount of work has been done in the past in order to apply response functions to the different mechanisms of streamflow generation and then incorporate these with the appropriate response zones and time scales so as to derive catchment scale flows and solute concentrations (McDonnel and Stewart, 1991; Kirchner *et al*., 2001).

According to Lorentz, *et al.,* (2003), **the analysis of streamflow generating mechanisms follows three distinctive steps**. The first consists of the recognition of the dominant mechanisms of streamflow generation, the second a physical quantification of the magnitude and response timing of the systems and the third, the definition of characteristic response functions that are able to represent the dominant mechanisms throughout an assortment of events. These functions can then be used in designing modifications to catchment scale models. Lorentz and Hickson (2001) applied a straightforward technique using the convolution integrals to transform the excitation function (excess rainfall or percolation dynamics) into simulated responses per unit length of stream. “The methodology is offered, not as an alternative technique for catchment runoff simulation, but as a technique for identifying and quantifying the volumes, residence times and transfer rates of sources and streamflow generation mechanisms in order to parameterise or refine algorithms, already inherent in most physically based catchment scale

simulation models" (Lorentz *et al*., 2003). "The convolution integral methodologies are particularly appropriate for defining sources, residence times and fluxes during rainfall events as well as during low flows" (Lorentz *et al*., 2003).

Streamflow generation mechanisms have been described in a number of studies, throughout the development of the Weatherley catchment, (Esprey, 1997, Lorentz and Esprey, 1998, Lorentz *et al.*, 1999, Lorentz, 2001a). "Three dominant streamflow generation mechanisms (overland flow, near surface macro-pore flow and groundwater flow) are assumed to contribute to the stream and also the local seepage zones linked to the stream during a precipitation event" (Lorentz *et al*., 2003). These streamflow generation mechanisms were first quantified using simple, physically based techniques and then applied to the measured soil water dynamics and runoff data from the beginning of January till the end of October 2001. "In addition to the physically based techniques, simple unit response functions, comprising an advection-dispersion model (ADM) were then selected to represent the response of the three streamflow generation mechanisms" (Lorentz *et al*., 2003). "These were then used in the convolution integrals to translate the excitation function (excess rainfall or percolation dynamics) into simulated responses per unit length of the stream" (Lorentz *et al*., 2003). The stream length was separated into 100m reaches and the overland flow, macro-pore flow and groundwater flow ADM's were solved for both sides of the stream and then subsequently linked with seepage zones and routed through to the weirs in the upper catchment (UC) and lower catchment (LC) independently. The simulations demonstrate an astonishingly good fit to the observed data for single events in this case, even though the macro-pore response seems to over simulate the recession limb. In both the upper and lower catchment, the near-surface discharge yields significantly more water than the surface runoff component. "In the upper catchment, the macro-pore layers yield approximately 70% of the discharge while in the lower catchment this source yields roughly 92% of the total streamflow generated" (Lorentz *et al*., 2003). "The methodology is robust, provided the excess rainfall is properly quantified using a physically based Green-Ampt runoff/infiltration generation algorithm"

(Lorentz *et al*., 2003). The analyses confirm that the antecedent water conditions and rainfall intensity control the streamflow generation response, above all because they have a large influence on the near surface macro-pore response (Lorentz *et al*., 2003).

"The overland flow mechanism is considered to contain an advection and dispersion component and adhere to the mass balance of an advection-dispersion model (ADM)" (Lorentz *et al*., 2003). The ADM corresponds to the travel time distribution of flows contributing towards the surface runoff flows in the catchments. "An analytical solution, comprising some degree of asymmetry, is used to describe the surface runoff, q_{out}, based on a dispersion coefficient, *D* and a mean residence time, t " (Stewart and McDonnell, 1991). "This diagnostic solution characterizes the response of the mechanism to a unit impulse" (Stewart and McDonnell, 1991) and is illustrated in Figure 2.4.

The observed runoff response is then simulated using the analytical solution in a convolution integral:

$$q_{out} = \int_0^{\infty} g(t').d(t-t').dt' \qquad (2.1)$$

where $d(t)$ is the excitation function, in this instance, the time series of excess rainfall, i_e. q_{out} is the runoff response. Applying this excitation to the unit response function, $g(t)$, (Figure 2.4), generates the ADM simulated runoff for the subcatchment. The function g(t) is given as:

$$g(t) = \left(\frac{4pDt}{t}\right)^{-1/2} t^{-1} e^{\left(-1(1-t/t)^2 t/(4Dt)\right)} \qquad (2.2)$$

Where $g(t)$ is the unit response function, D is the dispersion coefficient, describing the spread of travel times and T is the response time. The ensuing convolution integral solution, used in a one minute time step produces an accurate simulation to the observed runoff plot data (Lorentz and Hickson, 2001).

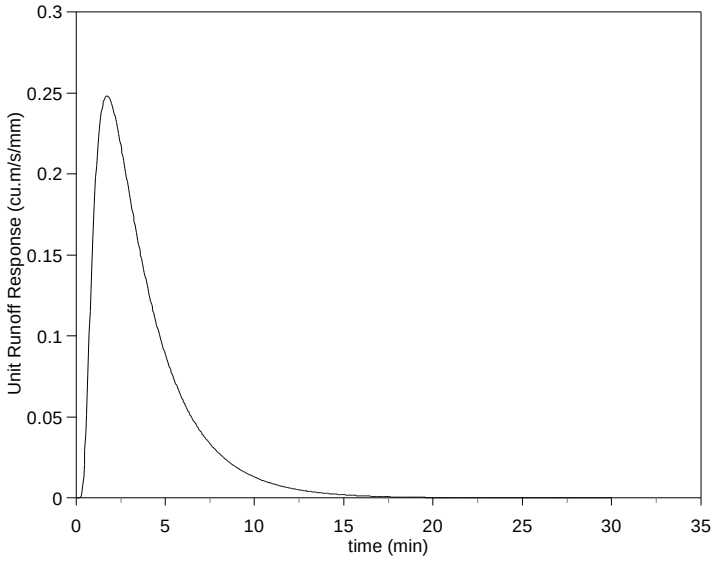

Figure 2.4. The Advection-Dispersion Model unit response function used to simulate the surface runoff (D = 0.25 m^2/s; τ = 3 min) by Lorentz and Hickson (2001a).

The **precursors of the response functions** developed in this case are used to calculate approximately the runoff in the Weatherley research catchment and to present guiding principles for application in deterministic modelling at larger scales (Lorentz *et al.*, 2003). "While the methodology demonstrated here is not intended as a new modelling technique, it is intended as a method for characterising responses of runoff and subsurface storage and release for various typical formations throughout South Africa" (Lorentz *et al.*, 2003). "Once characterised in this way, the results can be used to improve the parameterisation or algorithms of the many catchment models which already include quick, slow and baseflow response components, such as those included in the *ACRU*" (Schulze, 1994) and HYMAS, (Hughes and Sami, 1994) models. "It is particularly important to define these responses when land use changes are to be simulated " (Lorentz *et al.,* 2003), and then adding that "erroneous definition of source zones and discharge rates may cause inaccurate end results in the simulations of low flow responses" (Lorentz *et al.*, 2003). "Errors will occur, if, for example, these low-flows are then assumed to be generated from a fractured aquifer source, whereas, in reality,

the water is still resident on the hillslope and thus available for uptake by trees, which may have been introduced" (Lorentz *et al.,* 2003).

While it is imperative to distinguish and parameterise the reservoirs or source mechanisms contributing to streamflows (Uhlenbrook and Leibundgut, 2002), it is similarly important to characterize the residence times and the rates of transfer connecting dynamic reservoirs as well as from reservoirs to the stream (Hooper, 2001). These responses, predominantly between shallow unsaturated and saturated zones have the propensity to have long tailed travel time distributions. "Deterministic models that use exponential decay curves for these transfers, such as in the *ACRU* model, could well under predict discharges during dry periods" (Lorentz *et al.*, 2003).

Transfer functions are therefore a convenient and effective technique for hydrograph separation, because of their simplicity and simple application to rainfall-runoff modelling. **Hydrographs are therefore an attractive focus for hydrologic research**: "they use readily available hydrological data that integrate the variety of terrestrial runoff generation processes and upstream routing" (Weiler *et al.*, 2003). They can also be applied to specific areas of hydrologic response (macropore, groundwater and overland flow) and ought not to be contradictory when spatially upscaled. They can also be employed to scrutinize the changing spatial and temporal flow patterns throughout various hydrological situations, such as low flows and high flows (Wenninger *et al.*, 2004) and they can also be used to derive streamflow hydrographs produced by various storms without having to changing the models parameters for a given basin or catchment (Yue and Hashino, 2000). They can simulate hydrographs fairly accurately and can furthermore account for the long tail encountered on the receding limb of the hydrograph, which becomes particularly essential in times of low flows. "The model, its resulting runoff and the transfer functions as well as their parameterisations could then be used to study the scaling behaviour of the residence time of water in the watersheds in a much more efficient and straight forward way than is possible with existing techniques" (Weiler *et al.*, 2003a).

In order to utilise transfer functions in the future within the Weatherley catchment, the actual fluxes in and out of the source areas need to be defined and then also quantified using a physically based model. The source areas have been identified as the contributing hillslopes within the catchment and will be identified in chapter 4. Once they have been identified, the HYDRUS-2D model is used to simulate the observed tensions and water contents. The use of HYDRUS-2D was thought to be crucial, because of HYDRUS-2D being a physically based model with which to simulate the actual fluxes. Once this is adequately done, the actual fluxes entering and exiting the contributing hillslopes can be used to develop transfer functions for the Weatherley catchment in a future study. The HYDRUS-2D model routines that were used in this study are described below.

2.3 The HYDRUS-2D model

The importance of the unsaturated zone as an essential part of the hydrological cycle has long been acknowledged (Ŝimůnek *et al*., 1999). According to Ŝimůnek *et al*., (1999), "this zone plays an inextricable role in many aspects of hydrology, including infiltration, soil moisture storage, evaporation, plant water uptake, groundwater recharge, runoff and erosion". They also acknowledge that the past several decades have seen significant advancement in the conceptual perceptions and mathematical depictions of water flow as well as of solute transport processes in the unsaturated zone. There is now a selection of analytical and numerical models available to envisage water transfer processes connecting the soil surface and the groundwater table (Ŝimůnek *et al*., 1999). One of the most popular of these models remains the Richards' equation for variably saturated flow (Ŝimůnek *et al*., 1999). "The HYDRUS-2D program numerically solves the Richards' equation for saturated-unsaturated water flow and also includes, within the flow equation, a sink term to account for water uptake by plant roots" (Ŝimůnek *et al*., 1999). The program can also be used to investigate "water movement in unsaturated, partially saturated, or fully saturated porous media" (Ŝimůnek *et al*., 1999). The model can cope with flow domains delineated by

irregular boundaries and water flow can occur in the vertical or horizontal planes (Ŝimůnek *et al*., 1999).

2.3.1 Variably Saturated Water Flow

2.3.1.1 The Governing Flow Equation

Ŝimůnek *et al*., (1999) derives the physics of two-dimensional Darcian-type flow of water in a variably saturated rigid porous medium and assumes that the air phase plays an insignificant role in the liquid flow process. The prevailing flow equation for these aforementioned circumstances is given by the subsequent modified form of the Richards' equation (Ŝimůnek *et al*., 1999):

$$\partial\Theta/\partial t = \partial/\partial x_i \left[K(K_{ij}^A \, \partial h/\partial x_j + K_{ij}^A)\right] - S \qquad (2.3)$$

where Θ is the volumetric water content (L^3L^{-3}), h is the pressure head (L), S is a sink term (T^{-1}), x_i (i = 1,2) are spatial coordinates (L), t is time (T), K_{ij}^A are components of a dimensionless anisotropy tensor K^A, and K is the unsaturated hydraulic conductivity function (LT^{-1}) given by:

$$K(h,x,z) = K_s\,(x,z)\, K_r(h,x,z) \qquad (2.4)$$

where K_r is the relative hydraulic conductivity and K_s the saturated hydraulic conductivity (LT^{-1}).

2.3.1.2 Root Water Uptake

According to the literature by Ŝimůnek *et al*., (1999), the sink term, S, in Eqn 2.3 corresponds to the volume of water removed per unit time from a unit volume of soil due to plant water uptake. Feddes *et al.,* (1978) defined S as:

$$S\,(h) = a(h)S_p \qquad (2.5)$$

where the water stress response function a(h) is a prescribed dimensionless function (Figure 2.5) of the soil water pressure head ($0 \leq a \leq 1$), and S_p is the potential water uptake rate (T^{-1}). Ŝimůnek *et al*., (1999) highlights that Figure 2.5 gives a schematic plot of the stress response function as used by Feddes *et al.,* (1978).

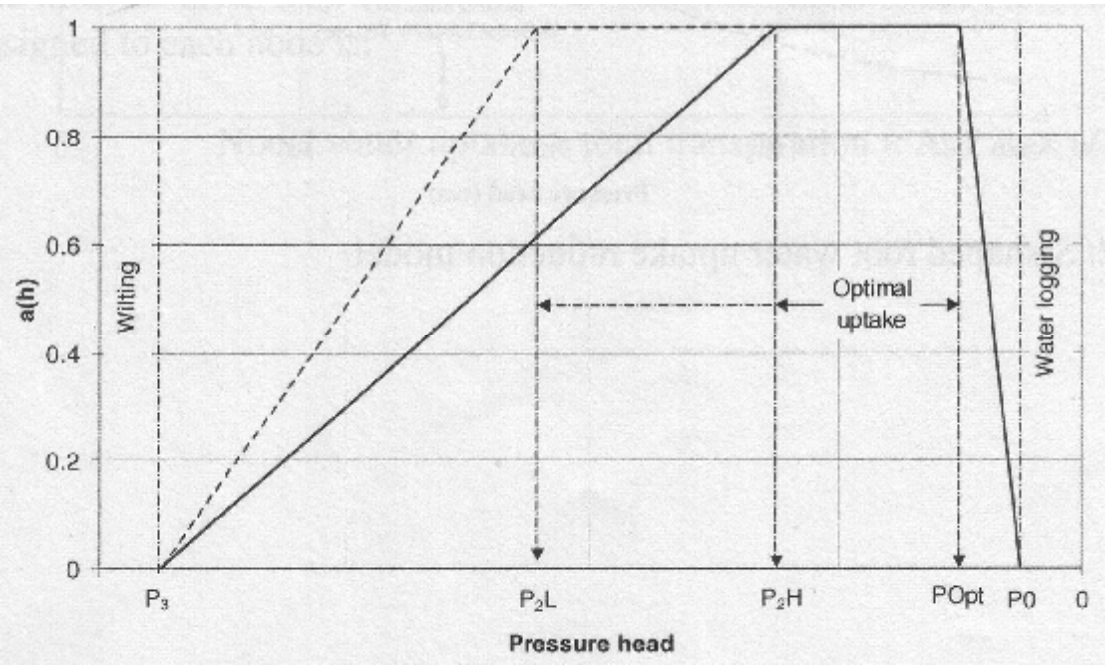

Figure 2.5 Schematic diagram of the plant water stress response function, α(h), as used by Feddes *et al*., (1978) taken from (Ŝimůnek *et al*., 1999).

Ŝimůnek *et al*., (1999) also noted that the water uptake is assumed to be zero close to saturation (ie, wetter than some arbitrary "anaerobiosis point", h_1) and for $h<h_4$ (the wilting point pressure head), water uptake is also assumed to be zero. Water uptake is considered to be most favourable between pressure heads h_2 and h_3, whereas for the pressure head between h_3 and h_4 (or h_1 and h_2), water uptake decreases (or increases) linearly with h (Ŝimůnek *et al*., 1999). Also according to Ŝimůnek *et al*., (1999), the variable S_p in Eqn 2.5 is equivalent to the water uptake rate throughout periods of no water stress when a(h) = 1.

2.3.1.3 The Unsaturated Soil Hydraulic Properties

According to Ŝimůnek *et al*., (1999), the unsaturated soil hydraulic properties, Θ(h) and K(h), in Eqn 2.3 are commonly highly non-linear functions of the pressure head and the HYDRUS-2D model allows the use of three different analytical models for the hydraulic properties (Brooks and Corey, 1964; van Genuchten, 1980; and Vogel and Císlerová, 1988).

In the HYDRUS-2D modelling exercise of this study, the van Genuchten (1980) soil hydraulic function was selected. This incorporates the use of the statistical pore-size distribution model of Mualem (1976) to acquire a predictive equation for the unsaturated hydraulic conductivity function in terms of soil water retention parameters (Ŝimůnek *et al*., 1999). The expressions of van Genuchten's (1980) water retention characteristic (Eqns. 2.6 and 2.7) and the hydraulic conductivity characteristic (Eqns. 2.8 and 2.9) are given by:

$$\theta(h) = \{\theta_r + (\theta_s - \theta_r) / [1 + |\alpha h|^n]^m\} \qquad h<0 \qquad (2.6)$$

$$\theta(h) = \{\theta_s \qquad h\geq 0 \qquad (2.7)$$

$$K(h) = K_s S_e^l [1-(1- S_e^{l/m})^m]^2 \qquad (2.8)$$

where

$$S_e = \theta - \theta_r / \theta_s - \theta_r \qquad (2.9)$$

$$m = 1 - 1/n, n>1 \qquad (2.10)$$

The above equations contain five independent parameters: θ_r, θ_s, α, n, K_s. The pore-connectivity parameter "l" in the hydraulic conductivity function was estimated by Mualem (1976) to be 0.5 as a typical value for various soils (Ŝimůnek *et al*., 1999). The parameter n is the pore size distribution index and m is a parameter in the soil water retention function; they are empirical coeffecients affecting the shape of the hydraulic function.

In the next chapter, the research catchment description and the qualitative streamflow generating processes are discussed followed by the methodology that was used in preparing the data for the HYDRUS-2D simulation, the simulations themselves and the contributing hillslope fluxes that were outputted from HYDRUS-2D model are described in detail.

3. METHODOLOGY

In this chapter, the Weatherley research catchment is described in detail as to its geographical position, topography, climate, soils, landuse and its instrumentation. Thereafter, the various processes and responses that have been conceptualised within the catchment are discussed and graphically presented. These processes or responses are developed into fluxes and will be subsequently transformed into the transfer functions, in a future study, for the various source areas within the catchment in developing the Weatherley catchment transfer function model. The Weatherley catchment is well suited to this study due to flow accumulation occurring as a result of hillslope convergence and divergence, which led to the transects within the Weatherley catchment being specifically sited on uniform transverse slopes.

In order to fit the various transfer functions to their related contributing source areas, the fluxes entering and exiting the contributing areas have to be quantified. It was decided that the HYDRUS-2D simulation model would be the most suitable for the task, due to its physically based parameter options and the variations required in the output including tensions, water content and cumulative fluxes. HYDRUS-2D was also found attractive in this study, because simulated tensions could be compared to those observed both vertically and laterally along the slope. The whole scope of the hillslope hydrological cycle processes, including fluxes of the conceptualized source areas within the Weatherley catchment with corresponding timing and quantities can be obtained from the HYDRUS- 2D model. In modelling at the small scale, like at a nested observation point, the model can be used very effectively with the simulated tensions following the observed ones, thereby describing the complexity of the natural flow regimes with accuracy and flexibility. When moving to modelling at a larger scale like hillslope and wetland areas, the optimization becomes more difficult with a much larger area being modelled with the same simple parameters. This then calls for the generalization of the hillslope section characteristics, causing the simulated output to deviate from the accuracy found at the smaller nested scale. With

this in mind the best first approximation of modelling is presented here in order to simulate the tensions and water contents and thus to obtain the fluxes from the model output to build transfer functions for the conceptualised hillslope soil water source areas within the Weatherley catchment.

3.1 The Weatherley Research Catchment

The Weatherley catchment is a research catchment in the Umzimvubu basin located on the footslopes of the Drakensberg mountain range of the northern Eastern Cape Province. The research site is the one of the upper-most catchments of one of the small tributaries feeding the Mooi River. There is no inflow of water into this catchment, making it a headwater catchment and thus highly attractive for hydrological studies at various scales (Van Huyssteen *et al.,* 2005). For this reason, the catchment is ideal for experimental purposes especially since "this area is highly susceptible to anthropogenic influences, where commercial agriculture, irrigation, household and rural settlements and forestry all contend for water use and allocation, therefore a sufficient supply of water to this region is seen as essential due to the recent establishment of forest cultivation" (Lorentz, 2001b). This is perfect in order to carry out a sound evaluation of the impacts of the afforestation, which is required by many researchers and stakeholders, but the hydrological processes on typical Molteno-Elliot sedimentary formations must be clearly understood first (Lorentz, 2001b). "Thus, a comprehensive hillslope and nested sub-catchment experiment has been initiated in a 1.5 km^2 research catchment, representative of the soils, geology, topography and climate of the region" (Lorentz, 2001a). "The Weatherley research catchment was established in 1995 and has been developed into a major research location involving many institutions" (Lorentz, 2001a). The research catchment is the idyllic situation for hydrological experiments and it was intended for the long-term surveillance and study of hillslope processes preceding and following the afforestation of the catchment (Esprey, 1997, Lorentz and Esprey, 1998, Hickson *et al*., 1999). The research catchment is located in the northern Eastern Cape Province and can be found approximately 5 km south west of Maclear, on the road to Ugie (31^o 06' 00" S, 28^o 20' 10" E) at an altitude of approximately 1 300 m above mean sea level

(Lorentz, 2001a). The research catchment was selected for its typical Molteno-Elliot formation hillslope profiles and has been described in detail in Lorentz (2001a). “The catchment drains in a north easterly direction, with the eastern, southern and western slopes being closed with the contributing hillslopes being divided longitudinally into two segments, separated by a prominent Molteno sandstone outcrop” as can be seen in Figure 3.1 (Lorentz, 2001a).

The catchment contains steep slopes, with an average slope of 12% on the eastern and southern slopes where a sandstone outcrop forms a distinctive shelf and 18% on the western slope were the outcrop is not as characteristic (Lorentz, 2001a). There is definite indication of other sandstone layering which is visible in various places on the upper half of the hillslopes (Lorentz, 2001a). The hardened sandstone shelf occurs at around 1320 m above mean sea level and has been formed primarily due to the resistance of the Elliot sandstone against weathering (Van Huyssteen *et al.,* 2005). The highest point in the catchment, at 1352 m, is situated in the south western part of the catchment and the lowest occurring along the stream flowing in a north easterly bearing from a height of 1286 m and discharging from the catchment at 1254 m (Van Huyssteen *et al.,* 2005).

The land cover at Weatherley is primarily Highlands Sourveld grassland (Acocks, 1975), which is usually in a moderate condition with a basal cover of 50-75% on the hillslopes (Esprey, 1997). Wetland environments are present along the whole reach of the stream, and sometimes up into the slopes depending on the wet season and vary in width from 100 to 400 m, being widest where marshy conditions are coupled with seepage lines from the hillslopes (Lorentz, 2001a).

Weatherley is considered to be situated in a marginal rainfall region for timber production with a Mean Annual Precipitation (MAP) of 740 mm and a Mean Annual A-pan Evaporation (MAE) of 1488 mm (Esprey 1997). The climate of the region is considered to be cool and wet, with warm wet summers and cold dry winters (Van Huyssteen *et al.,* 2005). Average daily temperatures have

been measured to range from 11°C in the winter to 20 °C in the summer, with harsh frosts and frequent snowfalls taking place at higher altitudes in winter (Lorentz, 2001a). A monthly synopsis of the rainfall, evaporation and daily temperatures is presented in Figure 3.2.

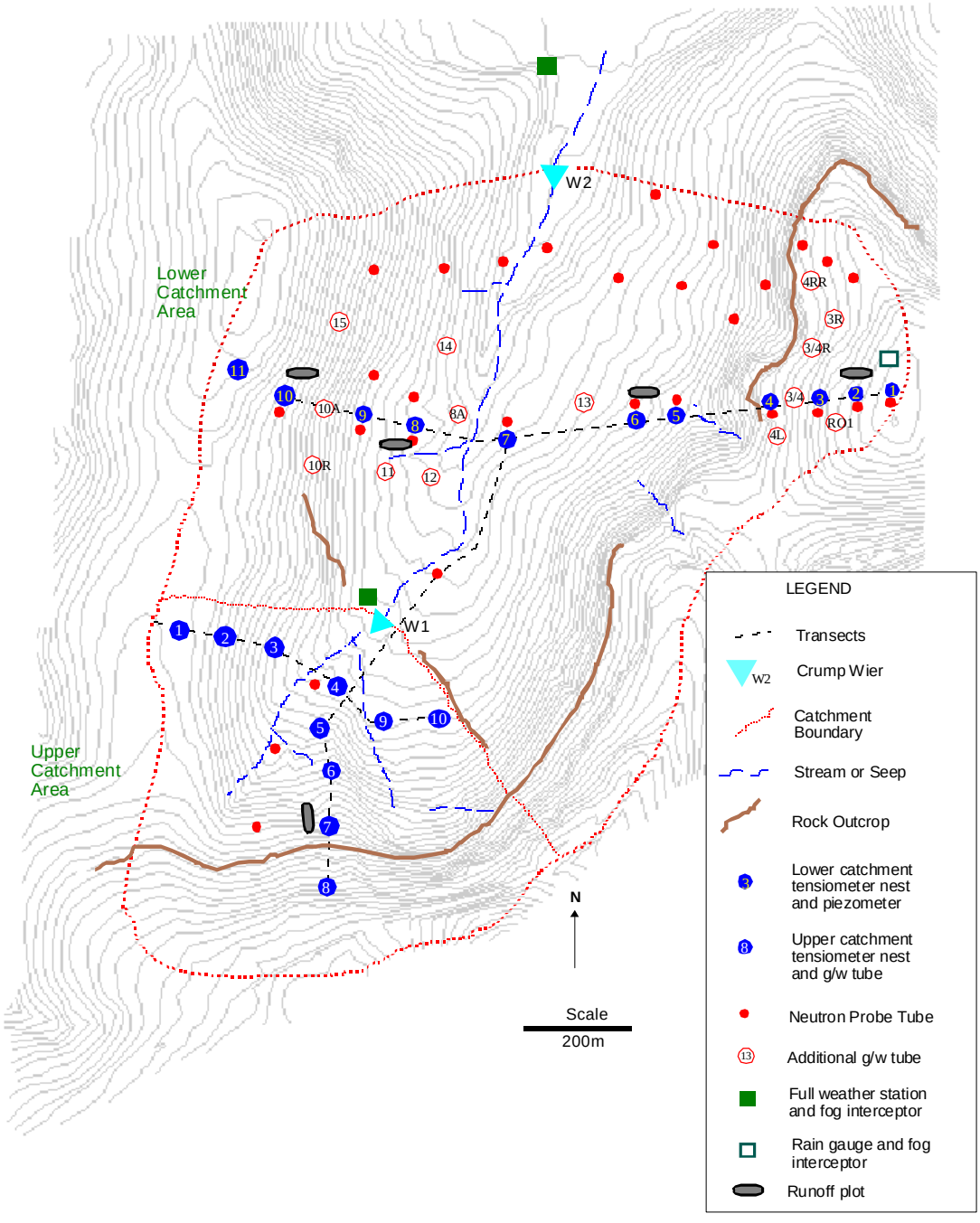

Figure 3.1 Layout of the experimental catchment, Weatherley, in the northern Eastern Cape Province, showing measurement instrumentation and structures (Lorentz, 2001a).

An especially intricate soil distribution exists with a large spatial variation (Lorentz, 2001a). “A comprehensive soil survey was initiated by the Institute for Soil, Climate and Water (ISCW) and 16 different soil forms were recognized within the 1.5 km^2 catchment boundary” (Roberts *et al.,* 1996). From this survey and further studies, it was found that due to the high rainfall and the siliceous lithology, the soils within the catchment are extremely acidic and have an exceedingly low cation exchange capacity as well (Van Huyssteen *et al.,* 2005). It was also discovered that these soils exhibit varying degrees of wetness and colour, ranging from red and yellow apedal mesotrophic soils to neocutanic and hydromorphoc soils (Lorentz, 2001a). The majority of the soils do, however, show apparent signs of water saturation. The instrumentation network in the catchment is extensive and has been systematically developed over the years as summarized in Table 3.1.

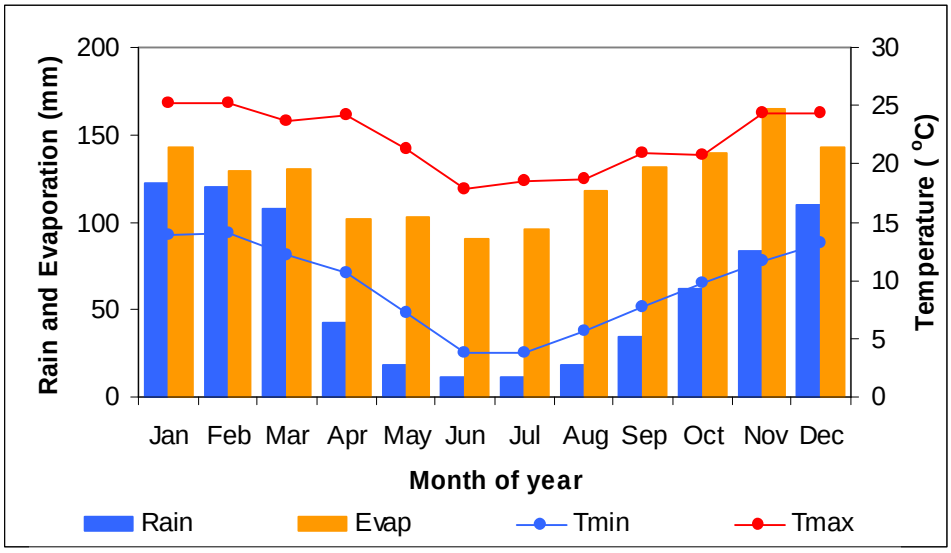

Figure 3.2 Climatic information recorded at the Weatherley experimental catchment (Lorentz *et al.*, 2003)

The instrumentation network of the research catchment consists of transects of automatic recording tensiometers and groundwater observation stations and neutron probe access tubes in the upper and lower sub-catchments, with each sub-catchment complete with a crump weir as can be seen in Figure 3.1 (Lorentz, 2001a). The lower sub-catchment transect, comprising of 11 stations, runs East-West, from the crest of the eastern slope in the lower sub-

Table 3.1. Highlights of Weatherley research catchment development from from 1995 – 2006 (after Lorentz, 2001a)

Year	Month	Description
1995	Apr.	Team assessment of research catchment
	Aug.	Neutron probe soil moisture stations 1 – 29
	Sep.	Detailed soil survey
	Oct.	Installation of rain gauge
1996	Jun.	Soil hydraulic property measurements at nests 1 – 4 and 8 - 10
	Aug.	Ground penetrating radar transect 1 – 7
	Sep.	Installation of meteorology stations at u/s and d/s weir locations
	Dec.	Installation of tensiometers and g/w wells at nests 1 – 4
1997	Jan.	Intensive monitoring period
	Feb.	Automation of tensiometers at nests 1 – 4
	Dec.	Upstream and downstream weirs completed and instrumented
1998	Jan.	Installation of tensiometers and g/w wells at nests 5 – 10
	Sep.	Installation of tensiometers and g/w wells at nests UC1 – UC10
	Nov.	Intensive monitoring period 2
	Dec.	Automation of selected g/w wells
1999	Jul.	Soil hydraulic property measurements at nests 5 – 7 and UC1 – UC10
2000	Feb.	Installation of ISCO water sampler at lower weir
	Sep.	Installation of surface runoff plots and instrumentation
2001	Mar.	First afforestation assessment
	Feb.	Second afforestation assessment
	Dec.	Source sampling of selected water quality species
2002	Jan.	Source sampling of selected water quality species
	Jun.	Local mapping of planned afforestation
	Aug.	Afforestation
2004	Apr.	Meteorological stations taken over by UKZN
2004	Feb.	Resistivity and TDR survey
2004	Nov.	Tensiometer and g/w well data monitoring halted due to vandalisation
2005	Jul.	Installation of boreholes around catchment
2006	Apr.	Workshop on Weatherley research catchment to determine future research possibilities, initiatives and capacity building

catchment, down into the wetland, traversing the stream and up the western slope, while another transect runs West-East in the upper sub-catchment and a final transect runs from the southern slopes of the upper sub-catchment, parallel with the stream, to overlap with the transect in the lower sub-catchment (Lorentz, 2001a). There are comprehensive meteorological weather stations positioned near the upper and lower weirs and there is also an additional rain gauge on the crest of the eastern hillslope near LC1 (Lorentz, 2001a). Overland flow runoff plots automated with tipping bucket mechanisms and Hobo loggers have been established and monitored on the upper and mid-slopes as indicated in Figure 3.1 (Lorentz, 2001a).

3.2 Qualification of the processes and responses in the Weatherley catchment

The distinction has to be made between hillslopes and wetlands as they exhibit distinct hydrological characteristic responses due to their location in the landscape and their vastly different combinations of local hillslope angle and upslope contributing area (McGlynn and McDonnell, 2003). McGlynn and McDonnell (2003) also stated in the same paper, that riparian zones respond (because of rising water tables) more rapidly to precipitation inputs than hillslope areas and this is also true for the Weatherley catchment, as evidenced from data collected from boreholes, piezometers, tensiometers and neutron probes as well as being witnessed within the catchment. These above-mentioned differences can be seen for the Weatherley catchment in Figures 3.3 (hillslope sub-area) and Figure 3.4 (riparian sub-area) respectively. In Figures 3.3 to 3.7, the legend indicates the location of the site followed by the depth that the data applies to. This difference in response areas is indicative of the higher antecedent soil moistures and more persistent water tables in the lower-lying near-stream positions and also because hillslopes drained more fully between events, resulting in higher between-storm soil moisture deficits (McGlynn and McDonnell, 2003).

According to McGlynn and McDonnell (2003), further complexity arises since the source areas change size and shape depending on whether further rainfall

occurs on the rising or the falling limb of the hydrograph, thereby expanding the irregular interface between the hillslope and riparian areas in headwater catchments. The antecedent soil water conditions also influence various patterns and dynamic responses, especially in semiarid, mountainous regions (Grant *et al*., 2004).

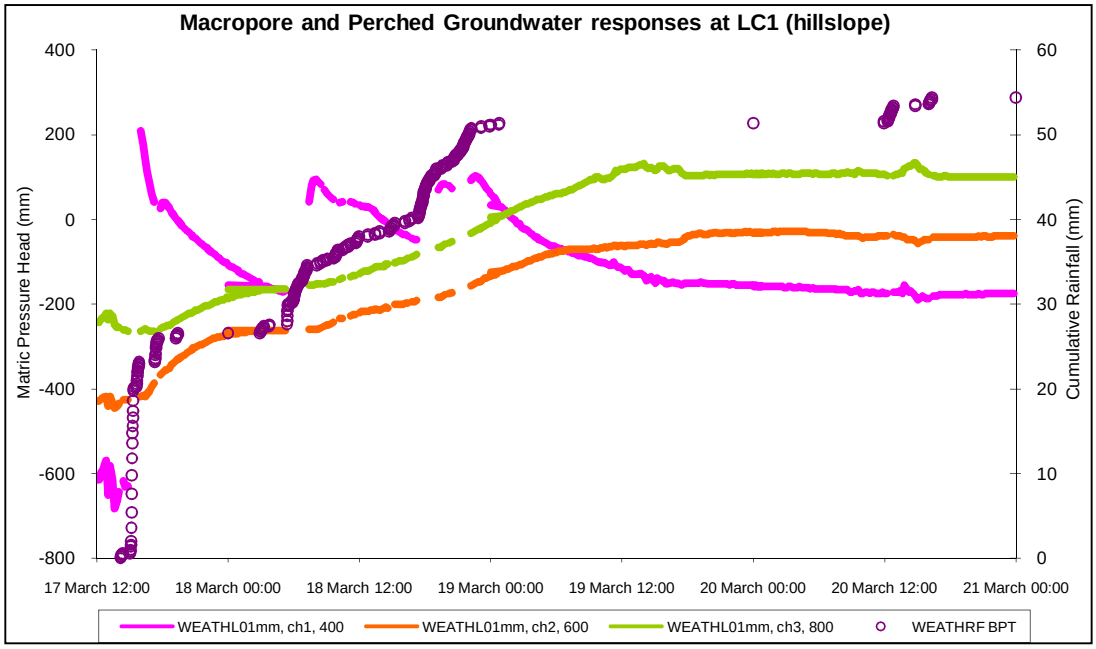

Figure 3.3 Examples of macropore and perched groundwater responses originating from upper hillslope areas at LC 1 (March 2001).

Hydrologic connectivity is the circumstance in which expanses of the hillslope, and the hillslope-stream system, are linked via lateral flow pathways, and is a significant factor that controls runoff response, nutrient transport, and many other hydrologic and ecologic functions of watersheds (Achet *et al*., 2006). This hydrologic connectivity is shown below by a series of graphs to demonstrate the connectivity between areas in the upper hillslopes (Figure 3.5 and 3.6) and also the connectivity between these upslope areas with those areas situated down in the wetland area (Figure 3.7 and 3.8).

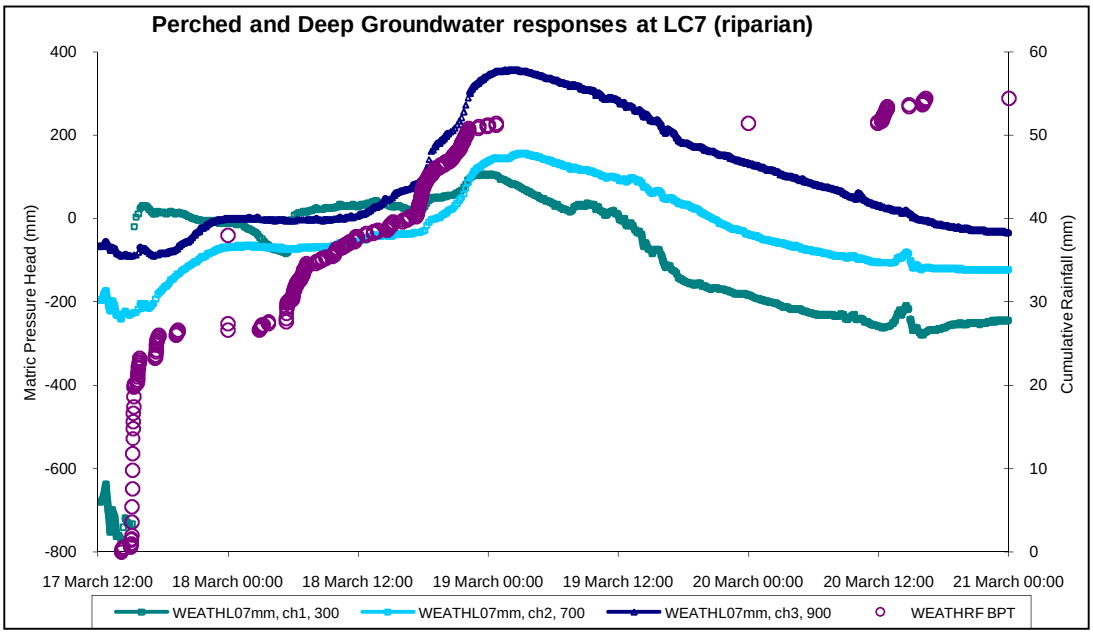

Figure 3.4 Examples of perched groundwater responses originating from riparian areas at LC 7 (March 2001).

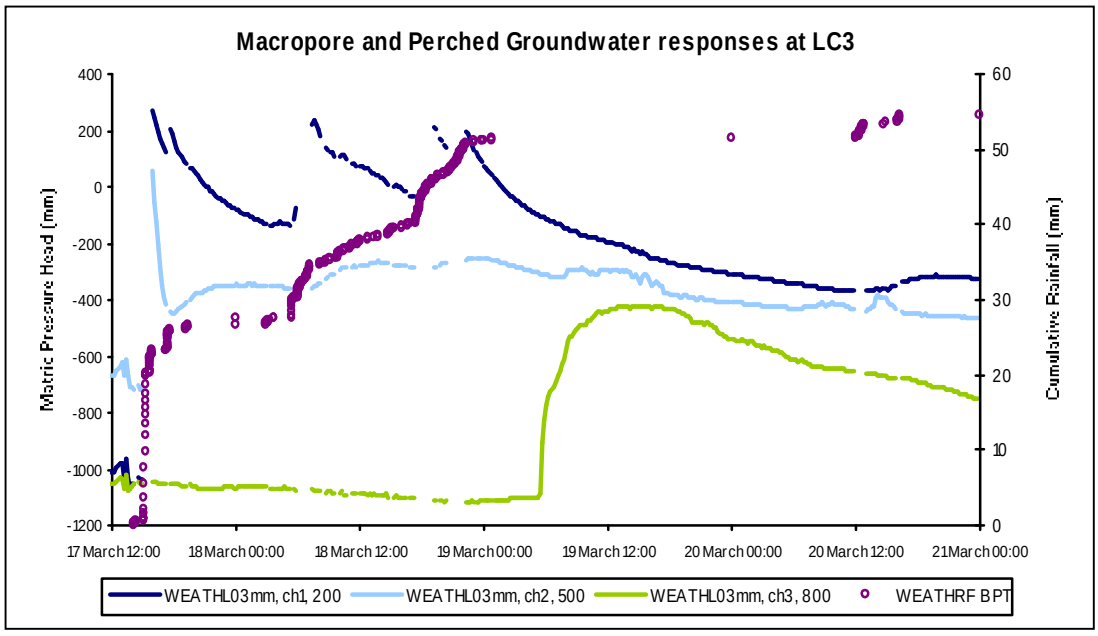

Figure 3.5 Examples of macropore and perched groundwater responses originating from upslope areas at LC 3 (March 2001).

The Figures 3.5 and 3.6 show that the data from these two sites (LC3 and LC4) are connected, with the shallow tensiometers responding at the exact same time, but to different degrees of inundation, showing the connectivity of the two sites through lateral processes during rainfall events. The differing

degrees of inundation could be indicative of this aforementioned connectivity. The deeper tensiometers (500 and 800 mm) show that there is connectivity between the two sites, but it is only partial due to the nonsteady state behaviour of the perched groundwater.

Figures 3.6 and 3.7 illustrate the connectivity between the upper hillslope area with the wetland area below it, from seepage taking place at the toe of the slope (LC4) to the groundwater recharge that occurs when the soil profile becomes inundated and the groundwater becomes connected to the shallower horizons through their saturation due to upslope contributions (LC6). Initially there is macropore type flow near the surface and this subsides quite rapidly in the late evening on 18 March (Figure 3.6), but the tensions indicate that there is still water moving into the wetland area from upslope even on 19 March at midday and still on the early morning of 20 March (Figure 3.7). This water emanates from seepage through the fractured bedrock from upslope to the wetland area below, thus proving connectivity between the two contributing areas. This connectivity will change the size and shape of the wetland contributing area, thus demonstrating the threshold behaviour of catchment runoff sources and the nonsteady state behaviour of discretised landscape unit hydrology.

The research catchments processes and responses are explained in a report based on extensive hydrometric observation and a thorough two week survey on the isotopic separation of the rainfall data and streamflow sources by Lorentz (2001a). The hillslope, wetland and riparian zone streamflow generation mechanisms were then construed from the hydrometric observations of the dynamics of soil water, groundwater and streamflow response to rainfall and evaporation. The dominant streamflow generation processes in the Weatherley research catchment have been generalised and represented in Figure 3.8 and described in Table 3.2. The streamflow generation mechanisms were then assembled into zones of similar response units as shown in Figure 3.9 and summarized in Table 3.3 Lorentz (2001a).

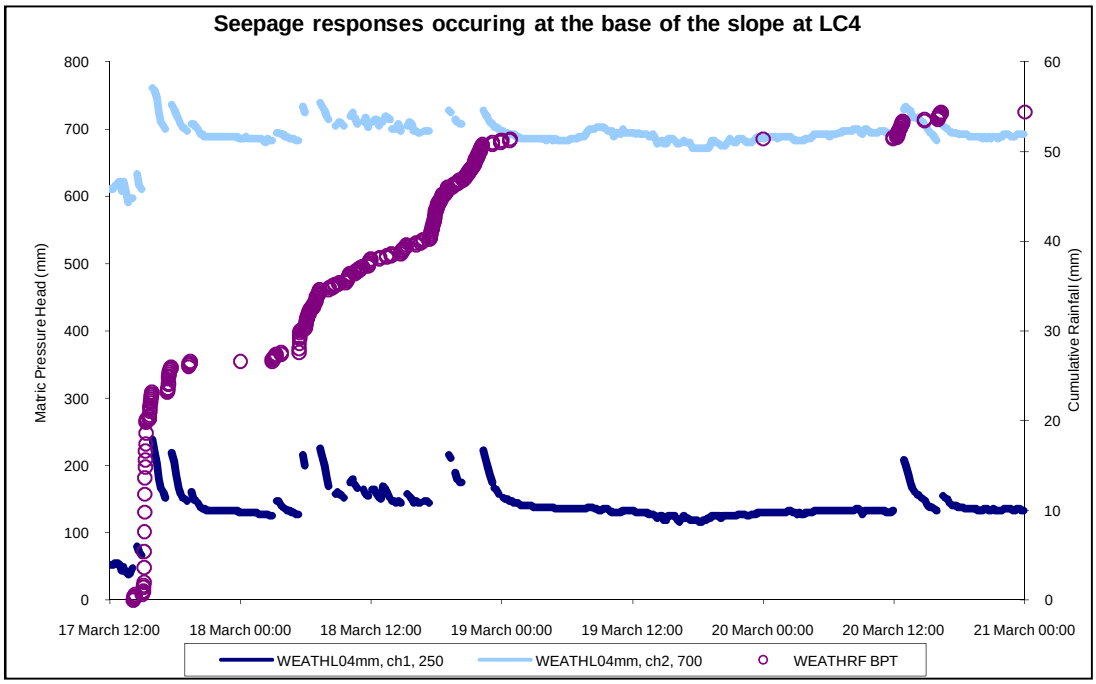

Figure 3.6 Examples of tension responses showing groundwater seepage responses originating from upslope areas at LC 4 and occurring due to the shallow bedrock interface (March 2001).

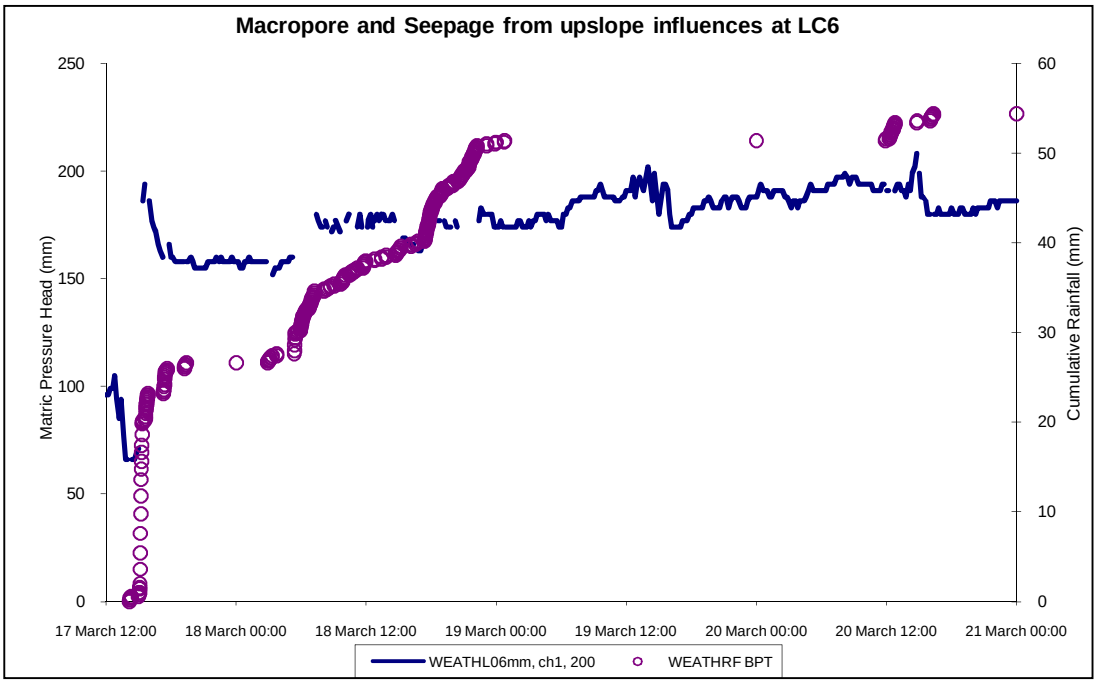

Figure 3.7 Example of tension response showing when groundwater recharge occurs at LC 6 originating from seepage from the toe of the upslope area at LC 4 (March 2001).

Three principal streamflow generation mechanisms, (overland flow, near surface macro-pore flow and groundwater flow), are believed to contribute to the stream and local seepage zones, linked to the stream, during a rainfall event (Lorentz *et al.*, 2003). This complicates the modelling in the studied catchment, because these sources of complex streamflow mechanisms have both fast and slow streamflow responses, which are difficult to model in conjunction with each other (especially with a simple two-parameter transfer function), based on natural thresholds, therefore the modelling is focussed on both the tensions and the water contents. In this distributed type modelling, the different streamflow generating mechanisms need to be generalized to a degree such as Becker and Braun (1999) have disaggregated the land surface into sub-areas of "quasi-homogenous" behaviour and Troch *et al.,* (2003), which distinguished between uniform, convergent and divergent hillslopes that are generally considered in geomorphology and hydrology. Source area modelling becomes possible in the Weatherley catchment where three different modelling segments are identified along the lower catchment's transect to be simulated with the HYDRUS-2D model. These identified generalized segments to be simulated are noted to be firstly, the transects LC 1-4 (west facing upper hillslope zone), then LC 5-7 (wetland and riparian zone) and LC 8-10 (east facing riparian, wetland and hillslope zone). These three segments encompass all the response zones that are identified in Figure 3.9 and described in Table 3.3.

With the frequent occurrence of water tables in the low-lying wetland areas the result is soil gleying, the accretion of fine sediments, and an increase in weathering and depositional processes (McGlynn and McDonnell, 2003). These basic differences in landscape units can be recognized because the topographic (Figure 3.8), hydrologic (Figures 3.3 and 3.4) and pedologic (Figure 3.10) variability that exists among hillslope and riparian areas contributing to a clear, unequivocal differentiation (Figure 3.9), and thus allowing mapping based on the solute signatures (or isotopic separation), soils, landform (toposequence) and response to storm precipitation (McGlynn and McDonnell, 2003). With this understanding, the hillslope, wetland and riparian areas can be more readily recognized and distinguished based on

landform, slope, elevation, moisture status, hydrological response, soil characteristics and also the proximity to the channel.

Weiler (2004) held that models simulating infiltration into soils containing macropores still present inadequate results, as existing models seem unable to encapsulate all the appropriate processes, with recent investigations revealing a distinctive flow rate variability depending on the initiation process, whether it be bypass flow, rapid lateral flow or due to a perched water table being developed. However, Achet *et al.,* (2002) states that in more arid environments this connectivity is relatively rare, with the water draining through a catchment following the same flowpaths and being spatially isolated for the majority of the year (Stieglitz *et al*., 2006), resulting in dramatic differences in hydrologic response and thus a range of ecological ramifications. This dynamic nature demonstrates the threshold behaviour of catchment runoff sources and the nonsteady state behaviour of discretised landscape unit hydrology. Therefore, according to McGlynn and McDonnell (2003), the “static mapping of similar source areas and their responses is a conservative approximation of the runoff generation from the principal landscape units”. The benefit of this approach of distributed modelling is in “capturing the complex interaction and system behaviour of the several factors in lateral unsaturated flow generation, the most appropriate unit of analysis is to follow the natural landscapes of topographic water flow or unsaturated response units” (Achet *et al*., 2002).

This distributed type modelling approach can be furthered by using transfer functions obtained from fluxes calculated from specific hydrological response areas. The Hydrus-2D model was used for this. The model was used primarily to estimate the fluxes in soil water dynamics, especially the discharge fluxes during the dry season from the soil matrix, thereby giving insight into low flow responses.

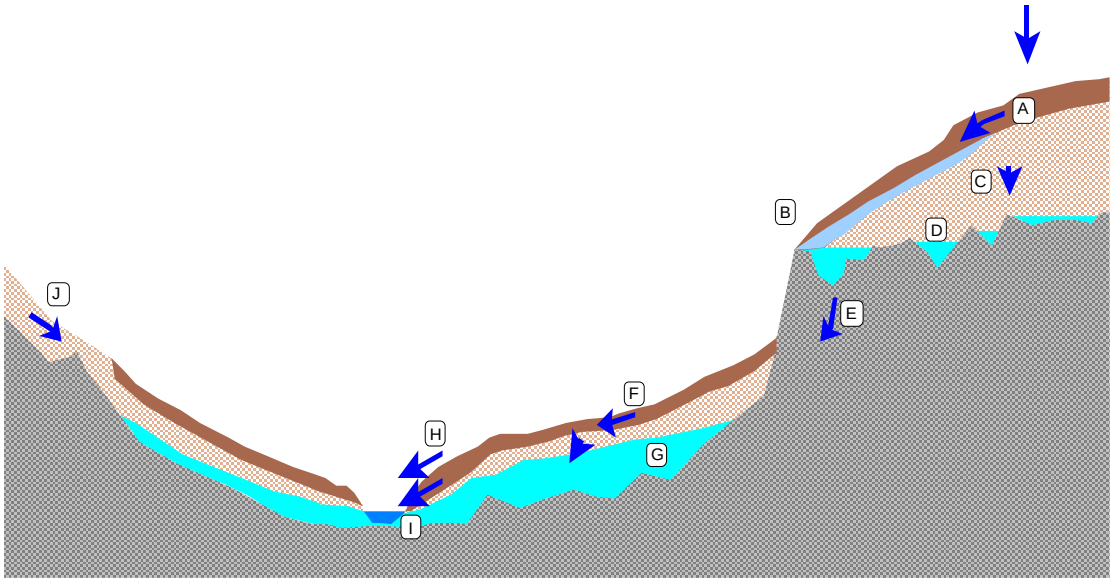

Figure 3.8 Schematic diagram of dominant flow processes and flow pathway zones (Depths of the soil profiles are exaggerated 4x the vertical scale) (after Lorentz and Hickson, 2001)

Table 3.2 Summary of flow mechanisms and their occurrence at Weatherley research catchment (after Lorentz and Hickson, 2001)

CODE	DESCRIPTION	OCCURRENCE
A	Rapid lateral flow near the surface due to macro-pore conductance. Local perched water table of short duration. Matric pressure head discontinuity with deeper perched water table, D.	In upper slope segments in downstream catchment during high intensity events and some low intensity events with large volumes (>30 mm).
B	Accumulation at the toe of the slope segment with emergence and flow over bedrock.	In upper slope segments in downstream catchment.
C	Slow percolation to water tables perched on bedrock.	In all slope segments for most events except low intensity and volume.
D	Water tables perched on bedrock and in bedrock hollows.	Disconnected from soil water in upper slopes of eastern side of downstream catchment, but connected in lower slopes and in upstream catchment during moderate to intense events.
E	Seepage of groundwater through fractured bedrock.	Assumed to occur in all slope segments.
F	Rapid macro-pore, lateral flow in flatter marsh slopes and infiltration to marsh ground water.	Vertical recharge is more rapid than lateral movement in lower slopes of downstream catchment and in upstream catchment, except when groundwater rises into macro-pore layers.
G	Marsh ground water level fluctuation	Rapid for most events in lower downstream catchment. Slower, but connected in upper catchment.
H	Exfiltration, surface runoff and macro-pore discharge to stream	In downstream catchment. Exfiltration not observed in upstream catchment.
I	Groundwater discharge into stream	Occurs in upstream and downstream catchments. Some near stream groundwater ridging during intense events.
J	Unsaturated redistribution of soil water to bedrock. No groundwater on soil/bedrock interface.	In upper parts of western slope. Generates slowly to soil/bedrock water table downslope.

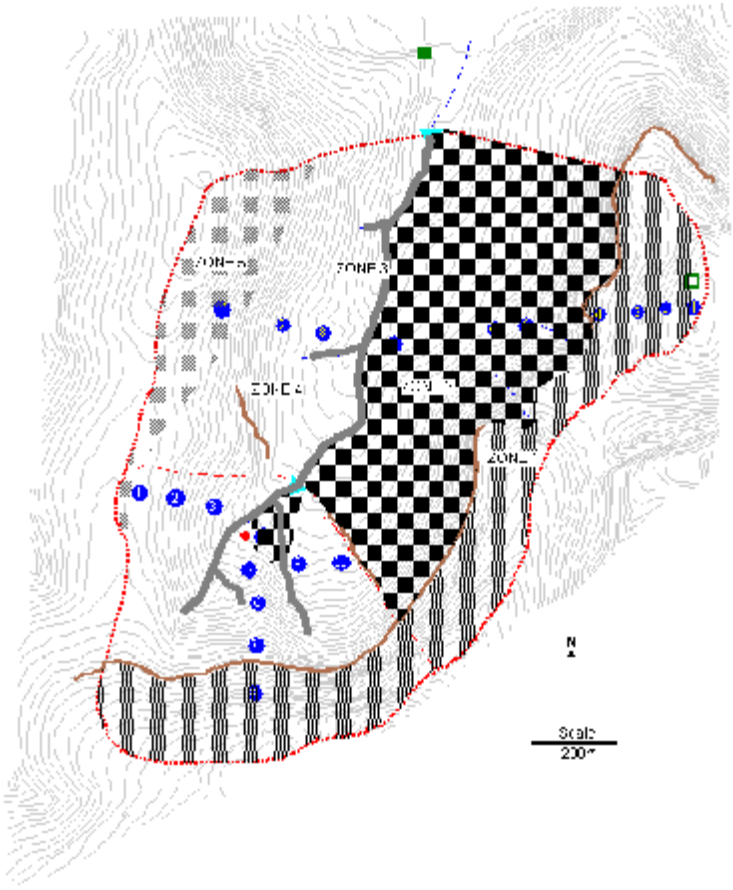

Figure 3.9 Zones of similar flow pathway zones, Weatherley. The Zone numbers refer to descriptions in Table 3.3 (Lorentz *et al.,* 2003)

Table 3.3 Summary of general flow generation zones, Weatherley research catchment (Lorentz *et al.*, 2003)

ZONE	DESCRIPTION
1	Upper slopes of eastern half of the catchment, where delivery of water in a disconnected near surface macro-pore zone delivers water to bedrock outcrop at the toe of the slope. Soil matric pressure is not continuous between responses in near-surface layers and deeper layers near bedrock. Surface water runoff generation for no more than 20 to 30m upslope contributes to flow at the toe. Slow deep groundwater from soil/bedrock interface recharges to toe and to lower slopes and bedrock. All water from this zone is delivered to Zone 2.
2	Recharge from upslope zone and infiltrating water raise groundwater levels at seepage lines and wetland areas. Some flow in near-surface macro-pores. However, it is normally associated with the resident groundwater rising into the macro-pore layers, particularly adjacent to the stream and seepage lines leading to the stream. Some groundwater ridging near the stream yields increased hydraulic gradients for short periods during moderate to intense events.
3	Near stream surface and near-surface water runoff, dominated by groundwater intersecting rapid delivery macro-pore layers.
4	Some flow in near-surface macro-pore layers, but mostly due to intersection of soil/bedrock perched water. There is generally soil matric pressure continuity between upper and lower layers. Near the stream, water is delivered through groundwater rising into macro-pore layers.
5	No perched water tables are evident, even during intense events. Little macro-pore discharge in near-surface layers, even during intense events. Significant wetting to deep horizons with slow delivery of unsaturated water to lower slopes.

3.3 HYDRUS-2D input file setup

The HYDRUS-2D model was run for the period from 1 January 2001 to the end of October 2001. The input file for running the model was made up from breakpoint rainfall data collected from the Weatherley subcatchment and evaporation data that was collected by the ARC-ISCW and patched by van Zyl and Lorentz (2001), since daily measured evapotranspiration for the veld in the Weatherley catchment was not available for this study. The evapotranspiration data were patched using daily FAO Penman-Monteith equation data for Weatherley and surrounding stations and was obtained from the ISCW (van Zyl and Lorentz, 2001). The stations and the periods of data reported include: Weatherley (31.1000 S, 28.3333 E), from 01 June 1997 up to 28 February 2001; Somerton (31.1567 S; 28.3843 E) from 01 January 1997 to 3 August 2003; Wildebees (31.2000 S; 28.2167 E) from 25 March 1997 to 28 February 2001; and Tsolo (31.3000 S; 28.7667 E) from 3 December 1997 to 6 January 2004.

The ETo data from all of the above stations contains many missing values. In order to fill the data gaps, Weatherley ETo data was regressed against ETo for a surrounding station for dates on which both stations had ETo data (Figure 3.11). ETo data from the three stations, namely: Somerton, Wildebees, and Tsolo, were found to fit Weatherley ETo data reasonably well. The scatter of the data and the subsequent regression equations indicate that Somerton Eto data, followed by Tsolo Eto data matched Weatherley Eto data fairly well. Wildebees Eto data showed a considerable scatter, specifically for ETo data values exceeding 4 mm day^{-1}. Missing daily Weatherley Eto data values were estimated using the above regressions in the following order of preference: Somerton, Tsolo and then Wildebees.

The breakpoint rainfall from the Weatherley catchment's raingauge (near the nest at LC1) was used with the Eto data to create an hourly input file, where the daily Eto rate was applied between the hours of 06:00 and 18:00 throughout the analysis period. The Atmosph.in file in HYDRUS-2D requires the separation of the potential evaporation (rSoil) and transpiration (rRoot)

data, which is done via spreadsheets and according to the crop factor selected. Interception was assumed to be part of Eto in this study.

The crop factors influence the partitioning of the potential evaporation (rSoil) and transpiration (rRoot) input data in the input file. The crop factor selected was the Highlands Sourveld grassland (Schulze and Pike, 2004). The crop factors are shown in Table 3.4 below. The crop factor in winter (June, July and August) was increased slightly in order to transpire more water out of the soil profile at a faster rate and to make transpiration take place when the crop factor was 0.2. According to the maximum transpiration from crop coefficients equation (Eqn 3.1), a crop factor of 0.2 signifies no transpiration occuring as there is scarcely enough canopy cover to transpire water. The crop factor for September and October was decreased in order to match the observed response, in the soil water tensions of those months, by not allowing as much water to transpire out the soil thereby maintaining a wetter soil. The crop factor affects the amount of transpiration occurring each day and so either it will increase or decrease the daily evaporation accordingly, as the evaporation cannot exceed the potential evapotranspiration for the day.

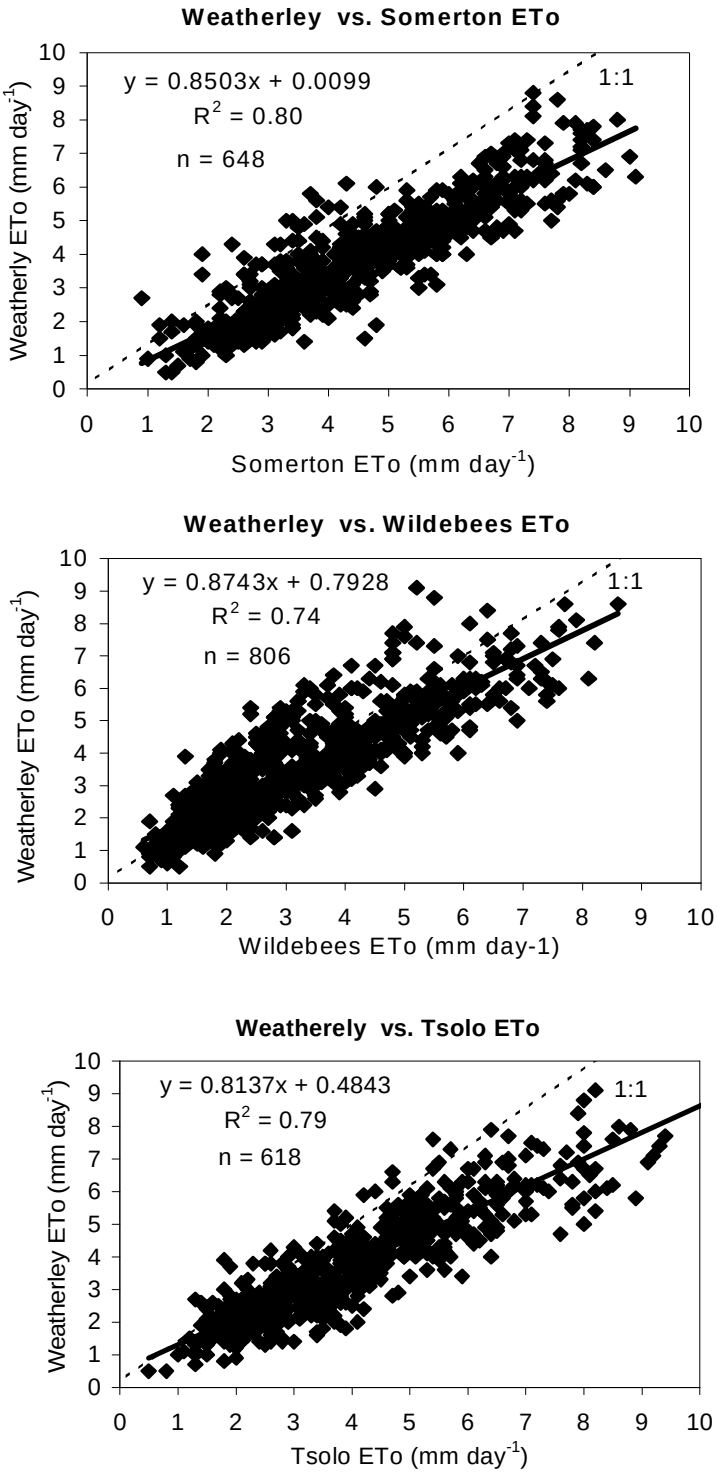

Figure 3.10 Regression equations for ETo values of Weatherley vs. surrounding stations from data obtained from ISCW climate database (van Zyl and Lorentz, 2001).

Table 3.4 Monthly Crop Factors (K_d) for Highland Sourveld (Schulze and Pike, 2004) and those used in the HYDRUS-2D model setup.

Month	K_d from Atlas	K_d used in HYDRUS-2D
January	0.7	0.7
February	0.7	0.7
March	0.7	0.7
April	0.5	0.5
May	0.3	0.3
June	0.2	0.25
July	0.2	0.21
August	0.2	0.21
September	0.5	0.25
October	0.65	0.27

These crop factors are used in conjunction with the maximum transpiration from crop coefficients equation (Eqn 3.1) used in ACRU (Schulze, 1995) and the daily evapotranspiration to calculate the amount of daily transpiration.

$$F_t = 0.95 * (\text{Monthly CAY} - 0.2)/ 0.8 \quad \text{when } K_d > 0.2 \qquad (3.1)$$
$$= 0 \quad \text{when } K_d \leq 0.2$$

where

F_t is the fraction of the total available transpiration and CAY is the average monthly crop coefficient

The inputs into the Hydrus-2D model are calculated by subtracting the daily potential transpiration from the daily potential evapotranspiration to calculate the amount of daily potential evaporation for the individual days of the month. These daily values for transpiration and evaporation are then divided into the daylight hours (i.e. 06:00 to 18:00). These values then become the daily rRoot and rSoil values respectably, which are used as input into the ATMOSPH.IN

file in the model. A portion of the ATMOSPH.IN file is presented in Appendix A in Table A1.

Once this is done a HYDRUS-2D file is created, where the type of simulation (water flow), the length units (mm), the type of flow (vertical plane), the number of materials (1), the time units (hours) and the number and timing of the print times are specified. The temporal discretization covers a 10 month (7296 hours) modelling period with a minimum time step of 0.01 hours and an initial time step of 0.0025 hours. The iteration criteria, the soil hydraulic model (van Genuchten) with no hysteresis was chosen. The root water uptake model is then selected in a similar way, with the Feddes water uptake reduction model with no stress being chosen and the Feddes root water uptake parameters being included as input.

A finite element mesh outline is created from geometric points capturing the hillslope section attributes of length, depth and slope. This is then converted into a mesh in HYDRUS-2D, specifying the number of boundary points needed for the required mesh detail. A high resolution of mesh detail was required in order to observe what is happening at different depth levels in the soil profile. The root zone is then defined in the finite element space in the model, with the depth of between 0.5 m and 1 m being specified. The initial conditions can be specified by the user or for a more realistic option; the initial conditions can be imported from a previous run, with the same geometry, where the moisture conditions have been naturally dispersed through the profile. Observation nodes are then specified at the same spatial and depth scales of the tensiometers and neutron probes along the transects as can be seen for the LC 1-4 section in Figure 3.12. Then boundary conditions are given to the sections of boundary of the mesh. In the upper east facing hillslope transect (LC1-4); a no flow boundary condition was used at the bottom of the domain, an atmospheric boundary condition along the top of the domain and a seepage face at the toe of the slope. In the lower east facing wetland transect (LC5-7), a constant pressure head boundary condition was specified at the bottom of the domain, an atmospheric boundary condition along most of the top of the domain with a small variable flux boundary

condition included where contributions occur from the upper hillslope area and a seepage face at the toe of the slope. The variable flux boundary condition occurs around nests LC5 and LC6 with the amount of seepage from the uplslope area being 0.05 mm/hr from January to April and 0.012 mm/hr for the remaining period. This equates to 162.5 mm, which is equivalent to the amount seeping out of the LC1-4 transect simulation (Figure 5.16), and comprises of water being contributed from the upslope area due to seepage through the fractured groundwater bedrock and from the toe of the upper hillslope transect. In the west facing hillslope transect (LC8-10) a no flow boundary condition was specified along most of the bottom of the domain with a constant pressure head boundary along the lower reaches of the bottom domain, an atmospheric boundary condition along the top of the domain and a seepage face at the toe of the slope. The soils measured soils hydraulic characteristic was used as a first estimate in the modelling. However, these characteristics shown in Figure 3.12 required modification in order to fit the observed tensiometer responses.

3.4 Fitting Water Retention Characteristics to the data

From laboratory suction tests that have been performed in the past on the soils from the Weatherley catchment (Lorentz *et al.*, 2001), water retention curves have been plotted for the nest sites at different depths along the transects. These data were found useful, but as one increased the area to be modelled, the parameters were found to be less applicable as they are very much site and depth specific. The soil retention and hydraulic conductivity functions require residual (Θ_r) and saturated (Θ_s) water content, saturated hydraulic conductivity (K_s), the inverse of the bubbling pressure or air entry value (α) and pore size distribution (n). Achet *et al.,* (2006), who also used the HYDRUS-2D model to simulate sections, noted a difference of several orders of magnitude in soil hydraulic properties between reported laboratory, in-situ measurements and the properties required to fit the field observations of soil water responses. Thus the parameters that were calculated from fieldwork do not necessarily correspond to the ones utilised within the model. In this study, the fieldwork was found helpful with the Θ_s and Θ_r values, but not greatly with

the alpha and n values and they are therefore only used as a guide. An example of a good fit against the observed water retention curve and their associated parameters is given in Figure 3.13, but these parameters were found to be inaccurate when modelling the dynamic tensions and water contents, so a trial and error exercise took place to derive the effective hydraulic characteristics to represent the whole hillslope segment.

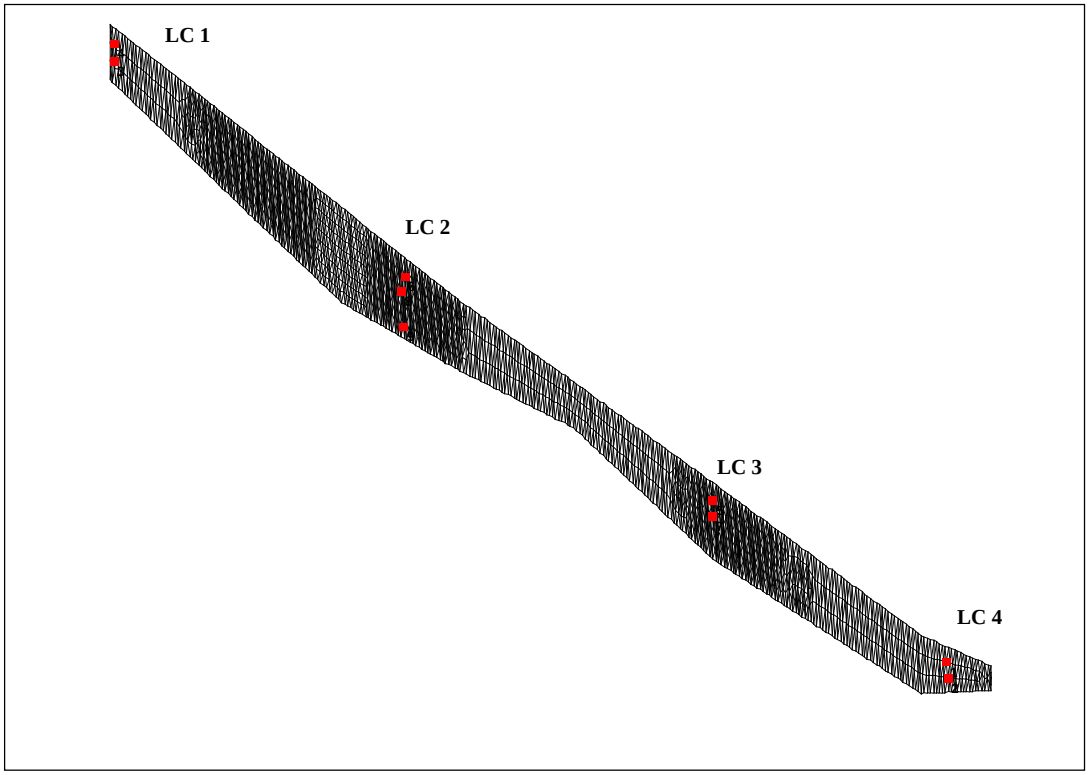

Figure 3.11 Finite element mesh showing actual locations and depths of the observation nodes reflecting the tensiometers and neutron probes occurring in transect LC 1-4

Thus the observed water retention curve was used to try various combinations of the soil hydraulic properties and finally an adequate simulated fit was found for the water retention curve as well as the simulated tensions and water contents. The resultant water retention curve is shown in Figure 3.14.

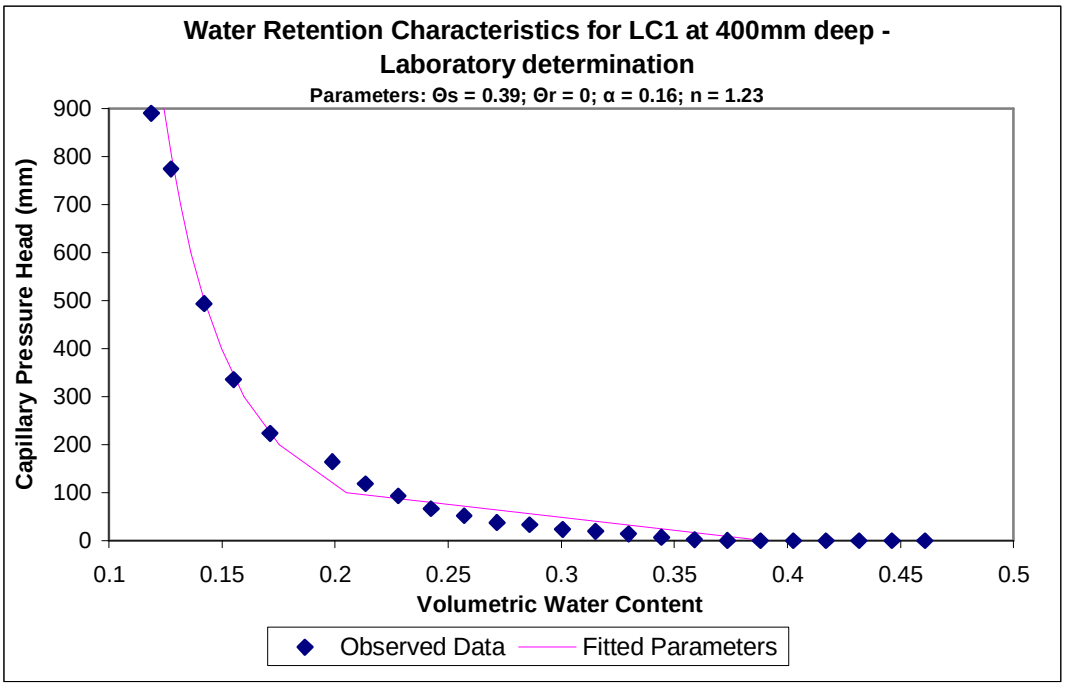

Figure 3.12 Laboratory water retention characteristics for Nest LC 1 at 400mm deep-resulted in poor HYDRUS-2D simulation parameters

3.5 Modelling with the HYDRUS-2D model

Simulating the observed tension and water content at each point in the vertical and lateral dimension of the 2-D transect required extensive iterative simulations. The first set of simulations was simple, for an overview of the HYDRUS-2D model, where a small section of the hillslope was modelled to avoid over complication early on and some initial problems were solved as a result. These included avoiding the numeric instability often encountered during modelling, by changing the finite element grid resolution, the time step and adjusting the hydraulic characteristics. Once this small site was adequately modelled, the area to be simulated was increased to cover the upslope section in the Weatherley lower catchment from nest 1 to 4. The modelling was done along the transect that runs along the east facing hillslope section (LC1-4) and at various depths, with the observation nodes within the model structure being set at the same position and depth as the tensiometers in the actual catchment. The model also simulated the seepage exiting out of the sandstone along the outcrop at the bottom of the upslope

section. The observed water table was included to further demonstrate simulation of the soil dynamics within the profile.

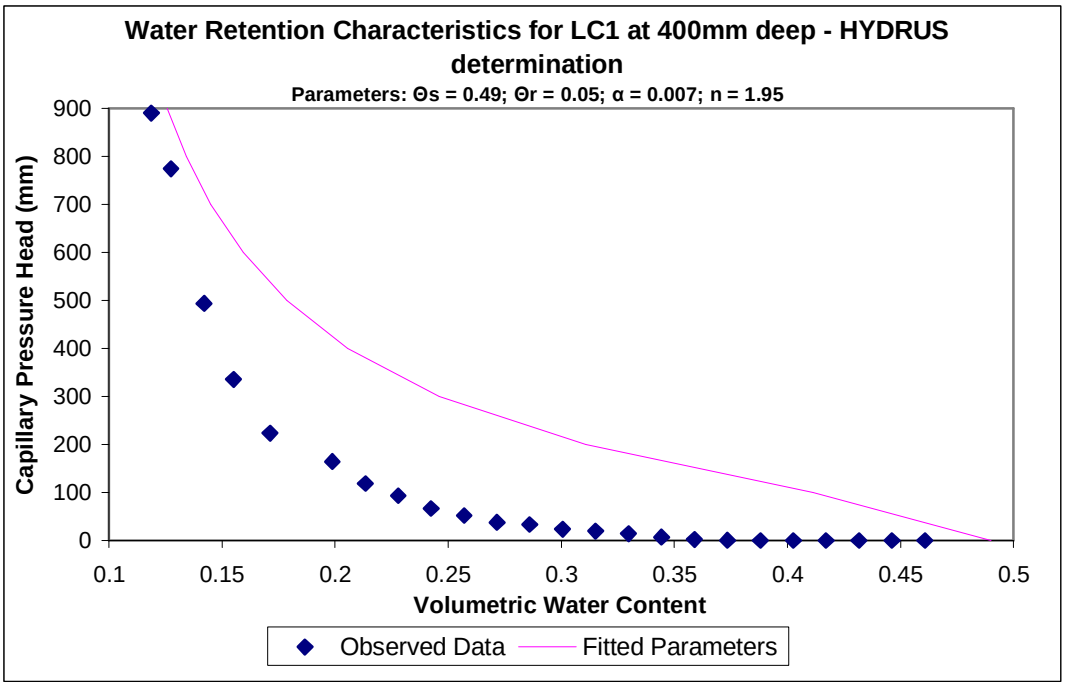

Figure 3.13 Water retention characteristics for Nest LC 1 at 400mm deep - resulted in good HYDRUS-2D simulation parameters

Once the simulated output had been adequately modelled to fit the observed results for all the transects within the Weatherley lower catchment, the fluxes are ready to be quantified and assigned to the various source areas. However, prior to this, the simulated flux results need to be converted into the same format as the data in the input file so that the runoff and seepage from the hillslope can be isolated. This needs to be done because the model input (Appendix A, Table A1) is at a rate (mm/hr) and the model output (Appendix A, Table A2), is a volume per model time step. This is achieved by inserting both the spreadsheets of model inputs (ATMOSPH.IN), the times steps and responses from the model output (Cum_Q.out) into a Microsoft Access file. Both the input and output files are converted to text format and rounded off uniformly to then be merged to form a combined text table with the input data at the output timestep. This precipitation, evaporation (rSoil) and transpiration (rRoot) text in the table is then converted back to values as shown in Appendix A, Table A3.

The Cum_Q.out file reported cumulative fluxes at each model output timestep as volumes and these need to be converted into depth (mm) so that they are easily comparable to the input data. In order to do this, an atmospheric boundary factor needs to be calculated to divide the cumulative flux output by, in order for them to be converted to mm. This is accomplished by graphically comparing the known input values (Precipitation, rSoil and rRoot), in their new output timestep, with their corresponding output cumulative fluxes (CumQAP, CumQRP, CumQA and Cum QR) along the length of atmospheric surface boundary such as in Figure 3.15. The corresponding HYDRUS-2D output yields volumetric output fluxes are described in Table 3.5.

Table 3.5 Description of the cumulative output fluxes from the Cum_Q.out file

Output Parameter	Explanation
CumQAP	Cumulative total potential surface flux across the atmospheric boundary (L^2)
CumQRP	Cumulative total potential transpiration rate (L^2)
CumQA	Cumulative total actual surface flux across the atmospheric boundary (L^2)
CumQR	Cumulative total actual transpiration rate (L^2)

The known inputs, like rainfall, potential evaporation and potential transpiration, across a boundary are compared with the input reflected in the simulated output file. This allows for a conversion factor to be calculated since these depend on the associated boundary length. The boundary conversion factor is determined by comparing known input values with reported output volumetric fluxes. However, HYDRUS-2D does not output rainfall and evaporation separately, but rather as QAP, so these need to be reproduced from input data before the boundary conversion factor can be determined.

The applicable equation follows:

$$ABF = KI\ (mm) / I\ (mm) \qquad (3.2)$$

where the ABF is the atmospheric boundary factor; KI is the known input and I is the input across the boundary from the simulated output file. The atmospheric boundary factor is then applied to the simulated responses across the boundary, like actual evaporation and transpiration as well as potential evaporation and transpiration.

These cumulative output fluxes need to be defined to isolate the various fluxes, so Es-P is:

$$(Es\text{-}P)_e = (Es - PPT) * (t_e - t_{e-1}) + (Es\text{-}P)_{e-1} \quad (3.3)$$

where Es-P is the input soil evaporation less precipitation cumulative flux rate remembering that there is no evaporation during rainfall; Es is the input soil evaporation; PPT is the input precipitation; $_e$ is the print timestep interval and t is the timestep. And Et is:

$$Et_e = Et\ (t_e - t_{e-1}) + Et_{e-1} \quad (3.4)$$

where Et is the input transpiration cumulative flux rate; $_e$ is the print timestep interval and t is the timestep.

The Cum_Q.out file has calculated cumulative seepage fluxes at each model output timestep as volumes and these also need to be converted into mm. In order to do this, a seepage factor needs to be calculated to divide the cumulative seepage flux by in order for it to be converted to mm per time step. This is accomplished by calculating the volumetric water content (Θ) for each print time specified, from the changing volume (V), and the constant area (A) from the cross sectioned transect profile:

$$\Theta = V / A \quad (3.5)$$

These volumetric water contents are then compared with those found in the time staggered graphical display of results featured in HYDRUS-2D as well as with the water contents outputs from the model in the ObsNod.out file. The change in soil storage (Δ SS) is then calculated in mm per time step:

$$\Delta SS = (\Theta_e - \Theta_{e-1}) * A / (L * 1) \quad (3.6)$$

where Θ is the water content; $_e$ is the print time; L is the length of the atmospheric boundary and A is the cross sectional area.

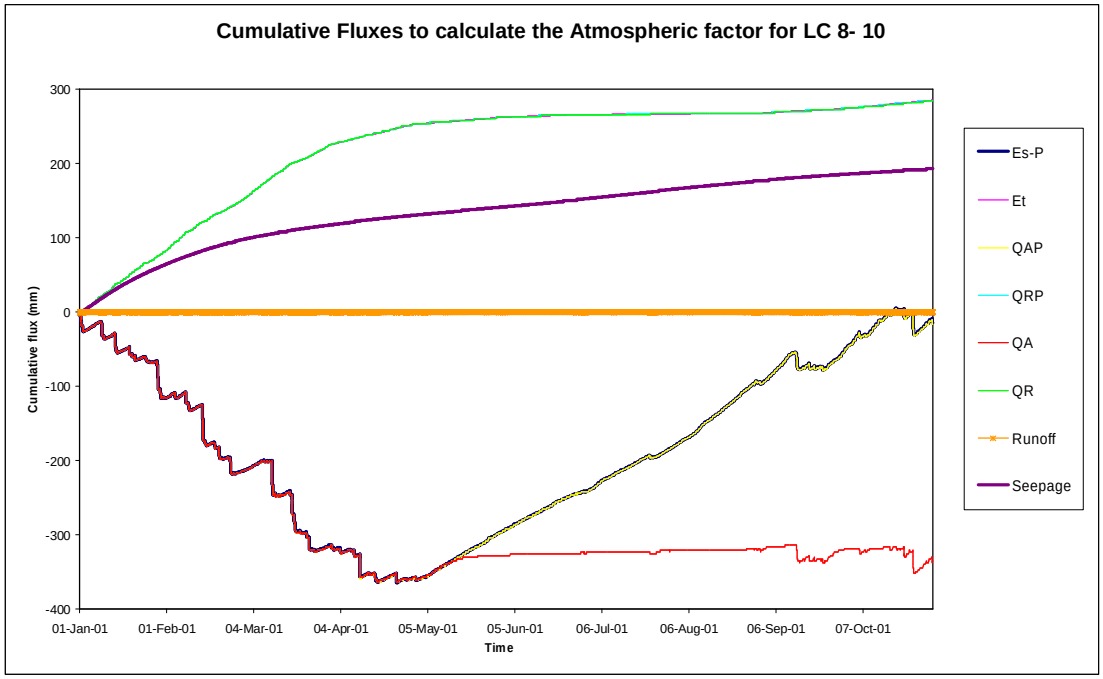

Figure 3.14 Diagram showing how the cumulative fluxes are compared in order to calculate the atmospheric boundary factor

A mass balance approach is then used to calculate the amount of seepage in mm per time step:

$$S = PPT_{act} – Et_{act} – Es_{act} – (\Delta \text{ Soil Storage}) \quad (3.7)$$

where S is the seepage (mm); PPT_{act} is the actual precipitation (mm); Et_{act} is the actual transpiration (mm) and Es_{act} is the actual soil evaporation. The seepage boundary factor can be calculated by forcing the seepage (mm) from the Cum_Q.out file to be equal to the seepage calculated by the above equation.

The surface runoff from the transects can be calculated by taking the cumulative total actual surface flux across the atmospheric boundary (QA) and dividing it by the atmospheric factor obtaining QA in mm per time step. This is manipulated by saying that if there is rainfall, take the QA value and if not zero. The runoff is calculated by subtracting the precipitation from the above statement and not accounting for a negative runoff, as this is not possible.

A time series is produced of the fluxes along the transect, where the actual runoff, seepage, precipitation, transpiration and the evaporation as well as the potential transpiration, evaporation and evapotranspiration rates are calculated. The change in soil moisture (mm per time step) is also included. The potential evaporation and transpiration (mm per time step) are calculated from the QAP and QRP fluxes respectively. The actual evaporation and transpiration (mm per time step) are calculated from the QA and QR fluxes respectively. The potential evapotranspiration (mm per time step) is calculated by combining the potential evaporation and transpiration fluxes.

3.6 Quantification of Water Balance Fluxes for the Weatherley Catchment

The quantification of the fluxes in the water balance was achieved by fitting the simulated output from the ObsNod.out file in HYDRUS-2D to the observed tensiometer and water content data collected at the Weatherley catchment. Once an adequate simulation was accomplished, the output cumulative fluxes from the Cum_Q.out file in HYDRUS-2D were converted into mm for easy manipulation. A cumulative time series was then presented of all the fluxes, from the identified source areas, in the simple water balance approach put forward for the Weatherley catchment to use for transfer function development.

3.7 Transfer Functions combined with Geographic Information Systems (GIS)

The various contributing areas within the Weatherley subcatchment have been delineated, and thus the fluxes of the streamflow components can be utilised to simulate the overall streamflow. The contributing areas are the upslope, wetland and riparian source areas, and these can contribute to streamflow from different aspects, such as quick, slow and baseflow response components and at different profile depths. These various responses can be either components like overland, macropore or groundwater flows or various combinations of each of them. These soil water component fluxes are then useful for the development of a transfer function model for the Weatherley catchment as well as the bigger Mooi River catchment in a future study.

4. PARAMETER SENSITIVITY

In this chapter, the different HYDRUS-2D parameters are discussed and the effect that they have on the capillary pressure head response. Initially, parameters were quantified by ensuring a close correspondence between specific characteristics of a hydrological time series and their observed equivalent, a procedure called parameter optimization (Schulze, 2006). Parameter optimisation was used in this study for estimating the unsaturated soil hydraulic parameters. This inverse method is typically based upon the minimization of a suitable objective function, which expresses the discrepancy between the observed values and the predicted system response (Ŝimůnek *et al*., 1999). In this parameter optimization, a manual approach was used in an iterative type procedure, where the values of one parameter at a time are manually modified and the resulting effect is observed and then repeated by trial and error until a desired degree of precision is obtained (Schulze, 2005). This is a time consuming exercise, particularly using HYDRUS-2D, as it is a multi-parameter model and there is a high degree of interaction between the parameters.

The parameters that are used in the analysis are the residual water content (Θ_r), the saturated water content (Θ_s), the inverse of air entry value or bubbling pressure (α), the pore size distribution index (n), the saturated hydraulic conductivity (Ks), the pore connectivity parameter (l) and one of the Feddes root water uptake parameters, specifically the pressure at which root water uptake ceases (P3). The parameters used in the simulation of LC 1 - 4 are tabulated in Table 4.1.

4.1 Residual Water Content (Θ_r)

Typically, Θ_r represents the point in the Soil-Water Retention Curve (SWRC) where only marginal changes in water content occur with a further increase in the soil's suction and transpiration is initiated. Therefore when Θ_r is lowered, the final water contents of the drying curve of the SWRC are lowered thereby

potentially allowing more transpiration as the soil becomes sandier in nature and releases soil water with more ease.

Table 4.1 Summary of parameters used to simulate transect LC 1 - 4

Base Line Hydrus Parameters in LC 1 simulation are:	
Residual Water Content **(Θ_r)**	0.05
Saturated Water Content **(Θ_s)**	0.49
Inverse of Air Entry Value or Bubbling Pressure **(α)**	0.007
Pore Size Distribution Index **(n)**	1.95
Saturated Hydraulic Conductivity **(Ks)** in mm/hr	50
Pore Connectivity Parameter **(l)**	0.6
Feddes Root Water Uptake Model Parameters:	
Pressure head value below which roots start to extract water from soil **(P0)** in Pa	-10
Pressure head value below which roots can't extract water at max rate **(P2H)** in Pa	-2500
As above, but for a potential transpiration rate **(P2L)** in Pa	-2500
Value of the pressure head below which root water uptake ceases **(P3)** in Pa	-50000

In HYDRUS-2D, if Θ_r is lowered, then the amount of water that can be drained or transpired from the soil is increased, as the portion of plant available water is increased. When the residual water content parameter is lowered, there is a net increase in summer soil water tensions and a net decrease in winter as well as spring.

Conversely, increasing Θ_r causes less water to be drained or transpired from the soil as the portion of plant available water is decreased and the soil becomes more clayey in nature thus not relinquishing the soil water as easily. Raising Θ_r, results in a net decrease in the simulated tensions in the time series.

4.2 Saturated Water Content (Θ_s)

Θ_s represents the point in the Soil-Water Retention Curve (SWRC) which theoretically corresponds to the soils porosity, but is often less than that due to dissolved and entrapped air (Rassam *et al.*, 2003). Therefore when Θ_s is lowered, the final water contents of the wetting curve of the SWRC are lower and this also means that a saturated state is attained sooner. When Θ_s is lowered in HYRUS-2D, the amount of water in the soil is less, as the portion

of plant available water is decreased. On the other hand, raising Θ_s allows more water to be drained or transpired from the soil as the portion of plant available water is increased when the soil becomes sandier and therefore porous in character.

4.3 Inverse Air Entry Value or Bubbling Pressure (α)

Characteristically, α represents the inverse of the critical suction value at which the largest pores in the soil matrix begin to lose water (Rassam *et al.*, 2003). When α is lowered in HYDRUS-2D, much like clay soils, more matric suction needs to take place for the soil to begin draining the largest pores. Once α is raised in HYDRUS-2D, it behaves like a sandier soil, requiring less matric suction to occur out of the soil to begin draining the larger pores and this tendency is true until the soil is drained of all it's available water.

4.4 Pore Size Distribution Index (n)

In HYDRUS-2D, n controls the shape of the SWRC and reflects the pore size distribution. Within the plant available water part of the SWRC graph, a unit increase in matric suction causes more water to be extracted from coarse textured soils than from fine textured soils (Rassam *et al.*, 2003). When n is lowered, the soils become more claylike in nature resulting in a net downward translation of the whole simulated time series. When n is raised, the soils become sandier in nature causing a net upward translation of the whole simulated time series of tensions.

4.5 Saturated Hydraulic Conductivity (Ks)

In HYDRUS-2D, Ks controls the amount of water that the soil is able to absorb and redistribute before the infiltration capacity of the soil is exceeded. If Ks is lowered, the upper soil horizons will remain wetter because of the retarded ability of the soil to redistribute the wetting front. When Ks is raised in HYDRUS-2D, there is an overall net decrease in the simulated time series. If Ks is raised, then the soil will take longer to become saturated with less runoff

occurring, but the soil will be drained much quicker causing the soil to have lower final water contents after wetting cycles due to the additional lateral and vertical flows.

The HYDRUS-2D is a complex model with a large understanding required to utilise it well. It was found to simulate the tensions, the parameters shown in Table 4.1, yielded the best fit to observed tensions. The simulations showed that the most sensitive parameters were the inverse of air entry value or bubbling pressure (α), the pore size distribution index (n) and the saturated hydraulic conductivity (Ks).

5. RESULTS AND DISCUSSION

The results from the modelling conducted and the further analysis of the outputs of the HYDRUS-2D model are presented in this chapter. These include the simulation results from the HYDRUS-2D model viewed comparatively with the tensions and water contents that have been observed at the Weatherley research catchment. The simulation occurs over the period from the beginning of January 2001 to the end of October 2001 and reflects a typical recession from wet to dry season. The primary focus of the study was looking at low flow generation, so macro-pore flow was not seen as important to model accurately. Once the tensions and water contents are adequately simulated, the cumulative fluxes for the afore-mentioned contributing areas (Figures 3.8 and 3.9) are calculated. In addition, seepage fluxes emanating from the hillslopes are reported. These fluxes will be used in developing transfer functions for the soil water discharge response emanating from the hillslopes in future studies, for which this work forms the basis of providing the details.

5.1 Water Retention Characteristics

Laboratory desorption experiments have been carried out in the past on the soil samples taken from the Weatherley catchment (Lorentz *et al.*, 2001) with water retention curves being plotted for the nest sites at different depths along the transects. These data were found to be helpful, but as one increased the area to be modelled from site to hillslope section, the parameters were found to be less and less related as they are very much site and depth specific. However, this was to be expected since a single material type was used to model the entire hillslope section. The HYDRUS-2D model requires residual (Θ_r) and saturated (Θ_s) water content, saturated hydraulic conductivity (K_s), the inverse of bubbling pressure or air entry value (α) and pore size distribution (n) as key input parameters. Achet *et al.,* (2006), who also used the HYDRUS-2D model, noted a discrepancy of several orders of magnitude in soil hydraulic properties between reported laboratory and the best

parameters for the simulated results. Thus the parameters that were calculated from fieldwork do not necessarily correspond to the optimum parameter sets utilised within the model. Nevertheless, the fieldwork is helpful with the Θ_s and Θ_r values, but not that helpful with the alpha and n values and they are therefore only used as an initial guide. An instance of a good fit, using the van Genuchten (1980) hydraulic characteristic relationships, compared to the observed water retention curve and their associated parameters are given in Figure 3.13, but these parameters were found to be inaccurate when modelling the observed hillslope tensions and water contents, so a trial and error exercise took place. The observed water retention curve was thus employed to find the correct combinations of the soil hydraulic properties. Eventually an adequate simulated fit was found for the van Genuchten (1980) retention curve as well as the simulated tensions and water contents in the HYDRUS-2D model. The fitted water retention curve is shown in Figure 3.14.

The laboratory determined water retention characteristics yielded a poor simulation of the tensions as well as the water contents in HYDRUS-2D and the adopted curve was one which best represented the behaviour of the tension time series at each location in the transect. This is due to the laboratory determined characteristics being based on a small sample, and thus mostly the matrix structure is represented with the macropore structure being poorly characterised. This supports what Achet *et al.,* (2002) claimed as a large discrepancy in some soil hydraulic properties between reported laboratory and the best parameters for the simulated results. The complete set of the fitted water retention characteristics used in the modelling with HYDRUS-2D for the other observation station sites is presented in Appendix B.

5.2 Tension and Water Content Modelling Results

The results from the simulation of the observed tensions and water contents are now discussed. A summary of the input menu for the different transects and their unique set of parameters values is presented in Appendix C.

The contributing source areas approach, where response zones are identified, was used in applying the HYDRUS-2D model to the lower catchment area of the Weatherley catchment since this was found to be the best advancement for transfer function development and application. By applying this approach, the contributing sources can be isolated and then disaggregated according to their topographic, hydrologic and pedologic variability that exists among hillslope and riparian areas contributing to a clear, unequivocal differentiation (McGlynn and McDonnell, 2003). This is beneficial in a catchment that has a high degree of heterogeneity with regard to its hillslope characteristics and streamflow generating mechanisms.

In simulating the lower catchment area at Weatherley, three contributing hillslope segments were selected that were considered representative of the lower catchment area hillslopes. These independent response zones have been identified as the transect above the sandstone outcrop containing LC 1-4 of about 190 metres (west facing upper hillslope zone), then below the sandstone outcrop to the stream encompassing LC 5-7 of about 535 metres (west facing wetland and riparian zone) and finally on the far side of the stream LC 8-10 measuring about 410 metres (east facing riparian, wetland and hillslope zone). These three segments encompass all the identified response zones that are represented in Figure 3.9 and described in Table 3.3. The simulations of LC 1 through to LC 4 are described in detail in this chapter, while the remainder are described in Appendix D.

5.2.1 West facing Upper Hillslope Transect (LC 1 to LC 4)

The transect was simulated as a whole hillslope segment, but the results are presented nest by nest. This transect was well simulated as a whole, as can be seen in Figures 5.1 to 5.12, especially considering that only one set of parameters was used in the model setup for this entire hillslope section. The shallow soil horizon (around 400 to 500 mm deep) yielded an excellent agreement between the simulated and observed tension time series, as can be seen in Figure 5.1 and Figure 5.5 respectively, and this shallow soil component would represent the upslope macropore type flow component that

was identified in Figure 3.8 and 3.9 respectively. The simulated tensions at this shallow depth were consistently in agreement with the observed data, with the simulated summer tension time series being especially accurate as can be observed in Figures 5.1 and 5.5 respectively. The winter recession in the tension time series was simulated adequately along with the last part of the simulation with the onset of precipitation in spring. At this depth the simulations at the toe of the slope transect (Figure 5.9), were a little less precise than the simulations at the other three sites (Figures 5.1 and 5.5 respectively as well as the first figure in Appendix D) with the summer, winter and spring simulated values all being a little bit drier than the observed data. This is probably due to the fact that the complexity of the dynamics leading to the build up of seepage water at the toe of a slope is not well translated in the HYDRUS-2D model. The simulated water contents for this depth over the entire hillslope segment were also modelled well (Figures 5.2 and 5.4) except for the site at the toe of the slope segment as seen in Figure 5.10. The simulated water contents in summer showed good variation as a result of frequent wetting and drying cycles due to ample precipitation and long, hot days as can be seen in Figures 5.2 and 5.6 respectively. This is not the case in Figure 5.10 where the wetting and drying cycles are less constant in the simulated time series as in the observed data. The winter recession was uneventful, with a steady decline in simulated water contents. The spring rains caused rapid simulated responses throughout the transect in late September and early October, but the responses lacked the magnitude of the responses observed as can be seen in Figures 5.1, 5.5 and 5.9 respectively.

The deeper soil water component (around 900 to 1000 mm deep) represents flow from perched water tables as well as soil water contributing towards a groundwater component in this transect and the tension time series was simulated adequately. The simulated tensions mimic the observed data well, but the timing of the peaks and troughs were not in sync, due to the simulated response not being sharp or regular enough, as can be observed in Figure 5.7. The tensions in summer respond well to rainfall with the anticipated drop in tension (increase in matric pressure head) and the associated increase during subsequent drying phases occurring, but the peaks and troughs are

delayed as well as the peaks being smaller and the troughs being deeper as can be perceived in Figures 5.3 and 5.7. It can also be noted from Figures 5.3, 5.7 and 5.11, that the wetting and drying cycles were not adequately modelled with the finer fluctuations not being evident in the simulated values. The winter recession was rather monotonous but well modelled as can be observed in Figures 5.3, 5.7 and 5.11. The spring precipitation was poorly modelled, with no response being imminent as can be seen in Figures 5.3, 5.7 and 5.11, where it is noted that the simulated tensions are generally more positive than the observed tensions at the beginning of the simulation. The observed values are difficult to simulate mainly because the crop factors hardly allowed transpiration to take place, due to the frost during the winter months (Schulze, 2006), as well as the roots being incapable of reaching to that depth in the profile and scarcely any evaporation taking place at this depth. Also, the HYDRUS-2D model does not simulate the transference of deeper soil water down the hillslope well in this instance. There is no development of a simulated perched groundwater table at the toe of the slope since only one type of soil being specified, with no change with increasing depth throughout the transect. The net result is that no rapid transfer of water to the toe is simulated, but also because no macropore mechanism was included in the simulation, even though variations in the saturated hydraulic conductivity were experimented with in attaining the final simulated time series, where the saturated hydraulic conductivity was varied from 2 to 200 mm/hr. Thus the complex soil water dynamics are represented quite well, but the lateral interactions of the various processes are not mimicked adequately, as is the problem with models with regard to the B-horizon such as ACRU because of the poor routines for the transference of soil water to deeper horizons through processes such as bypass and lateral flow.

5.2.1.1 Comparison of Simulated Results against Observations at Lower Catchment 1 (LC 1)

The observed tensions and water contents for LC1 at 550 mm deep were simulated well, with the simulated values following the trends of the observed data closely as can be seen in Figure 5.1 between January and May during

summer and also in the spring rainfall response in late September. The simulated tension time series values follow the same close agreement, especially during summer, to the observed data without ever totally encapsulating the smaller fluctuations in tensions, while managing to mimic the overall water dynamics that are present at the site (Figure 5.1).

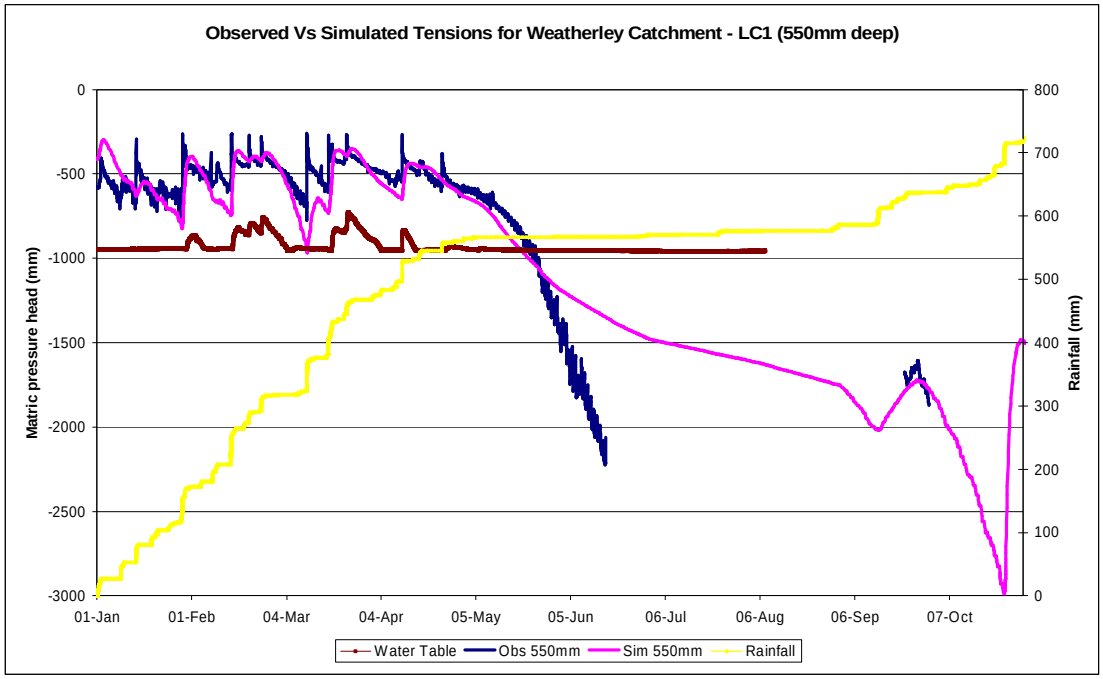

Figure 5.1 Observed vs Simulated Tensions from the HYDRUS-2D model for LC 1 at 550 mm deep (Borehole data is reflected as a depth below surface on the matric pressure head axis).

When the soil gets drier in the summer months, the simulation tends to dry the soil out further than the observed (Figure 5.1 at about 10 March), with the peaks never reaching the highs of the observed data (Figure 5.1 at about 6 February, 15 and 28 March). The observed water table responds with the same timing and frequency, as the observed and simulated tension time series, once the soil has dried considerably as can be noted in Figure 5.1 at about 6 February and 11 April. As can be seen in Figure 5.1, the simulated winter tension time series recession period dries out well initially in May, according to the observed tension data, but then does not mimic the severe drying curve out found in the later winter month of June. This is because the crop factors used in winter are slightly higher than the ones in the literature for

the Highlands sourveld, with some transpiration occurring when the literature indicated none due to the frost (Schulze, 2006). When precipitation takes place again in the spring, the simulation is good with the observed tension data being well represented by the peak in the tension time series as can be seen in Figure 5.1 in late September. This is also due to the crop factors in spring being set lower than the prescribed values in the literature in order to gain the indicated response. The poor observed data were omitted, due to technical problems with the tensiometers, in this period from mid June to the end of September and also from early October until the end of October.

The simulated water contents for LC1 at 550 mm deep performed adequately compared to the observed data, but lacked accuracy during drying phases between the rainfall events with the simulated values showing rapid drying while the observed data indicate a slower drying process (Figure 5.2 at 10 and 29 March as well as at 3 April). There are definite responses to rainfall, which are rapid during the more constant rainfall events of the summer months as can be seen in Figure 5.2 at 3 April. The initial response to the spring rainfall was a little retarded in its magnitude, with the observed data showing far wetter conditions earlier and also larger responses being noted in Figure 5.2 at about 15 September and 22 October. There was a lot of poor observed data from technical problems with the neutron probe at this site and these data were discarded from the observed record, leaving too few data points to be conclusive.

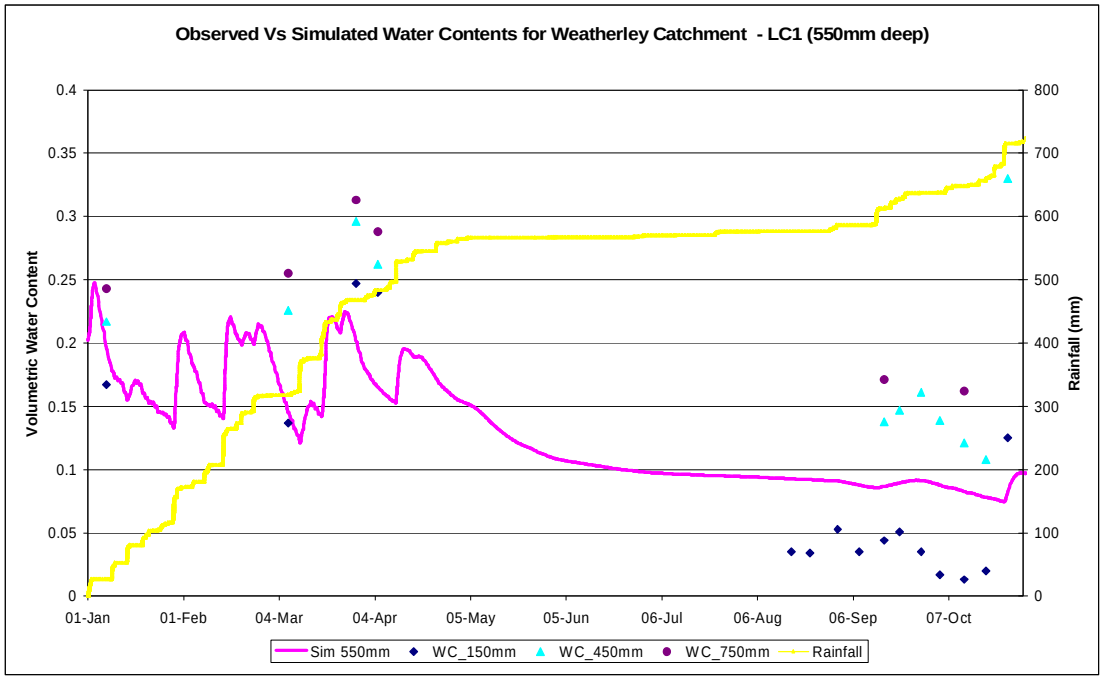

Figure 5.2 Observed vs Simulated Water Contents from the HYDRUS-2D model for LC 1 at 550 mm deep.

The simulation of the observed tensions for LC1 at 1000 mm deep was satisfactory, with the simulated values remaining close to the observed data record as can be seen in Figure 5.3 especially from mid May onwards. The tensions in the summer months did not capture the complex interplay of the water dynamics well as can be perceived from Figure 5.3 from January until mid July, but the values were still in the region of the observed data. The tensions from early to late winter were well simulated, with the simulated recession fitting the observed data, this was due to the crop factors hardly allowing transpiration due to the frost during these months (Schulze, 2006), as well as the roots do not reach to that depth in the profile and scarcely any evaporation takes place at this depth. In spring the simulated values were not well simulated, although there was no good observed data available, with no response being evident in Figure 5.3 from the precipitation events of early September and late October. The water table responded well in respect of the timing and magnitude compared with the observed data in Figure 5.3 at 6 February and 15 as well as 23 March. Periods of erroneous observed data were omitted at this site, due to technical problems with tensiometers, from late March until mid May as well as mid July onwards in Figure 5.3.

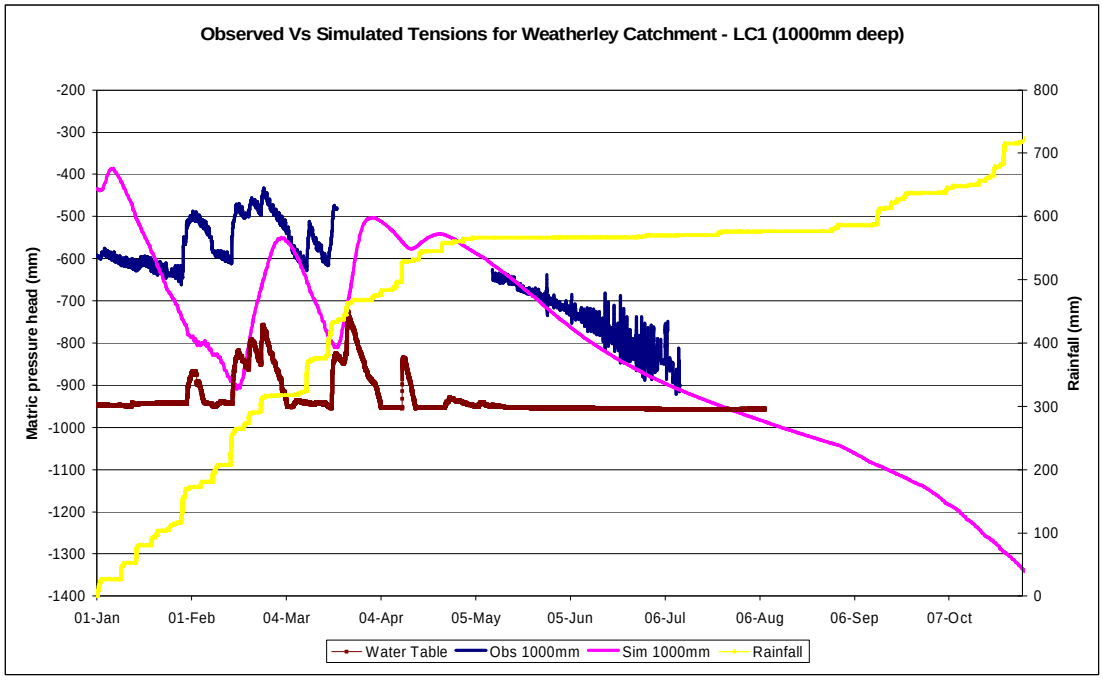

Figure 5.3 Observed vs Simulated Tensions from the HYDRUS-2D model for LC 1 at 1000 mm deep (Borehole data is reflected as a depth below surface on the matric pressure head axis).

The simulated water content values were poor compared to the observed data for LC1 at 1000 mm deep, although the trend is well represented (Figure 5.4). The simulated values responded well to precipitation inputs and were adequately lagged, but were never mimicking the observed data as can be seen at about 9 and 29 March as well as 3 April in Figure 5.4. This is due to the B-horizon being difficult to model using the same parameters as those used for this entire transect, especially when only one soil type was specified and no variation was allowed with the increasing depth. Large amounts of the observed neutron probe data were left out at this site as well due to these being flagged as poor data because the neutron probe was reading the same erroneous observed values for every measurement.

The simulated tension time series for Lower Catchment 2 (LC 2) was put into Appendix D were similar to those discussed in the next section on Lower Catchment 3 (LC 3).

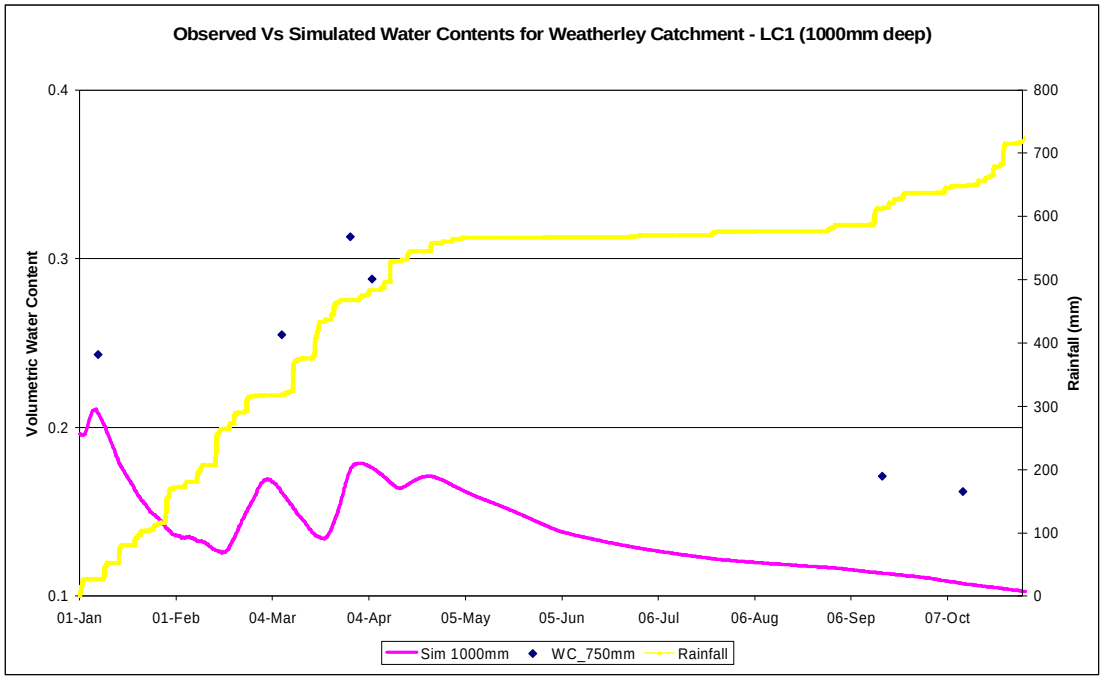

Figure 5.4 Observed vs Simulated Water Contents from the HYDRUS-2D model for LC 1 at 1000 mm deep.

5.2.1.2 Comparison of Simulated Results against Observations at Lower Catchment 3 (LC 3)

The simulation of the transect LC 1 – 4 allows comparisons of responses at LC 3. The simulated tension time series and water content for LC3 at 440 mm deep was excellent, with the simulated values following the tendencies of the observed data. The simulated tension values follow the same trends as the observed data, but never quite take on the smaller fluctuations in tensions (January until Apr in Figure 5.5), although imitating the overall soil water processes that are observed at the site. During the summer months in Figure 5.5, at 10 March for example, the simulation tends to not dry the soil out as much as the observed tension time series, although the shape of the observed data is followed. The peaks during the summer months never reach the amplitude of the observed data as can be seen in Figure 5.5 at 6 February, but once again the general pattern is present. The observed water table responds well with timing and frequency of the simulated data in summer, as can be noticed in Figure 5.5 at 26 February and 14 April, but is more dramatic due to the upslope contributions. There are no water table

responses to the rainfall occurring in the springtime. In the winter recession period, the simulation dries out initially well in May (Figure 5.5), as according to the observed tension data. Thereafter there is no more data for this site as it had to be left out because it was flagged as poor data. Precipitation in spring causes rapid wetting of the profile and the simulated tension time series responds at the onset of even frontal rainfall events of 25 mm with low intensities. There are no observed data to compare with the simulated tension time series.

The simulated water contents for LC3 at 440 mm deep were well modelled when compared with the observed data, but the simulated values were sometimes found to be higher during drying phases of summer and lower in the winter (Figure 5.6 at about 10 March and then during May respectably). There are distinct responses to precipitation in the simulated tension time series, especially to the larger, more regular rainfall events of the summer months as can be noted in Figure 5.6 at 19 March and 11 April. The first simulated responses to the spring precipitation were smaller in magnitude, with the observed data showing slightly wetter conditions earlier and also larger responses being forthcoming at the end of the simulation as can be noted between late September and mid October in Figure 5.6. There were poor observed data from the neutron probe at this site and these data were unused.

The simulation of the observed tensions for LC3 at 990 mm deep was mediocre based on visual analysis, with the simulated values continuing close to the observed data (Figure 5.7). The simulated tensions did not mimic the intricate interaction of the soil water dynamics effectively as can be seen during February in Figure 5.7, but the values still remained close to the observed data.

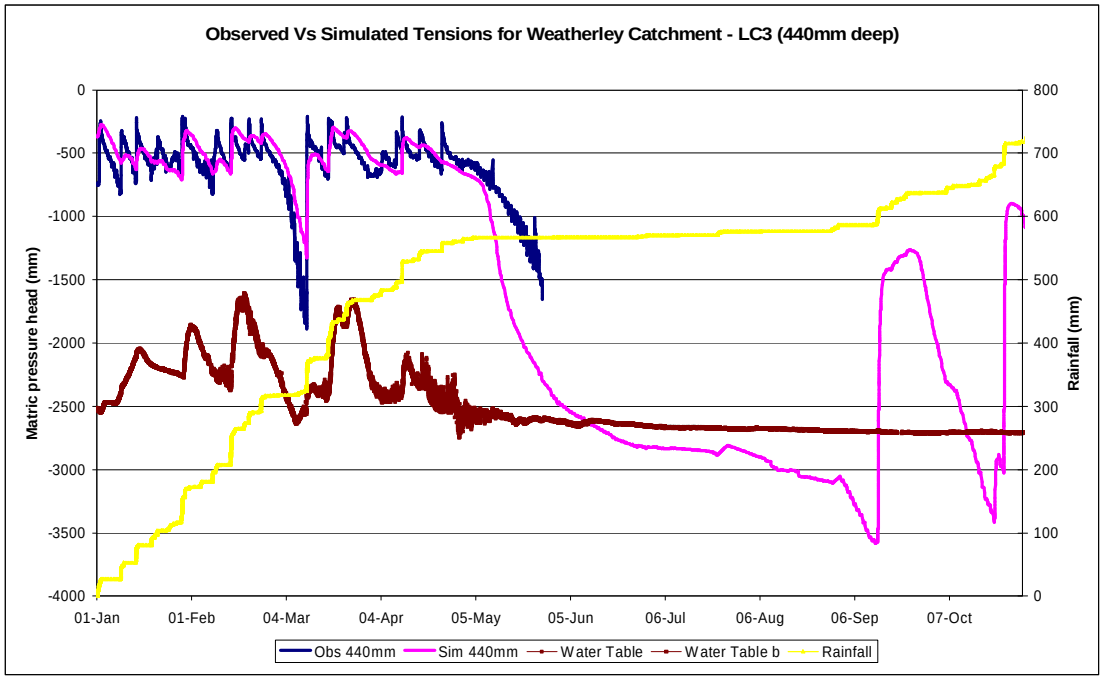

Figure 5.5 Observed vs Simulated Tensions from the HYDRUS-2D model for LC 3 at 440 mm deep (Borehole data is reflected as a depth below surface on the matric pressure head axis).

The peaks and troughs of the simulated values were delayed when compared with the observed data during February and March in Figure 5.7, showing that model was not able to simulate the transference of deeper soil water down the profile and hillslope well. The simulated values being delayed is also due to the B-horizon being complex to model using the identical parameters as those used for this whole transect, especially when only one soil type was specified and no variation was permitted with increasing depth. The tensions for the entire period were over simulated, but not by a great deal, mainly because the crop factors barely permitted transpiration to take place, due to the frost during those months (Schulze, 2006), as well as the roots not being specified at this depth in the profile. The observed water table responded well in respect to the timing and magnitude of the observed tension data. Periods of erroneous observed data were omitted at this site from after May due to these being flagged as poor data.

.

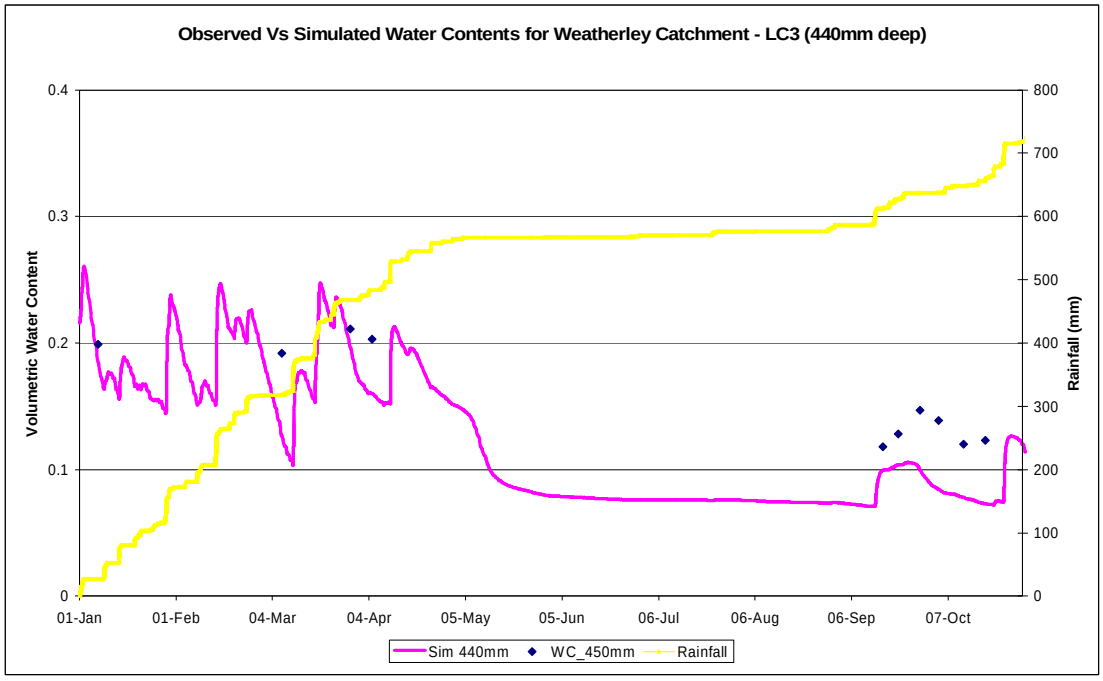

Figure 5.6 Observed vs Simulated Tensions from the HYDRUS-2D model for LC 3 at 440 mm deep.

The simulated water content values were not simulated well when compared with the observed data for LC3 at 990 mm deep (Figure 5.8), as they were grossly under simulated throughout the simulation period. The simulated values responded to rainfall inputs and were predictably lagged, but were certainly not in close agreement with the observed data. This is mainly because the B-horizon is complicated to represent using the same parameters as those used for the entire transect, particularly when only one soil type was specified and no variation was permitted with the increasing depth. A number of the observed neutron probe data were omitted due to these being flagged as poor data because the neutron probe was reading the same erroneous observed values for every measurement.

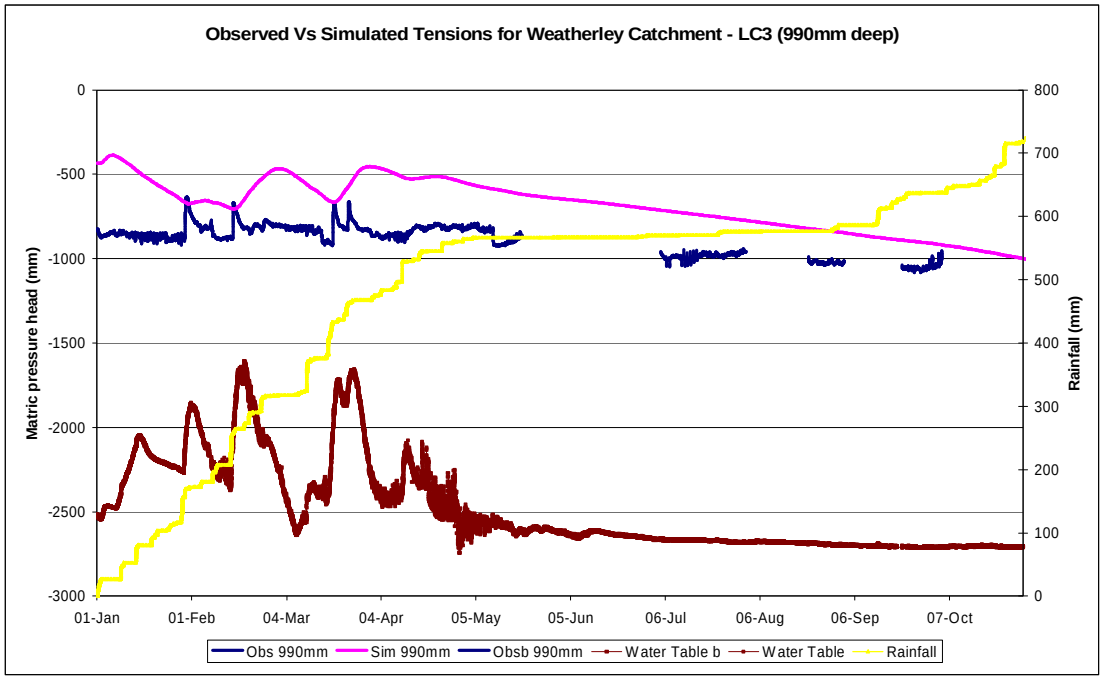

Figure 5.7 Observed vs Simulated Tensions from the HYDRUS-2D model for LC 3 at 990 mm deep.

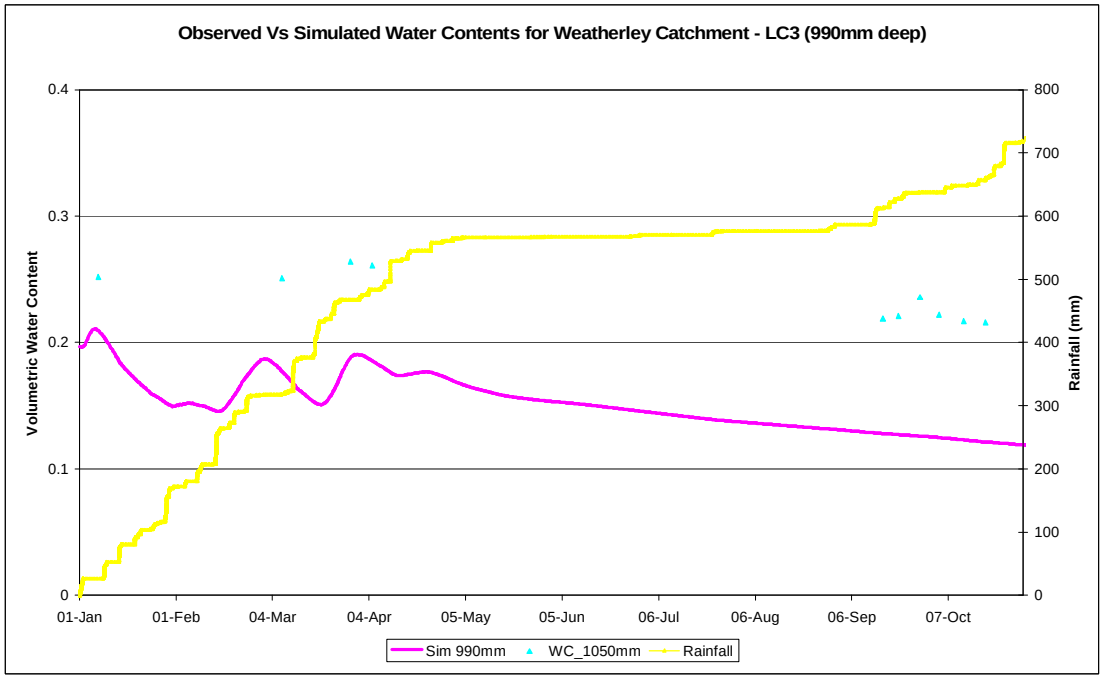

Figure 5.8 Observed vs Simulated Water Contents from the HYDRUS-2D model for LC 3 at 990 mm deep.

5.2.1.3 Comparison of Simulated Results against Observations at Lower Catchment 4 (LC 4)

The simulation of the observed tensions and water contents for LC4 at 440 mm deep was good, with the simulated values mimicking the overall tendencies of the observed data well, but the simulated tension time series was always undersimulated as can be seen in Figure 5.9. The simulated tensions follow similar trends as the observed records, but never mimic the minor fluctuations in tensions, although imitating the overall soil water processes present at the site (Figure 5.9).

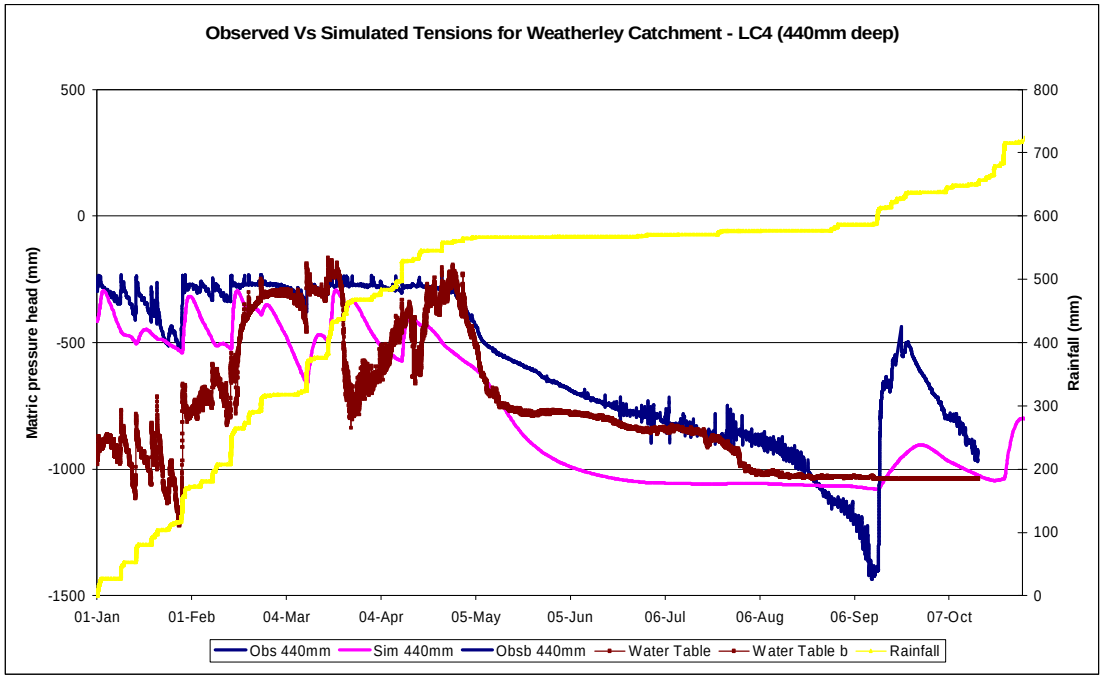

Figure 5.9 Observed vs Simulated Tensions from the HYDRUS-2D model for LC 4 at 440 mm deep.

The simulated values are more pronounced in variation during the summer months, as can be noted at about 3 February and 24 March in Figure 5.9, with the simulated values being drier. The peaks during the summer months never attain the highs of the observed data (Figure 5.9 at about 3 Feb and 24 March), although the drying cycles are so severe that they don't allow the simulated tensions to attain similar peaks as the observed data, but once again the general pattern is present. The troughs in the simulated tension time

series during summer were too deep, compared to the observed data, due to the severe wetting and drying cycles at this location. The water table is well synchronised with the timing and frequency of the simulated data responses, but is more responsive in summer (Figure 5.9) owing to the upslope contributions and because of this, seepage water flows out of the toe of the hillslope for about two months from 16 February until 6 May. In winter, the simulation of the tension time series recession period is satisfactory with the simulated values not quite attaining the degree of wetness of the observed tension data, but overall the trend is similar as can be seen in Figure 5.9 from May until the end of July. During the spring rains, the simulated values respond abruptly but do not reach the level of magnitude of the observed record as can be noticed in Figure 5.9 from mid September. The observed record is good at this site, with hardly any data being unused.

The simulated water contents for LC4 at 440 mm deep poorly modelled compared with the observed data and was once again found to be inaccurate during drying periods (Figure 5.10 at about 7 January and 10 March). There are distinctive responses to rainfall in the simulated water content time series, particularly to the larger, more constant rainfall events of the summer months such as the ones seen in Figure 5.10 at about 12 February, 20 March and 11 April. The initial simulated responses to the spring rainfall were subdued in their magnitude, with the observed data having prevailing wetter conditions earlier and also bigger responses being observed at the end of the simulation as can be witnessed from mid September to October in Figure 5.10. There were lots of poor observed data at this site, which was unused due to these being flagged as poor data because the neutron probe was reading the same erroneous observed values for every measurement.

The simulation of the observed tensions for LC4 at 890 mm deep was mediocre, with the simulated values continuing to be proximal to the observed data (Figure 5.11). The simulated tensions did not represent the involved relationships of the soil water dynamics efficiently. The peaks and troughs of the simulated values were lagged compared with the observed data as seen in Figure 5.11 at about 20 February, showing that model was unable to

simulate the movement of deeper soil water along the hillslope section and down the soil profile adequately. The simulated values being lagged is owing to the B-horizon being complex to model using the same parameters to model the entire transect, especially when only one soil type was specified and no variation was permitted with the increasing depth. The simulated tensions for the summer months were drier than those of the observed data record as can be noticed from January until April in Figure 5.11. The tensions for the winter and spring period were over simulated, which is noticeable in Figure 5.11 from May onwards, mainly because the crop factors scarcely allowed transpiration to take place, owing to the frost during those months (Schulze, 2006), as well as the roots not being specified to that depth in the soil profile and barely any evaporation thus taking place at this depth. The observed water table responded to the precipitation events with the timing being similar in comparison with the observed tension data as seen on 12 February in Figure 5.11, but the connectivity of the groundwater is periodic, depending on upslope contributions. Most of the observed data record were utilised for this site and depth.

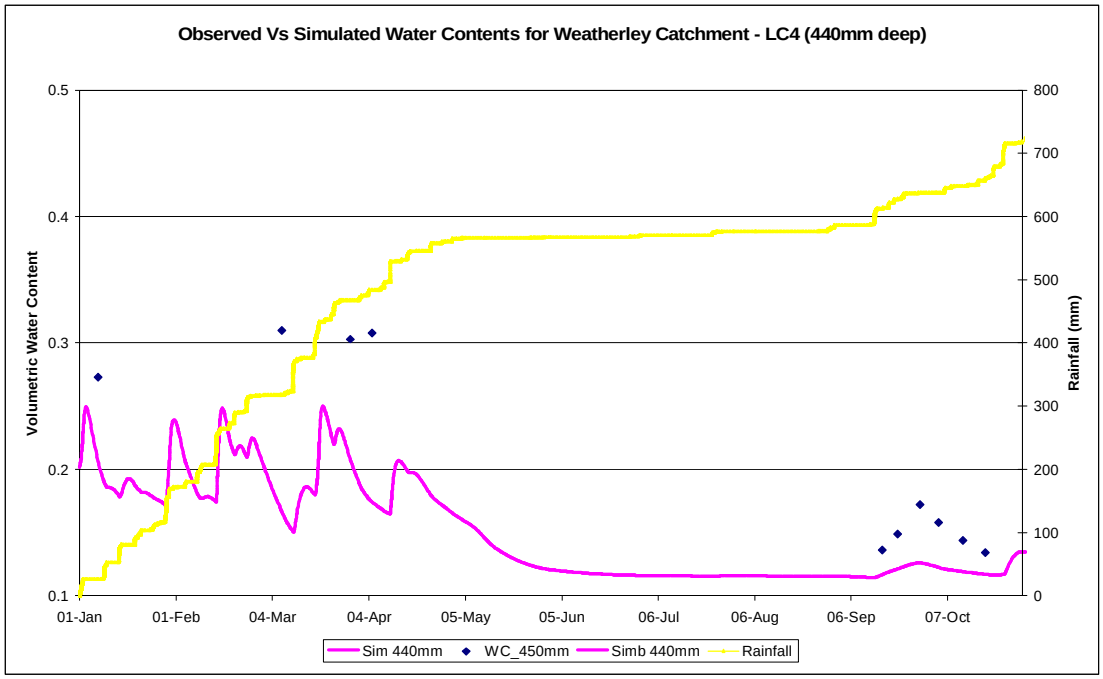

Figure 5.10 Observed vs Simulated Water Contents from the HYDRUS-2D model for LC 4 at 440 mm deep.

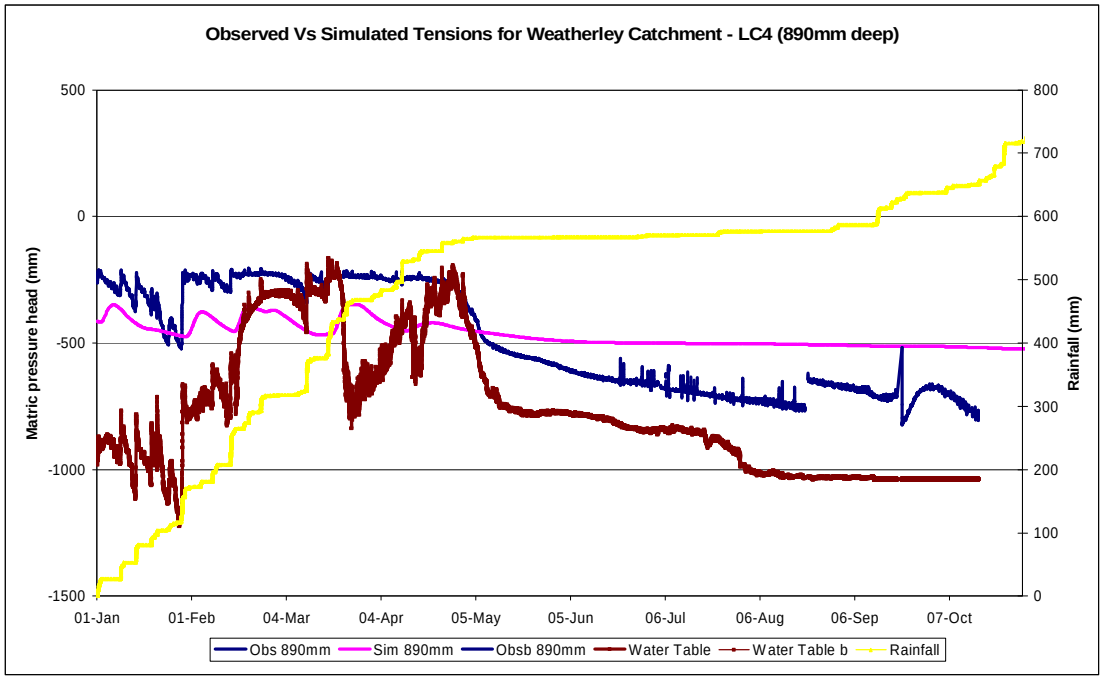

Figure 5.11 Observed Vs Simulated Tensions from the HYDRUS-2D model for LC 4 at 890 mm deep.

The simulated water content values were not well simulated compared with the observed data for LC4 at 890 mm deep (Figure 5.12). The simulated values responded well to rainfall inputs and were predictably lagged, as can be seen at about 6 February and 30 March in Figure 5.12, but were never in close approximation with the observed data. This is because the B-horizon is difficult to model using the same parameters as those used to model the whole transect, especially when only one soil type was specified and no variation was permitted with the increasing depth. There was no simulated response to the winter recession or spring rains at this depth. Large quantities of the observed neutron probe data were left out at this station due to being flagged as poor data.

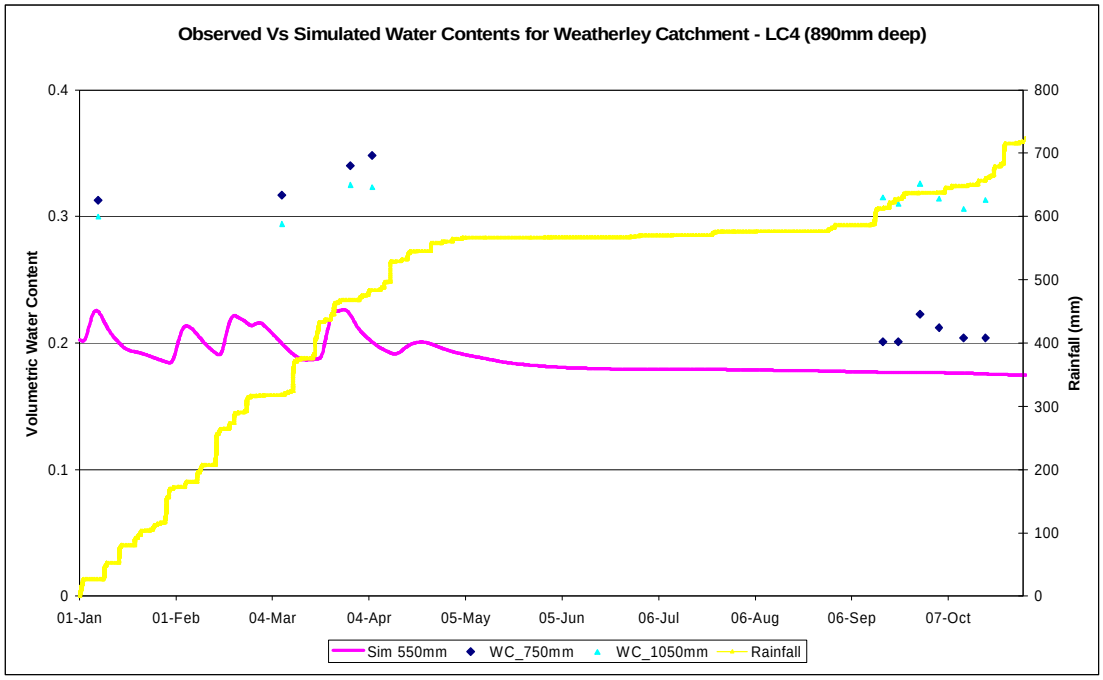

Figure 5.12 Observed Vs Simulated Water Contents from the HYDRUS-2D model for LC 4 at 890 mm deep.

5.2.2 West facing Wetland Transect (LC 5 to LC 7)

This transect was adequately simulated, but the simulated tension time series does not show the interaction of the complex processes accurately and the simulated values are not in close agreement with the observed data as can be seen in Appendix D in Figures D.7 through to D.17 respectably. This is acceptable for a first attempt at modelling with HYDRUS-2D, particularly taking into consideration that merely one set of parameters was utilised in the model setup for this whole hillslope section. The shallow soil horizon (around 300 to 500 mm deep) was modelled well and this shallow soil component would represent the wetland macropore type flow component that is identified in Figures 3.8 and 3.9 respectively. The simulated tensions at this shallow depth were in close agreement with the observed data, with the summer tensions being especially well modelled as can be seen in Figure D.13 from January through until April. The simulated values for this depth at LC 6 were moderately mimicked, with the simulated tension time series not being in close agreement to the observed values. This was mainly due to the variable flux boundary condition that was included to account for the seepage flows

coming from the above hillslope transect. Prior to the inclusion of the variable flux boundary condition at the expense of an atmospheric boundary condition, the simulated values were poorly mimicked. The simulated water contents at this depth were not modelled well.

The deeper soil water component (around 740 to 900 mm deep) represents flow from perched water tables as well as soil water contributing towards a marsh groundwater component in this transect and this was simulated with mediocrity based on a visual comparison. The agreement between the simulated tension time series and the observed data was not good as well as the interactions of the subsoil not being entirely captured as can be perceived in Appendix D in Figures D.7 and D.15. The simulated tension time series for this deeper soil water component were not good, considering the timing of the peaks (14 February in Figure D.15) and troughs (14 February in Figure D.7 as well as the 3 February in Figure D.15) were out of phase. The summer tension time series at LC 7 responded well to rainfall, as can be seen in Figure D.15 at about 18 March and 3 April, with the associated lagging taking place but the tensions at LC 5 did not respond to mimic the observed data. The winter recessions in the simulated time series for LC 5 and LC 7 were uneventful, but well modelled with a steady decline in tension being noted in Figures D.7 and D.15 respectably. The spring precipitation resultant tensions were poorly modelled at LC 5 and LC 7, with no response being forthcoming (Figures D.7 and D.15) where it is noted that the simulated tensions are generally wetter than the observed tensions at the beginning of the simulation. The observed values are difficult to simulate mainly because the crop factors hardly allowed transpiration to take place, due to the frost during the winter months (Schulze, 2006), as well as the roots being incapable of reaching to that depth in the profile and scarcely any evaporation having taking place at this depth. In addition, the HYDRUS-2D model does not simulate the conveyance of deeper soil water down the hillslope suitably in this instance, since there is no perched groundwater table because only one soil material was specified and there was no change in soil properties with increasing depth throughout the transect. The net result is that no rapid transfer of water to the toe is simulated, because no macropore mechanism was included in

the simulation, even though variations in the saturated hydraulic conductivity were experimented with in attaining the final simulated time series. Consequently the intricate soil water dynamics are characterized fairly well, but the interactions of a variety of the processes are not mimicked sufficiently, as is the predicament with a lot of models when considering the B-horizon.

The deep soil water component (more than 1100 mm) characterizes flow from the perched water tables as well as soil water contributing towards a marsh groundwater component in this transect and this was simulated tolerably. The simulated tension time series for this deep soil water component were good, with the simulated values being in close proximity with the observed data especially from mid April until the end of July in Figures D.9 and D.17 respectively. The summer tension time series did not respond well to precipitation, with the wetting and drying cycles amplitude and frequency not being captured well as can be seen in Figures D.9 and D.17 respectively, probably due to the deep soil water component being modelled inadequately for the aforementioned reasons. The winter recession was modelled moderately, with a steady decline in tension being noted, but not to the magnitude of the observed data as can be noted in Figures D.9 and D.17 respectively from mid April to July. The spring rainfalls ensuing tensions were inadequately modelled, with no response occurring.

This proved to be the most difficult of the transects to model, due to the detached upslope contributions and the different flow generating mechanisms that occur within a wetland with different amounts and intensities of rainfall as well as the varying antecedent moisture conditions. Thus, the amount of seepage water exiting transect LC 1 – 4, was added in tiny daily increments over the whole simulation period to transect of LC 5 – 7. According to McGlynn and McDonnell (2003), further intricacy arises since the source areas alter size and shape depending on whether additional precipitation occurs on the rising or the falling limb of the hydrograph, thereby expanding the irregular interface between the hillslope and riparian areas in headwater catchments. The antecedent soil water conditions also control various

patterns and dynamic responses, more than ever in semiarid, mountainous areas (Grant *et al.*, 2004).

The simulated tension time series and water contents for Lower Catchment 5 (LC 5) through to Lower Catchment 7 (LC 7) were included in Appendix D.

5.2.3 East facing Hillslope and Wetland Transect (LC8 to LC10)

This transect was simulated well based on visual comparison, except for the simulation in spring, particularly taking into thought that just one set of parameters was used in the model scenario for this entire segment (Figures D.18 through to D.33). The shallow soil horizon (around 400 to 550 mm deep) was well modelled. This shallow soil component would characterize the wetland macropore type flow component from groundwater rising as well as from slow unsaturated redistribution of the soil water to the bedrock with delivery of unsaturated water to the lower slopes and these are identified in Figures 3.8 and 3.9. The simulated tension time series at this shallow depth showed a close agreement with the observed data, with the summer tensions being accurate. The timing of the peaks and troughs in summer is good at LC 10 where no upslope water interferes with the contributions and therefore the lagging of the flow dynamics, but the simulated tensions are over simulated. The simulated values for this depth at LC 8 and LC 9 were reasonably modelled, but were mostly under simulated with the general shape following that of the observed data record well. The winter recession period was adequately mimicked, with the trends being followed. With the onset of the spring rains, the responses vary from each site at this depth. At LC 8 (Figure D.18), there is no response, whereas at LC 9 (Appendix D) there are sharp responses to the rainfall inputs but they never reach the magnitude seen in the observed data. At LC 10 (Figure D.28), the response is initially poorly modelled, although it does intensify towards the end of the simulation, and again does not attain the magnitude noted in the observed record. The simulated water contents at this depth were not modelled well, except for those in summer at LC 10.

The deeper soil water component (around 800 to 900 mm deep) represents slow unsaturated redistribution of soil water to the bedrock with delivery of unsaturated water to the lower slopes as well as soil water contributing towards a marsh groundwater component in this transect, as summarised in Figures 3.8 and 3.9 respectively. This deeper soil water component was simulated adequately based on visual comparison with the observed values. The simulated tensions for this deeper soil water component were well modelled, with the simulated values being in close proximity to those of the observed data, but the peaks and troughs were not in phase. The summer tensions at LC 8 and LC 9 responded well to large precipitation events, with the expected lagging occurring but both locations were slightly under simulated. The tensions at LC 10 responded favourably, but the responses occurred more rapidly and in tandem with the observed data but were over simulated. The winter recession period was non-responsive, with a steady decline in tension being fairly well modelled. The spring rainfalls ensuing tensions were ineffectually simulated, with no response being simulated, but this is perhaps due to the soil horizons not yet being saturated enough at this period of the simulation. This is predominantly because the crop factors scarcely permitted transpiration to occur, owing to the frost throughout those months (Schulze, 2006), as well as the roots being specified to not reach that depth in the profile and thus barely any evaporation takies place at this depth. Also, the HYDRUS-2D model does not replicate the transference of deeper soil water down the hillslope and the soil profile properly in this simulation because only one soil material was specified and there was no change of water retention characteristics with increasing depth in the transect. Consequently the complex soil water dynamics are represented reasonably well, but the relationships of a variety of the processes are not simulated satisfactorily, as is the dilemma with a lot of models when considering the deeper B-horizon.

The deep soil water component (more than 1300 mm) typifies the slow unsaturated redistribution of soil water to the bedrock as depicted in Figures 3.8 and 3.9 respectively, with considerable wetting to the deep horizons and slow delivery of unsaturated water to the lower slopes in this transect

occurring. This deep soil water component was simulated acceptably, based on visual comparison with the observed values. The simulated tensions for this deep soil water component were well modelled, with the modelled values being in close proximity to the observed data record. The summer tensions responded to larger precipitation events as can be seen in Figures D.22, D.27 and D.32 in Appendix D respectably, but the responses were predictably lagged and at times the simulation responded too dramatically. The winter recession was modelled well, with a stable decline in tension being noted in close proximity to the observed data. The spring rainfalls ensuing tensions were insufficiently simulated, with no response taking place.

The simulated tension time series and water contents for Lower Catchment 8 (LC 8) through to Lower Catchment 10 (LC 10) were included in Appendix D.

The simulated tensions were compared against the observed tensions for each of the sites, at the same times, to produce a goodness of fit statistic. These statistics are discussed in the next sub-section.

5.3 Goodness of fit Statistics

The simulated tensions were matched up against the observed tensions for each of the tensiometer sites at their respective depths, at the same times, to generate a goodness of fit statistic which is shown in Table 5.1. From the table it is clear that some of the locations at certain depths have been simulated well (Lower Catchment 1 at 550 mm deep) and other locations were poorly simulated (Lower Catchment 1 at 1000 mm deep). It can be seen from looking at the table that, at certain locations, at various depths, the simulation shows that some valuable lessons and parameterizations have been achieved. Conversely, at other locations and depths, the simulation shows that further studies need to be done, in order to achieve the desired simulation accuracy.

Table 5.1 Goodness of fit statistics of the simulated hillslope sections

	R^2	n
Lc1 at 550mm deep	0.84	36
Lc1 at 1000mm deep	0.16	28
Lc2 at 450mm deep	0.23	13
Lc2 at 840mm deep	0.96	34
Lc2 at 2040mm deep	0.16	52
Lc3 at 440mm deep	0.5	35
Lc3 at 990mm deep	0.42	37
Lc4 at 440mm deep	0.83	56
Lc4 at 890mm deep	0.76	57
Lc5 at 740mm deep	0.00002	39
Lc5 at 1280mm deep	0.62	57
Lc6 at 320mm deep	0.61	52
Lc7 at 460mm deep	0.73	41
Lc7 at 880mm deep	0.25	34
Lc7 at 1100mm deep	0.52	53
Lc8 at 490mm deep	0.57	56
Lc8 at 820mm deep	0.64	54
Lc8 at 1450mm deep	0.08	48
Lc9 at 440mm deep	0.62	42
Lc9 at 850mm deep	0.86	59
Lc9 at 1300mm deep	0.67	48
Lc10 at 530mm deep	0.14	42
Lc10 at 830mm deep	0.2	50
Lc10 at 1390mm deep	0.42	50

5.4 Cumulative Contributing Hillslopes Flux Results

This section contains the cumulative flux results from the contributing hillslopes identified in Chapter 3. The results were obtained from the Cum_Q.out file from the HYDRUS-2D output and these cumulative fluxes are then converted to mm by dividing the flux values by a factor that is dependent on the geometry of the represented transect. This factor is different for each of the hillslope sections and also for the seepage area at the toe of the hillslopes. In these graphs of cumulative fluxes, the actual soil evaporation; the potential soil evaporation; the potential transpiration; the actual transpiration; the rainfall; the potential evapotranspiration; the runoff; the seepage and the change in soil moisture are presented. A table summarising the contributions of the different components as a percentage of the rainfall is presented below in Table 5.2.

Table 5.2 Contributions of the different cumulative fluxes for the various transects

Contributions from Different Components as % Rainfall **% Cum Discharges for Whole Period**									
Transect	Component	**Rainfall**	**Act Soil Evap**	**Pot Soil Evap**	**Act Trans**	**Pot Trans**	**Pot EvapoTrans**	**Runoff**	**Seepage**
LC 1 - 4	Cum Flux (mm)	725.1	388.7	716.9	279.6	287.2	1004.1	0	162.5
	% of Rainfall		53.6	98.9	38.6	39.6	138.5	0	22.4
LC 5 - 7	Cum Flux (mm)	725.1	390.6	709.3	284.0	285.2	994.6	0	169.1
	% of Rainfall		53.9	97.8	39.2	39.3	137.2	0	23.3
LC 8 - 10	Cum Flux (mm)	725.1	371.5	677.9	273.6	284.7	962.6	0	193.1
	% of Rainfall		51.2	93.5	37.7	39.3	132.8	0	26.6
% Cum Discharges for Summer Period (January - April and October)									
Transect	Component	**Rainfall**	**Act Soil Evap**	**Pot Soil Evap**	**Act Trans**	**Pot Trans**	**Pot EvapoTrans**	**Runoff**	**Seepage**
LC 1 - 4	Cum Flux (mm)	652.4	273.7	331.3	261.6	265.9	597.2	0	81.7
	% of Summer Rainfall		42.0	50.8	40.1	40.8	91.5	0	12.5
	% of Total Rainfall	90.0	37.8	45.7	36.1	36.7	82.4	0	11.3
LC 5 - 7	Cum Flux (mm)	652.4	280.5	318.2	263.8	264.2	582.3	0	107.3
	% of Summer Rainfall		43.0	48.8	40.4	40.5	89.3	0	16.5
	% of Total Rainfall	90.0	38.7	43.9	36.4	36.4	80.3	0	14.8
LC 8 - 10	Cum Flux (mm)	652.4	265.8	313.4	252.9	263.2	576.5	0	138.0
	% of Summer Rainfall		40.7	48.0	38.8	40.3	88.4	0	21.1
	% of Total Rainfall	90.0	36.7	43.2	34.9	36.3	79.5	0	19.0
% Cum Discharges for Winter Period (May - September)									
Transect	Component	**Rainfall**	**Act Soil Evap**	**Pot Soil Evap**	**Act Trans**	**Pot Trans**	**Pot EvapoTrans**	**Runoff**	**Seepage**
LC 1 - 4	Cum Flux (mm)	72.7	115.0	385.6	18.0	21.3	406.8	0	80.8
	% of Winter Rainfall		158.2	530.4	24.7	29.2	559.6	0	111.1
	% of Total Rainfall	10.0	15.9	53.2	2.5	2.9	56.1	0	11.1
LC 5 - 7	Cum Flux (mm)	72.7	110.1	391.2	20.1	21.1	412.3	0	61.8
	% of Winter Rainfall		151.4	538.1	27.7	29.0	567.1	0	85.0
	% of Total Rainfall	10.0	15.2	54.0	2.8	2.9	56.9	0	8.5
LC 8 - 10	Cum Flux (mm)	72.7	105.7	364.5	20.7	21.5	386.1	0	55.2
	% of Winter Rainfall		145.5	501.5	28.5	29.6	531.1	0	75.9
	% of Total Rainfall	10.0	14.6	50.3	2.9	3.0	53.2	0	7.6

Table 5.2 is useful as it outlines the water distribution in the catchment as a percentage of the rainfall within the simulation period. The contributions from the different flux components are graphically presented below for the whole period (Figure 5.13). The potential evapotranspiration is highest for LC 1 - 4, therefore more water should be lost from the transect by actual evaporation and transpiration causing there to be less water in the soil, thereby reducing the amount of seepage flowing from the toe of the slope. This is correct except that LC 5 - 7 actually evaporates and transpires more water, due to their being more readily available water in the larger wetland and riparian area than at top of the hillslope, thereby allowing the actual evaporation and transpiration to be driven accordingly. Therefore LC 1 - 4 has less seepage occurring from the transect than LC 5 - 7 as well as less actual evaporation and transpiration; so then more water is being stored proportionally in that transect of the catchment. The potential evapotranspiration, actual evaporation as well as the actual transpiration are the lowest in LC 8 - 10, meaning that there is more opportunity for either seepage or soil moisture storage to occur, hence that this transect has the most seepage occurring proportionally in the catchment. LC 8 -10 has the exact same amount of potential transpiration as LC 5 - 7, but LC 5 – 7 has more actual transpiration occurring from it which can only be explained by there being more wetland and riparian area allowing more transpiration to occur because of their being more plant available water. It is also interesting to note that the actual evaporation is only half that of the potential evaporation due to there not being enough readily available water to satisfy the evaporative demands. There is no runoff occurring from any of the transects, meaning that the soil continued infiltrating water because the saturated hydraulic conductivity could not be lowered enough without causing numeric instability within the model output.

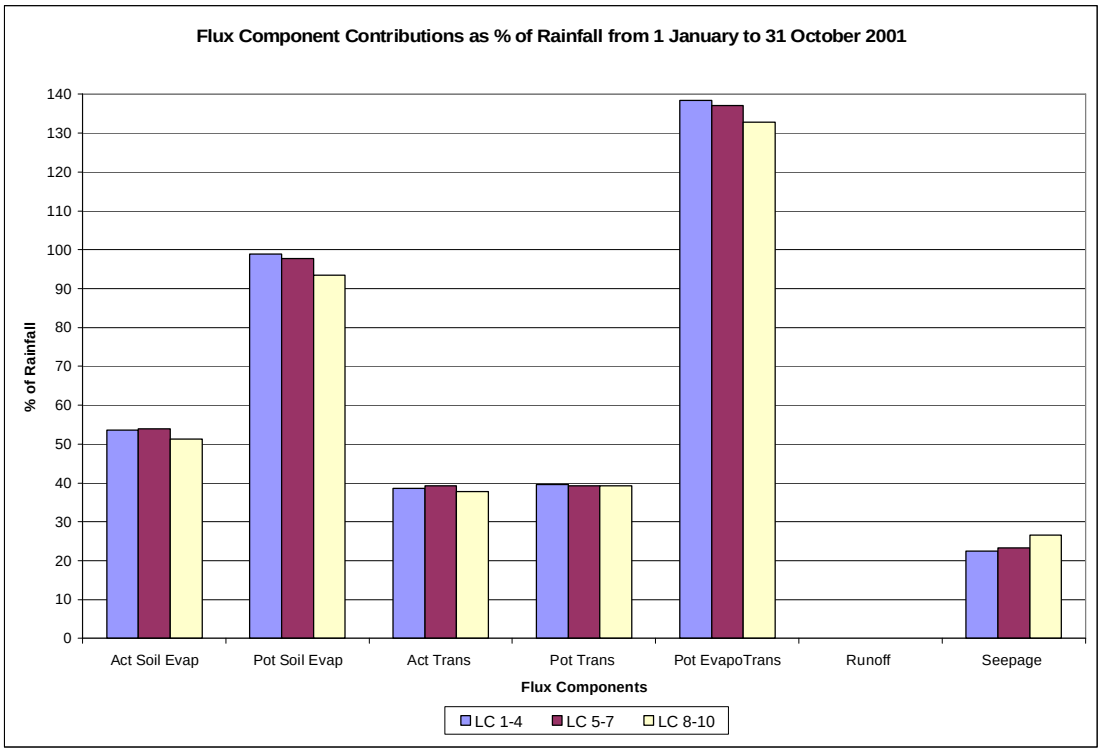

Figure 5.13 Flux component contributions for entire simulation period.

Table 5.2 also separates the contribution percentages of the various components of flow for the simulation period into high flow months (January to April as well as October) and low flow months (May to September). The contributions from the different flux components are graphically presented below for the high flow period from January to April and also including October 2001 (Figure 5.14). Once again in the high flows partitioning of the components, the potential evapotranspiration is highest for LC 1 - 4, consequently more water should be lost to the atmosphere from the transect by actual evaporation and transpiration which results in there to be less water in the soil profile thus decreasing the amount of seepage flowing from the toe of the slope. Again this is all true except that LC 5 - 7 actually evaporates and transpires more water, but this is owing to their being additional readily available water in the greater wetland and riparian area than in the upslope area, thus permitting the actual evaporation and transpiration to be driven accordingly.

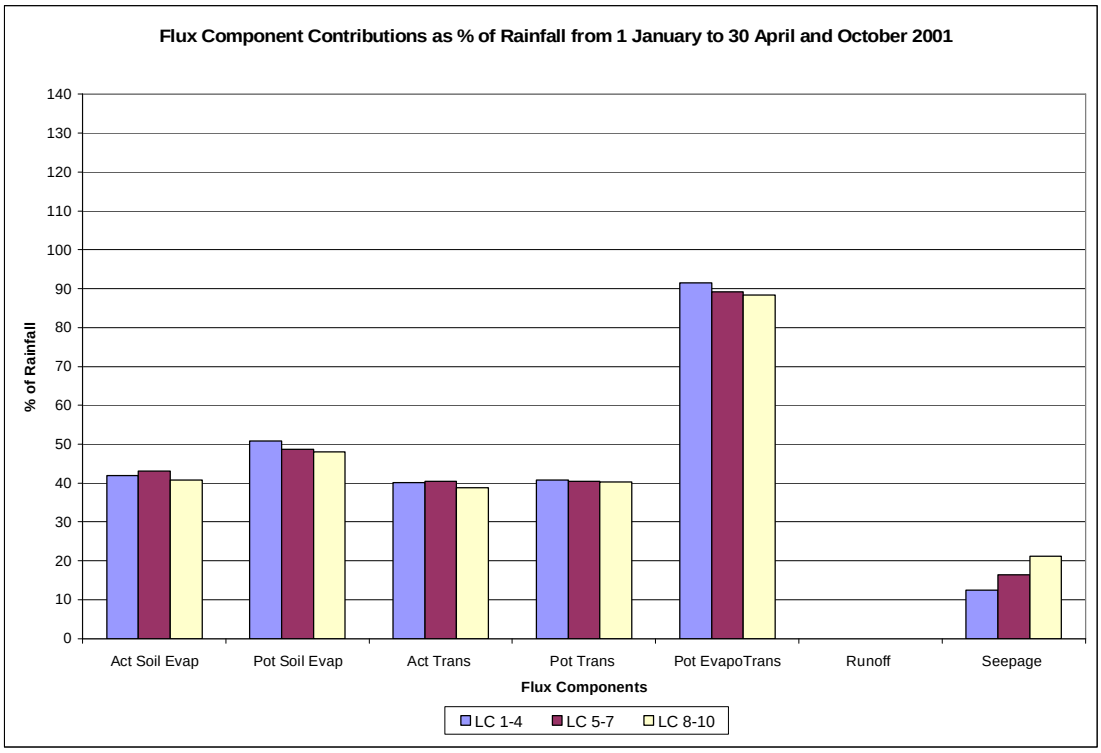

Figure 5.14 Flux component contributions for the high flow simulation period

Thus LC 1 - 4 has a lesser amount of seepage taking place from the transect than LC 5 - 7 as well as less actual evaporation and transpiration; therefore more water is being stored proportionally in that transect of the catchment. The potential evapotranspiration, actual evaporation as well as the actual transpiration are also the lowest in LC 8 - 10 for the high flows partitioning of the components, signifying that there is more likelihood of either seepage or soil moisture storage occurring, hence this transect has the most seepage occurring proportionally in the catchment again. In the partitioning of the high flow components, it can be noticed that all the transects have almost precisely the same amount of potential transpiration taking place, but LC 5 - 7 has more actual transpiration occurring which supports that the wetland and riparian area permits more transpiration to take place because of their being additional plant available water. The proportions of seepage flow from the various transects calls for some discussion, as the seepage from LC 1 - 4 is far less proportionately than that of LC 5 - 7 and LC 8 - 10 meaning that more water is stored in the soil during the high flows in this transect.

The contributions from the different flux components are graphically presented below for the low flow period from May to September 2001 (Figure 5.15). The actual evaporation is less than a third of the potential evaporation showing that the there is not enough readily available water to satisfy the high evaporative demands during times of low flows. The potential evaporation of LC 1 - 4 is lower proportionately to LC 5 - 7 during times of low flows, which is perhaps due to LC 1 - 4 being west facing and in winter the amount of solar energy is not enough to drive the potential evaporation as in the summer. The potential and actual transpiration during the low flow are very low proportionately because there is less plant available water in all the transects. The seepage in times of low flows are interesting, as the seepage from LC 1 - 4 is greater than the other transects, which is the opposite way round from Figures 5.13 and 5.14 respectively. The seepage from LC 5 - 7 is also more than that from LC 8 - 10, due to there being approximately 160 mm being added to transect LC 5 - 7 through a variable flux boundary condition to simulate the transference of the seepage water from the upslope transect of LC 1 - 4. This inversion of the seepage flow amounts is probably because LC 1 - 4 did not deliver as much seepage water as the other transects during the high flow months and therefore stored more water which got released from the hillslope to sustain the streamflow during times of low flow. The residence times of the upslope soil water would also be longer with the stored soil water only emerging from the hillslope as seepage flow during the winter period.

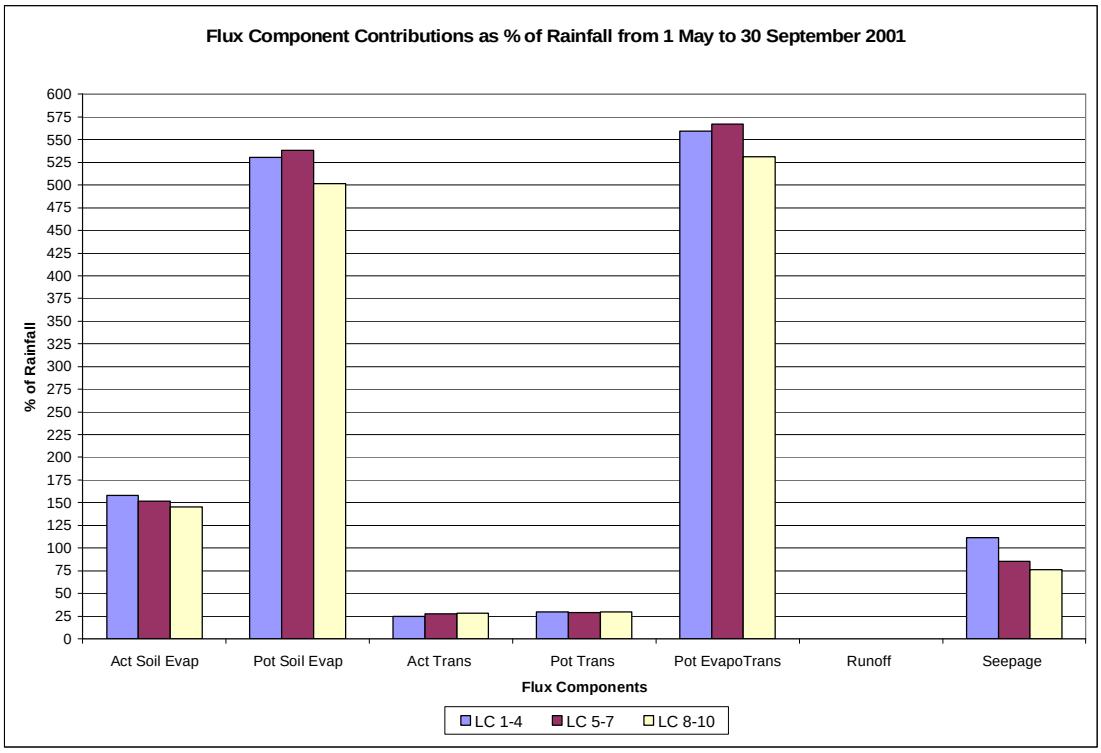

Figure 5.15 Flux component contributions for the low flow simulation period

5.4.1 Cumulative fluxes for the West facing Upper Hillslope Transect (LC 1 to LC 4)

The fluxes for this transect can be seen in Figure 5.16. There is no runoff from any of the transects because the HYDRUS-2D model is not sufficiently capable of taking the rainfall intensities into account properly; the model not being able to run adequately without the specified saturated hydraulic conductivity being very high, thereby requiring more intense precipitation events to produce runoff and the runoff exits the transect by way of seepage instead. The seepage is quite uniform in its flow out of this transect, which is not realistic, but there is a lot of seepage (about 165 mm) which suggests that some of the water that would have been surface runoff has emerged as seepage water from the transect. The change in soil moisture displays prominent changes during the summer after large, intense rainfall events, as can be seen at about 12 and 20 February, with a steady decline occurring in winter and a series of rather subdued springtime responses taking place from mid September onwards. The cumulative actual and potential transpiration fluxes are constantly shadowing each other with the final actual transpiration

cumulative flux being about 280 mm, with the cumulative potential transpiration flux being slightly higher for most of the simulation. The cumulative potential soil evaporation flux follows the cumulative actual soil evaporation flux closely, but remaining slightly above, until about mid May when the cumulative actual soil evaporation flux flattens out with the arrival of the winter temperatures.

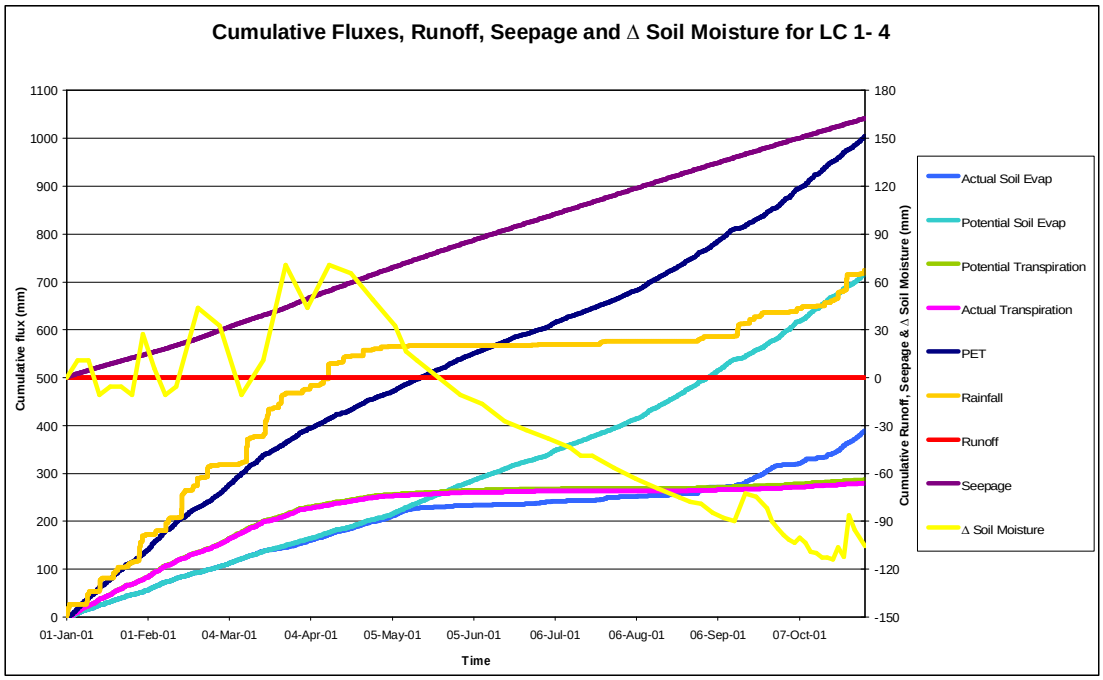

Figure 5.16 Cumulative Fluxes, Runoff, Seepage and Δ Soil Moisture for the transect of LC 1 - 4.

5.4.2 Cumulative fluxes for the West facing Wetland Transect (LC 5 to LC 7)

The cumulative fluxes, runoff and seepage flows for this transect can be seen in Figure 5.17. The seepage component's magnitude is slow initially in January and February in its flow out of this transect until the beginning of March, with advent of large, intense precipitation events (10 and 17 March) and high soil moisture values, a rapid increase in magnitude occurring until midway through May where it begins to taper off until the end of the simulation. The soil moisture exhibits less pronounced variation during the summer after large, intense rainfall events, as can be seen at about 12 and 20

February, compared with the fluxes of LC 1 - 4. In winter there is initially a rapid decline in soil moisture due the decrease in the amount of seepage flowing through from the upslope area and then a steady decline for the rest of the winter recession. There is a response to the spring rainfall but the response is only to larger rainfall events and is somewhat dampened. The cumulative actual and potential transpiration fluxes are continually close to each other with the final actual transpiration cumulative flux being about 284 mm, with the cumulative potential transpiration flux being a little higher for most of the simulation. The cumulative potential soil evaporation flux shadows the cumulative actual soil evaporation flux strongly, but remains slightly higher than it until about mid May when the cumulative actual soil evaporation flux levels out with the onset of the winter temperatures.

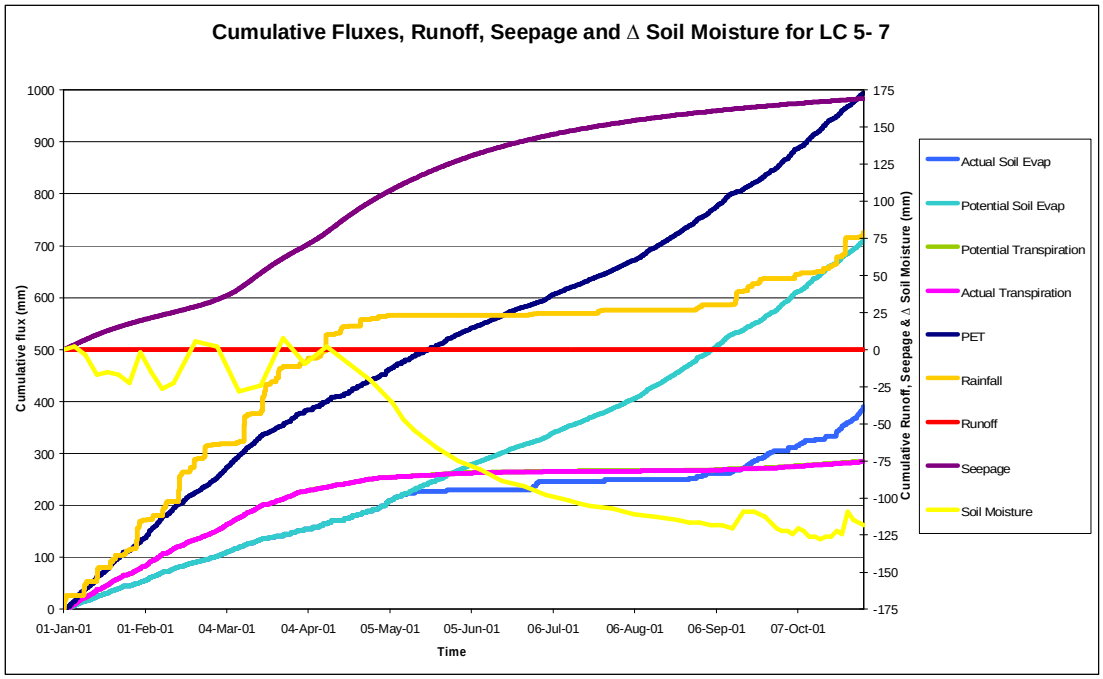

Figure 5.17 Cumulative Fluxes, Runoff, Seepage and Δ Soil Moisture for the transect of LC 5 - 7.

5.4.3 Cumulative fluxes for the East facing Hillslope and Wetland Transect (LC 8 to LC 10)

The fluxes for this transect can be seen in Figure 5.18. The seepage flow is fairly rapid in its surge out of this transect until the end of February and from

then on it starts to ebb in its flow to some degree until the end of the simulation. This is because of a combination of large, intense precipitation events, such as on the 13, 18, 20, 28 and 29 January, and high antecedent moisture conditions. This transect released the most seepage water, with the final cumulative seepage flow being 193 mm. The soil moisture demonstrates distinct fluctuations for the duration of the summer compared with the retarded fluctuations in soil moisture of LC 5 - 7. In winter there is again a steady recession of the soil moisture, followed by a dampened response to the onset of precipitation in the springtime. The cumulative actual and potential transpiration fluxes are incessantly in close agreement with each other, with the final actual transpiration cumulative flux being about 274 mm, with the cumulative potential transpiration flux remaining higher for most of the simulation. The potential evaporation follows the actual evaporation soundly, but continues faintly higher than it until about mid May when the actual evaporation flux levels out with the onset of the winter temperatures.

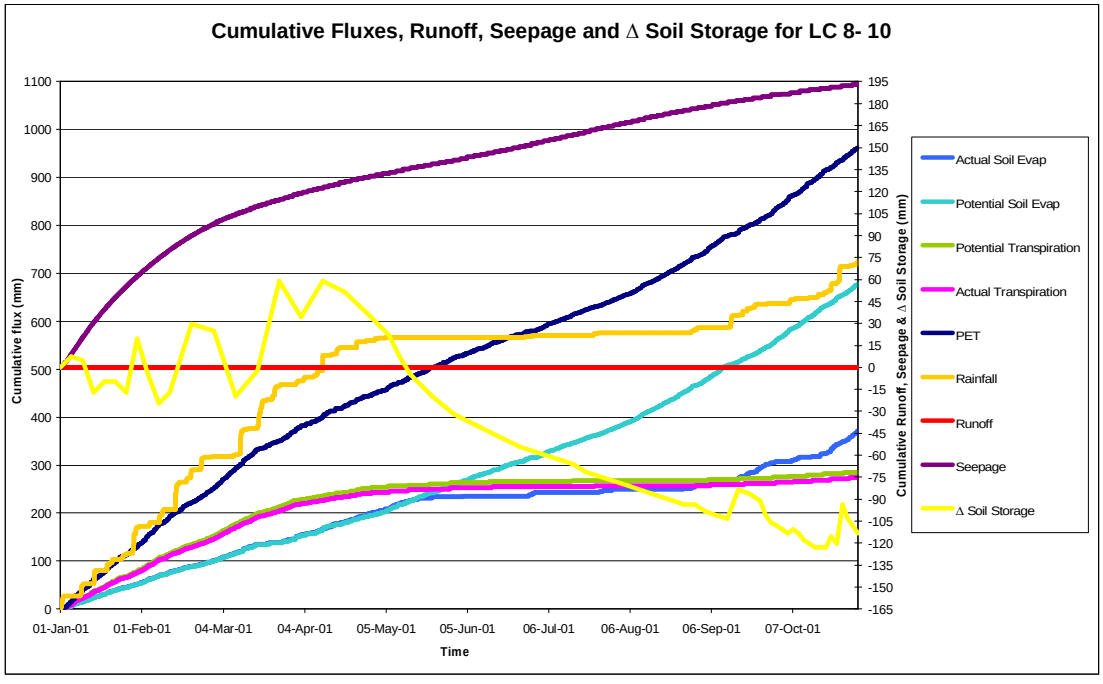

Figure 5.18 Cumulative Fluxes, Runoff, Seepage and Δ Soil Moisture for the Transect of LC 8 - 10.

5.5 Seepage Hydrographs of the Contributing Hilslopes

The seepage hydrographs for the transects were a good first approximation in determining seepage fluxes which can later be used to formulate seepage transfer functions for the Weatherley Catchment.

5.5.1 Seepage Hydrograph for the West facing Upper Hillslope Transect (LC 1 to LC 4)

The seepage hydrograph for LC 1 – 4 can be seen in Figure 5.19. The seepage hydrograph for LC 1 – 4 exhibits both large, quick responses as well as smaller responses to rainfall depending on the antecedent moisture conditions and the characteristics of the rainfall event being responded to. There is a lag response of about fifteen days to the large rainfall events. The fluctuations of the responses are more pronounced during the late summer and spring. There is a steady increase in the amount of seepage per day in the second month of the simulation, where larger and more intense rainfall events cause the amount of seepage to increase by more than 0.1 mm/day. This increase in seepage is attributed to soil water accumulating and moving along the interfaces between different soil horizons, soil types and the soil-bedrock interface, where soil water steadily flows down the soil profile to emerge at the base of the slope as seepage.

5.5.2 Seepage Hydrograph for the West facing Wetland Transect (LC 5 to LC 7)

The seepage hydrograph for LC 5 - 7 can be seen in Figure 5.20. The seepage hydrograph for LC 5 – 7 also exhibits large, quick responses as well as smaller responses to rainfall depending on the antecedent moisture conditions and the characteristics of the rainfall event being responded to. There is a distinct variation in amplitude compared to the responses of LC 1 – 4, where the responses of LC 5 – 7 have smaller fluctuations to individual rainfall events, but there is a more prominent rise of the seepage hydrograph in summer with the long tail of the winter recession being evident. The steady

increase in the amount of seepage per day, from February to April of the simulation, where larger and more intense rainfall events occurred, caused the amount of seepage to increase by more than 1mm/day.

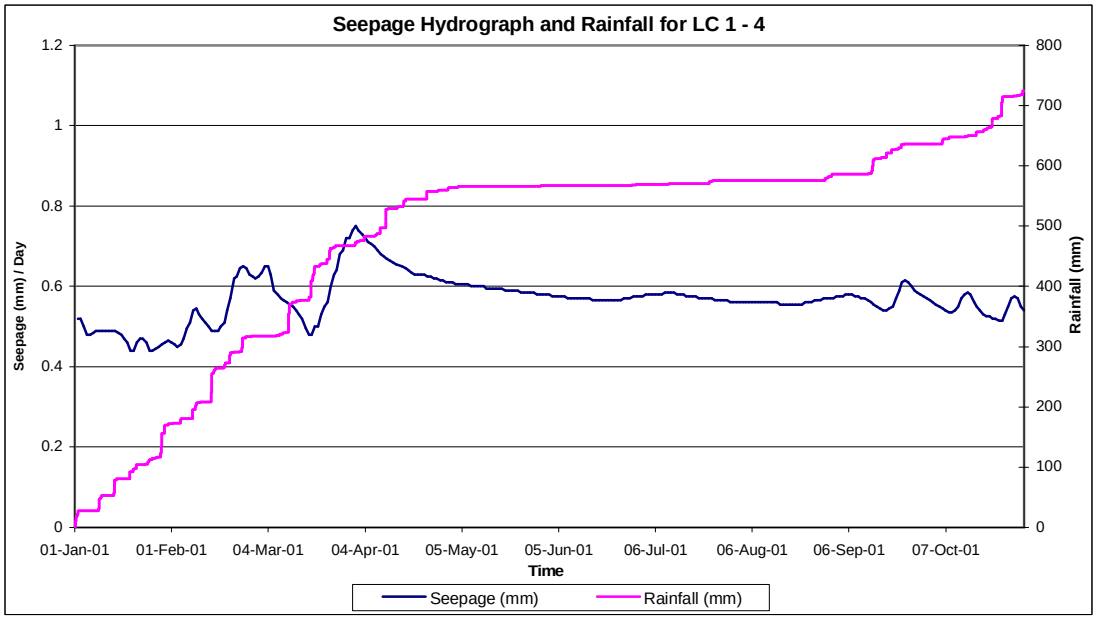

Figure 5.19 Seepage Hydrograph for transect LC 1 - 4.

5.5.3 Seepage Hydrograph for the East facing Hillslope and WetlandTransect (LC 8 to LC 10)

The seepage hydrograph for LC 8 – 10 can be seen in Figure 5.21. The seepage hydrograph for LC 8 – 10 was far less eventful, with the responses tapering off from an initial rapid and large not seem to depend response. The responses thereafter are erratic, but similar in magnitude with responses still being evident throughout winter and their recurrence becoming less often through the spring. The responses of LC 8 – 10 do not seem to vary in magnitude or timing according to the antecedent moisture conditions and the characteristics of the rainfall event being responded to like the seepage responses of the other two transects.

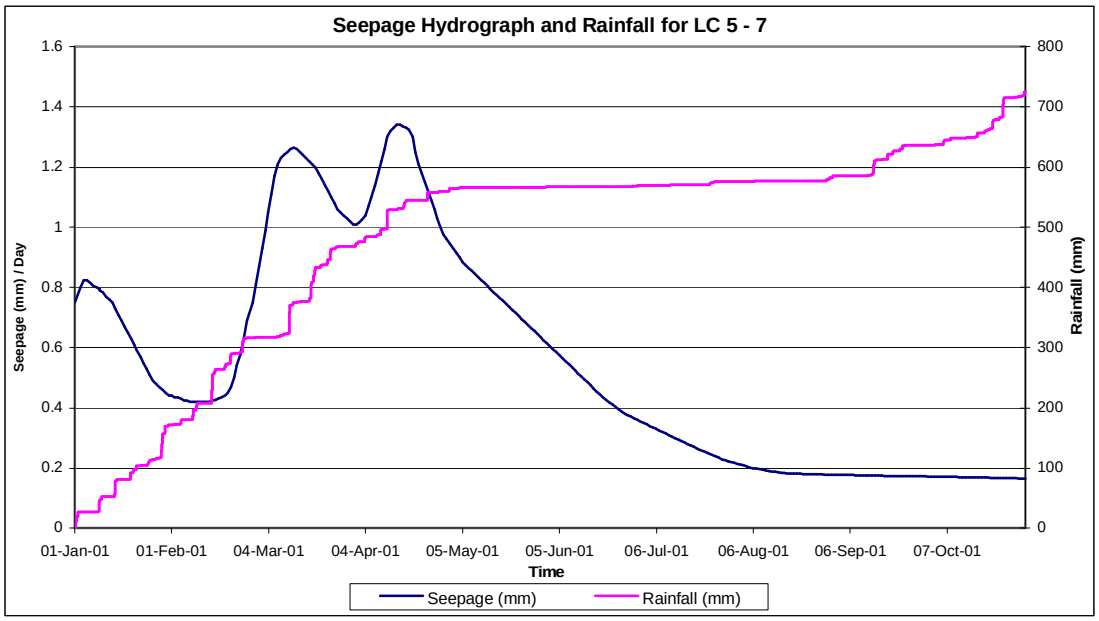

Figure 5.20 Seepage Hydrograph for transect LC 5 - 7.

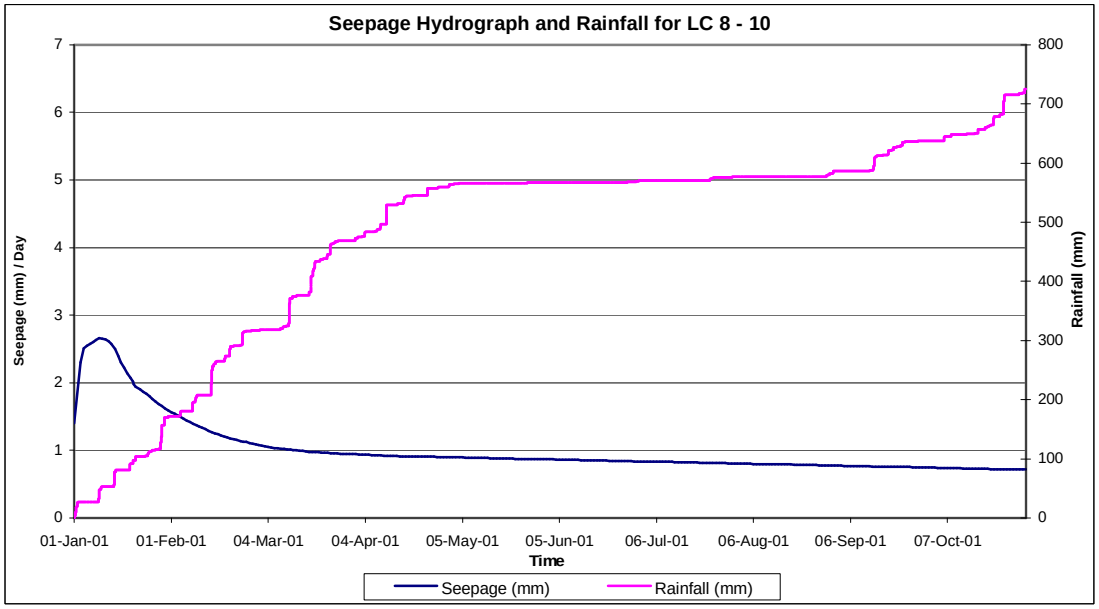

Figure 5.21 Seepage Hydrograph for transect LC 8 - 10.

These results are useful as a first approximation to determining seepage fluxes. The use of these results is offered in developing a transfer function model for the Weatherley catchment.

6. SUMMARY AND CONCLUSIONS

As can be seen from the Weatherley Catchment time series of hillslope tensions and water contents, the streamflow generated from the contributing hillslopes are part of a highly complex series of interactions between the surface and subsurface processes. These processes, their interactions and their degree of connectivity are often not fully understood and adequately captured by catchment modellers, which concurs with Stieglitz *et al*., (2002), who stated that it is apparent that more understanding needs to be gained about the connectivity between these various source areas in order to understand fully the prevalent streamflow generating processes. The understanding of the subsurface dynamics is often thought to be far more complex than the surface dynamics and is frequently a major factor affecting the runoff responses from small catchments. Due to the magnitude of these subsurface contributions to the overall streamflow, the HYDRUS-2D model was used in a first attempt to quantify the contributing fluxes from the hillslopes within the Weatherley Catchment. The hillslope flux responses are thus determined for later translation into a hillslope seepage transfer function calculated from simulating the hillslope soil water component of catchment responses.

After quantifying the contributing hillslope fluxes, the next step would be to develop transfer functions for the various types of flow, at different depths for the previously identified contributing hillslope transects. Transfer functions were found to be the most suitable method for modelling the Weatherley catchment because of their simplicity and easy application to rainfall-runoff modelling. They can be applied to specific areas and depths of hydrologic response and should not be inconsistent when spatially and temporally upscaled (Weiler *et al.*, 2003). Transfer functions can also be used to examine the changing spatial and temporal flow paths during different hydrological situations such as low flow and high flows (Wenninger *et al.*, 2004). They can be used to derive streamflow hydrographs produced by various storms without resorting to changing the model parameters for a given basin (Yue

and Hashino, 2000). They can also simulate hydrographs quite accurately and can account for the long tail encountered on the receding limb of the hydrograph, which becomes especially important in times of low flow (Weiler *et al.*, 2003a). The use of transfer functions should offer a comprehensive quantification of the contributing hillslopes in assessing the contributions to the Weatherley Catchment's streamflow.

Once a clear understanding of how the hillslope processes affect the catchment response was gained from observation, methods for determining the hillslope processes were devised (Hickson, 2000). These methods included using data from a comprehensive monitoring network established within the Weatherley Catchment including tensiometers, piezometers, crump weirs, a raingauge and individual water content measurements (Hickson, 2000). Also, soil physical and hydraulic characteristics were determined from in field and laboratory experiments. From laboratory suction tests that have been performed in the past on the soils from the Weatherley catchment (Lorentz *et al.*, 2001), water retention curves have been plotted for the nest sites at different depths along the transects which were then used to try various combinations of the soil hydraulic properties. These observed measurements were then compared with the simulated time series of the tensions and water contents from a modelling exercise performed with HYDRUS-2D for each site along the transects which were modelled according to the refined simulated soil hydraulic properties.

The methodology on how to quantify the hillslope fluxes began with using the HYDRUS-2D model and using the comprehensive data collected from the Weatherley Catchment to create a HYDRUS-2D input file. The breakpoint rainfall from the Weatherley catchment's raingauge (near the nest at LC1) was used with the ETo data to create an hourly input file throughout the analysis period from 1 January 2001 until 31 October 2001. The HYDRUS-2D input file requires the separation of the potential soil water evaporation (rSoil) and vegetation transpiration (rRoot) data, which is done using the applicable crop factor. Rough estimates of the water retention characteristics are determined from observed data and then refined during the modelling

exercise. The measured parameters for the various sites extracted from the literature were found to be less and less accurate as the area to be modelled increased. The observed parameters were found to be very much site and depth specific.

The simulated tensions were well modelled in the higher lying areas (LC 1 – 4 and LC 10), but the simulations in the lower lying regions were only passably modelled due to the model being unable to properly account for the water table and the fluctuations thereof mainly because the lateral flows are influenced by the macropore structures which were not well simulated. The simulated water contents did not have the same precision as the simulated tensions did, but the simulated water contents were once again modelled better in the high lying areas than the lower lying regions.

The timing of the tension response to precipitation events was in general well simulated, with the summer responses being rapid and consistent. The responses in winter were tolerably simulated, with the winter recession being present but not occurring at the same rate as the observed recession. The responses in spring were adequate, with the responses being rapid but also intermittent. The timing of the simulated water content response to precipitation events was hard to distinguish (except for the spring, where a host of individual observations were made) because of the sporadic observations. In the spring, the water contents were modelled adequately when compared to the observed data in the upper west facing hillslope transect (LC 1 – 4) in the shallow horizon, where the responses to rainfall were rapid.

The shallow horizons were well modelled compared to the deeper horizons at all sites within the hillslope transects. This is due to a much greater degree of complexity being present the deeper down one gets from the soil surface. The complexities lie in the connectivity and location of the deeper horizons, the thickness of them, the conductivity of the deeper layers and of those delivering soilwater to them as well as the location of the bedrock. This is a common problem with a lot of hydrological models, even though the deeper

horizons have enormous impact on streamflow generation and contributions to baseflow and the groundwater.

Once the simulated output from the model has been adequately fitted to the observed results for all the transects within the Weatherley lower catchment, the contributing hillslope fluxes were quantified. A time series is produced of the cumulative fluxes along the transect, where the actual runoff, seepage, precipitation, transpiration and the evaporation as well as the potential transpiration, evaporation and evapotranspiration rates are presented graphically in mm. The change in soil moisture (mm) is also included. From these cumulative fluxes, the period of study is shortened to look more closely at the cumulative fluxes during rainfall events during the summer, winter and spring.

Cumulative fluxes were created where the different contributions of the components of the Weatherley catchment's soil dynamics are summarised in the form of high and low flow comparisons as well as comparisons of the components from each of the transects. During low flows, the actual evaporation is less than a third of the potential evaporation, showing that there is not enough readily available water to satisfy the high evaporative demands during times of low flows. The potential evaporation of LC 1 - 4 is lower proportionately to LC 5 - 7 during times of low flows, which is perhaps due to LC 1 - 4 being west facing and in winter the amount of solar energy is reduced compared to the summer. The potential and actual transpiration during the low flow are very low compared to the high flow period, because there is less plant available water in all the transects and lower potentials. In times of low flows the seepage from LC 1 - 4 is greater than the other transects. The seepage from LC 5 - 7 is also more than that from LC 8 - 10, due to there being approximately 160 mm being added to transect LC 5 - 7 through a variable flux boundary condition to simulate the transference of the seepage water from the upslope transect of LC 1 - 4. This inversion of the seepage flow amounts is in part because LC 1 - 4 did not deliver as much seepage water as the other transects during the high flow months and therefore stored more water which got released from the hillslope to sustain

the streamflow during times of low flow. The residence times of the upslope soil water would also be longer with the stored soil water only emerging from the hillslope as seepage flow during the winter period.

The seepage hydrographs for the transects were a good first approximation in determining seepage fluxes which can later be used to formulate seepage transfer functions for the Weatherley Catchment. The seepage hydrograph for LC 1 – 4 exhibits both large, quick responses as well as smaller responses to rainfall depending on the antecedent moisture conditions and the characteristics of the rainfall event being responded to. There is a lag response of about fifteen days. The fluctuations of the responses are more pronounced during the summer and spring. The seepage hydrograph for LC 5 – 7 also exhibits large, quick responses as well as smaller responses to rainfall depending on the antecedent moisture conditions and the characteristics of the rainfall event being responded to. There is a distinct variation in amplitude compared to the responses of LC 1 – 4, where the responses of LC 5 – 7 have smaller fluctuations to individual rainfall events, but there is a more prominent rise of the seepage hydrograph in summer with the long tail of the winter recession being evident. The seepage hydrograph for LC 8 – 10 was far less eventful, with the responses tapering off from a initial rapid and large not seem to depend response. The responses thereafter are erratic, but similar in magnitude with responses still being evident throughout winter and their recurrence becoming less often through the spring. The responses of LC 8 – 10 do not seem to vary in magnitude or timing according to the antecedent moisture conditions and the characteristics of the rainfall event being responded to like the seepage responses of the other two transects.

The main source of streamflow from the contributing hillslopes, their interactions, their connectivity and their effects on the small catchment runoff within the Weatherley Catchment have been identified, described (Hickson, 2000) and quantified. It is evident from this study and those preceding it, that there is a high degree of spatial heterogeneity that exists within the Weatherley Catchment and thus different soil forms and contributing hillslope

areas result in different physical and hydraulic characteristics along the hillslopes (Hickson, 2000). This dissertation has set out to provide a sound understanding of the subsurface processes that occur in the Weatherley Catchment, then describe as well as quantify the fluxes entering and exiting the contributing hillslopes. The use of these results is offered in developing a transfer function model for the Weatherley catchment. Continued research of this kind is necessary to provide insights into the effects of climate change, land use change, sediment yield studies, water quality scenarios, water allocation and water resource management.

7. RECOMMENDATIONS FOR FUTURE RESEARCH

The research work that has been conducted over the years at the Weatherley experimental research catchment has been most valuable indeed. Theses by Esprey (1997), Hickson (2000) as well as many research papers by Lorentz (2001a, 2001b and 2003) and the work presented in this dissertation supplies a complete and thorough account of the processes (surface and subsurface) that occur at Weatherley as well as how these affect the small catchment's runoff criteria. The catchment's streamflow generation mechanisms were successfully simulated using the Hydrus-2D model in conjunction with hillslope hydrological process observations including hydrometric and a simple natural isotopic sampling experiment. The simulated data was then used to describe the volumes and fluxes of the sources of streamflow in building a transfer function model for the Weatherley catchment. With the continuation of monitoring at the Weatherley catchment and the implications of using the transfer function methodology, recommendations for future research include the following:

- Lengthening the study period that the fluxes for transfer function modelling in the Weatherley catchment were developed from, for more rigorous and accurate distributed modelling of catchment runoff during and after afforestation. The study period length should also be extended so that key trends and findings, such as the responses to large summer thunderstorms and the winter recessions can be ascertained to determine whether they are isolated or common trends which can then be focussed on in future research. There is a considerble data set available (nearly ten years) that can be used to make significant improvements on the estimation of hillslope, wetland and riparian zone responses within the catchment.

- The suggested transfer function model for the Weatherley catchment should be developed. The HYDRUS-2D model has been used to quantify soil based responses. This modelling requires a sound

understanding of the hillslope processes by the modeller and for the model to be able to accommodate these processes adequately, which will be the case with HYDRUS-2D once some experience is gained making the transfer function model accurate and extremely useful.

- The suggested transfer function model for the Weatherley catchment should be revised and refined further with regard to the various source areas like macropore (preferential) flow, which contribute towards the streamflow generation. The fluxes should be calculated for individual sites within the transects so that the valuable soil physical and hydraulic characteristics data can be used effectively, thereby attaining greater accuracy spatially and also with depth in the soil profile. The subtler processes within the small catchment will then still be captured and the degree of detail should not be too high.

- Expanding the work done in this thesis to the rest of the Mooi river catchment, with more field study to be done in the greater catchment with regard to land use, soil, land cover, geology, streamflow contributing areas and a comprehensive time series surveys.

- Using the upscaled transfer function methodology to conduct modelling exercises for different scenarios within the Mooi river catchment including future climate change, land use change, low flow predictions and sediment yield studies as well as water quality scenarios.

- Monitoring within the Weatherley catchment should continue, in light of the recent afforestation, with regard to the rainfall, streamflow, sediment yield, surface runoff, tensiometer, piezometer and borehole data, groundwater fluxes and the subsurface fluxes.

- There is a need for more updated instrumentation in the Weatherley catchment, such as more accurate estimations of evapotranspiration and more automated instrumentation. Some of the instrumentation

should also be updated to more modern technologies such as incorporating Water Mark type sampling instead of using tensiometers as theft of the 6V logger batteries takes place in the field and the current loggers are becoming perished.

- The effective management of this pristine research catchment is somewhat compromised by the lack of training and the implementation of transparency in defining the various tasks and duties entailed from the capture of data to the input of the data into the Weatherley database.

- The catchment has been subjected to a large amount of vandalization and theft in 2005, so a more effective security effort is required for protecting and capturing this valuable data (especially the tensiometer and piezometer data). Also care needs to be taken by the employees of Mondi when burning firebreaks, as there is often negligence displayed with instrumentation being damaged.

- More hydrological data, with more temporal definition, needs to be included in the simulations to more accurately model the given hillslope transects with the HYDRUS-2D model. Hydrological data such as macropore flow occurrence, with focus on the amount of precipitation, the intensity of precipitation and the antecedent moisture condition before precipitation occurs in order to induce macropore flow. This type of flow in modelling is important because it contributes to the rapid responses within a catchment, which has implications for flood and sediment yield hydrology. More hydrological data is also needed in order to characterise the deep groundwater flow component accurately as this contributes largely to baseflow, which is thought to sustain low flows, especially in small headwater catchments.

- A more detailed sampling survey of the Weatherley catchment with natural isotopes or chemical species tracers needs to be undertaken

with a pre-survey tracer correlation test, and either a three or five component isotopic hydrograph separation leading to a successful end member mixing analysis (EMMA) in order to fully assess the soil water dynamics in the catcment.

- A study as to the near-stream flow generation mechanisms in the Weatherley catchment needs to be undertaken in order to qualify and quantify the fluxes associated with piston flow and groundwater ridging phenomena during and after rainfall events. This study should also divulge information as to the amounts and intensities of rainfall that initiate these types of streamflow generating mechanisms at different antecedent moisture contents. More accuracy is also required in the modelling routines as far as a macropore flow component and a deep groundwater flow component are concerned. This will cause the runoff dynamics to be more accurately modelled, as at the moment the simulated surface runoff is zero as it is all being transferred into the seepage flow component. The groundwater flow component will bring more accuracy to all the simulations, but especially to the wetland transect (LC 5 – 7), where a lot of rapid and slow streamflow responses are generated by the fluctuating water table.

- The connectivity of the hydrological processes between the profiles at individual nest sites, the individual sites within the transects and also the hillslope transects needs to be focussed on in more detail in order to describe and understand their interactions with each other better. There is still much to be studied as far as the connectivities of different source areas, their timings and their quantities. This will result in the hilllslopes and thus the streamflow being quantified with more precision.

- This thesis can then later be used in studies of soil water release as to the cumulative effects of baseflows from small catchments to the large catchment scale and studies concerning the accumulation of low flows

from smaller catchments to sustain the low flows at the larger catchment scale.

8. REFERENCES

Achet, S. H., McNamara, J. P. and Chandler, D. 2002. Control of Unsaturated Soil Moisture Dynamics on Hillslope Hydrological Connectivity. American Geophysical Union, Fall Meeting 2002, Abstracts.

Achet, S. H., J. P. McNamara and D. Chandler. 2006. Insights Into the Unsaturated Subsurface Flow Mechanism in Streamflow Generation In Semiarid Environment: Applying HYDRUS2D Combined With Field Experiments in Dry Creek, Boise, ID. Water Resources Research. In Press. (http://earth.boisestate.edu/home/sachet/publications.doc)

Acocks, J. 1975. Veld types in South Africa. S.A. Botanical Research Institute, Department of Agricultural Technical Services, Memoir 40. p 83.

Agnese, C., Baiamonte, G. and Corrao, C. 2001. A simple model of hillslope response for overland flow generation. Hydrological Processes, 15: 3225 - 3238.

Alila, Y., Beckers, J., Cathcart, J. and Mitraoui, A. 2001. Science and Engineering Perspectives on Non-Linearity in Watershed Response. AGU Chapman Conference on State-of-the-Art in Hillslope Hydrology. Sunriver, OR Oct 8-12, 2001. Abstracts. p33.

Asano, Y., Uchida, T. and Ohte, N. 2002. Residence times and flow paths of water in steep unchannelled catchments, Tanakami, Japan. Journal of Hydrology, 261: 173 - 192.

Ballantine, J. A. and Dunne, T. 2001. The Disparity Between Saturated Hydraulic Conductivities at Point and Catchment Scales. AGU Chapman Conference on State-of-the-Art in Hillslope Hydrology. Sunriver, OR Oct 8-12, 2001. Abstracts. p18.

Becker, A. and Braun, P. 1999. Disaggregation, aggregation and spatial scaling in hydrological modelling. Journal of Hydrology, 217(3): 239 – 252.

Beven, K. 2001. Learning About Places: A Philosophy for Environmental Modelling? AGU Chapman Conference on State-of-the-Art in Hillslope Hydrology. Sunriver, OR Oct 8-12, 2001. Abstracts. p17.

Bishop, K., Köhler, S. Laudon, H. and Hruska, J. 2001. Riparian Zone Controls on the Chemical Dynamics of DOC-Rich Runoff from a Hillslope with Transmissivity-Feedback Flow Paths. AGU Chapman Conference on State-of-the-Art in Hillslope Hydrology. Sunriver, OR Oct 8-12, 2001. Abstracts. p19.

Bogaart, P. W. and Troch, P. A. 2003. Improved Understanding of the 3-D Hillslope Spatial Structure as a Prerequisite for Understanding the Hydrological Behaviour of Ungauged Basins. American Geophysical Union, Fall Meeting 2003, Abstracts.

Brassard, P., Waddington, J.M., Hill, A.R. and Roulet, N.T. 2000. Modelling groundwater-surface water mixing in a headwater wetland: implications for hydrograph seperation. Hydrological Processes, 14: 2697 - 2710.

Brooks, R. and Corey, A. 1964. Hydraulic properties of porous media. Hydrology paper No. 3, Civil Engineering Department, Colorado State University, Fort Collins, Colorado.

Brown, V.A., McDonnell, J.J., Burns, D.A. and Kendall, C. 1999. The role of event water, a rapid shallow flow component, and catchment size in summer stormflow. Journal of Hydrology, 217: 171 - 190.

Burns, D. A. 2002. Stormflow-hydrograph separation based on isotopes: The thrill is gone – What's next? Hydrological Processes, 16: 1515 – 1517.

Buttle, J.M. 1994. Isotope hydrograph seperations and rapid delivery of pre-event water from drainage basins. Progress in Physical Geography, 18(1): 16 - 41.

Collins, R., Jenkins, A. and Harrow, M. 2000. The contribution of old and new water to a storm hydrograph determined by tracer addition to a whole catchment. Hydrological Processes, 14: 701 - 711.

Denic-Jukic, V. and Jukic, D. 2003. Composite transfer functions for karst aquifers. Journal of Hydrology, 274: 80 - 94.

Elsenbeer, H. 2001. Hydrologic flowpaths in tropical rainforest soilscapes – a review. Hydrological Processes, 15: 1751 – 1759.

Esprey, L. J. 1997. Hillslope experiments in the North Eastern Cape to measure and model subsurface flow processes. Unpublished M. Sc dissertation, Department of Agricultural Engineering, University of Natal.

Feddes, R. A., Kowalik, P. J. and Zarandny, H. 1978. Simulation of field water use and crop yield, John Wiley and Sons, New York, NY.

Flühler, H. and Hagendorn, F. 2001. Preferential flow from pore to catchment scale. AGU Chapman Conference on State-of-the-Art in Hillslope Hydrology. Sunriver, OR Oct 8-12, 2001. Abstracts. p18.

Grant, L. E., Seyfried, M. S., Marks, D. and Winstral, A. 2004. Simulation of vegetation, soil characteristics, and topography effects on soil water distribution and streamflow timing over a semi-arid mountain catchment. American Geophysical Union, Fall Meeting 2004, Abstracts.

Hickson, R., Lorentz, S. and Volans, S. 1999. Identifyind Dominant Hydrological Processes on Molteno Formations of the northern Eastern Cape Province. Ninth South African National Hydrology Symposium,

University of the Western Cape, November, 1999. p10.

Hickson, R. 2000. Defining Small Catchment Runoff Responses Using Hillslope Hydrological Process Observations. Unpublished M.Sc dissertation, Department of Agricultural Engineering, University of Natal.

Hjerdt, K. N., McGlynn, B., Tromp-van Meerveld, I., McDonnell, J. J. and Hooper, R. P. 2001. Thresholds in Subsurface Flow Generation: An Intercomparison of Three Different Headwater Catchments. American Geophysical Union, Fall Meeting 2001, Abstracts.

Hooper, R.P. and Shoemaker, C.A. 1986. A comparison of chemical and isotopic hydrograph separation. Water Resources Research, 22: 1444 - 11454.

Hooper, R.P. 2001. Applying the scientific method to small catchment studies: a review of the Panola Mountain experience. Hydrological Processes, 15(10): 2039 – 2050.

Hughes, D. A. and Sami, K. 1994. A semi-distributed, variable time interval model of catchment hydrology – structure and parameter estimation procedures. Journal of Hydrology, 155: 265 – 291.

Iorgulescu, I. and Beven, K.J. 2003. Data-based modelling of runoff and chemical tracer concentrations in the Haute-Mentue (Switzerland) research basin, EGS-AGU-EUG Joint Assembly, Nice, France.

Joerin, C., Beven, K.J., Iorgulescu, I. and Musy, A. 2002. Uncertainty in hydrograph separations based on geochemical mixing models. Journal of Hydrology, 255: 90 - 106.

Katsuyama, M., Ohte, N. and Kobashi, S. 2001. A three-component end-member analysis of streamwater hydrochemistry in a small Japanese forested headwater catchment. Hydrological Processes, 15: 249 - 260.

Kendall, C., McDonnell, J.J. and Gu, W. 2001. A look inside 'black box' hydrograph separation models: a study at the Hydrohill catchment. Hydrological Processes, 15: 1877 - 1902.

Kirchner, J. W., Feng, X. and Neal, C. 2001. Catchment-scale advection and dispersion as a mechanism for fractal scaling in stream tracer concentrations. Journal of Hydrology, 254: 82 – 101.

Labat, D., Ababou, R. and Mangin, A. 1999. Linear and nonlinear input/output models for karstic springflow and flood prediction at different time scales. Stochastic Environmental Research Risk Assesment, 13(5): 337 - 364.

Ladouche, B., Probst, A., Viville, D., Idir, S., Baque, D., Loubet, M., Probst, J.-L. and Bariac, T. 2001. Hydrograph seperation using isotopic, chemical and hydrological approaches (Strengbach catchment, France). Journal of Hydrology, 242: 255 - 274.

Lorentz, S and Kienzle, S. 1994. The merits and limitations of GIS linked transfer function modelling of basin scale sediment yield. GIS Workshop Presentation: 50 Years of Water Engineering in South Africa, 14-15 July, 1994. Water Engineering Division, South African Institution of Civil Engineers, University of the Witwatersrand, SA.

Lorentz, S. and Esprey, L.J. 1998. Baseline hillslope study prior to afforestation in the Umzimvubu headwaters of the North East Cape Province, South Africa. *in:* Kovar, K., Tappeiner, U., Peters, N. E. and Craig, R. G. (eds). *Hydrology, Water Resources and Ecology in Headwaters* (proceedings of the Headwater ’98 Conference held at

Meran/Merano, Italy, April 1998) IAHS Publ. No. 248: pp 267 – 273. Oxfordshire, U.K.

Lorentz, S. 2001a. Hydrological Systems Modelling Research Programme: Hydrological Processes. Phase I: Processes Definition and Database. Water Research Commision, Pretoria. Report 637/1/01.

Lorentz, S. 2001b. Hillslope monitoring on Molteno formations in the northern Eastern Cape, South Africa. AGU Chapman Conference on State-of-the-Art in Hillslope Hydrology. Sunriver, OR Oct 8-12, 2001. Abstracts. P26.

Lorentz, S., Goba, P. and Pretorius, J.J. 2001. Hydrological Processes Research: Experiments and Measurements of Soil Hydraulic Characteristics. Water Research Commision, Pretoria, Report 744/1/01.

Lorentz, S., R. Hickson, W-A. Flügel and J. Helmschröt. 1999. Hillslope and Nested Catchment Monitoring on Molteno Formations of the Northern Eastern Cape Province, South Africa. XXIV General Assembly of the European Geophysical Society Poster Presentation, Den Haag, The Netherlands, April 1999.

Lorentz, S. and Hickson, R. A. 2001. Applying hillslope hydrology observations to catchment modelling in Molteno Formations. Tenth South African National Hydrology Symposium: 26 – 28 September, 2001, Pietermaritzburg, South Africa. pp15.

Lorentz, S., Thornton-Dibb, S., Pretorius. and Goba, P. 2003. Hydrological Systems Modelling Research Programme: Hydrological Processes. Phase II: Quantification of Hillslope, Riparian and Wetland Processes. Water research Commision, Pretoria, Report K5/1061 and K5/1086.

McCartney, M. and Neal, C. 1999. Water flow pathways and the water blance within a headwater catchment containing a dambo: inferences drawn from hydrochemical investigations. Hydrology and Earth System Sciences, 3(4): 581 – 591.

McDonnell, J. J. 1990. A rationale for old water discharge through macropores in a steep, humid catchment. Water Resources Research, 26: 2821 – 2832.

McDonnell, J.J., Bonell, M., Stewart, M.K. and Pearce, A.J. 1990. Deuterium variations in storm rainfall: Implications for stream hydrograph separations. Water Resources Research, 26: 455 - 458.

McDonnell, J.J., Owens, I.F. and Stewart, M.K. 1991. A case study of shallow flow paths in a steep zero-order basin. Water Resources Bulletin, 27(4): 679 - 685.

McDonnell, J.J., Stewart, M.K. and Owens, I.F. 1991a. Effect of catchment-scale subsurface mixing on stream isotopic response. Water Resources Research, 27(12): 3065 - 3073.

McGlynn, B. L., McDonnel, J. J., Hooper, R. P. and Kendall, C. 2001a. On the relative roles of hillslopes vs. riparian zones in headwater catchment runoff volume, timing and composition. AGU Chapman Conference on State-of-the-Art in Hillslope Hydrology. Sunriver, OR Oct 8-12, 2001. Abstracts. P27.

McGlynn, B. L., McDonnel, J. J., Kendall, C. and Hooper, R. H. 2001b..The effects of catchment scale and landscape organization on streamflow generation processes. AGU Chapman Conference on State-of-the-Art in Hillslope Hydrology. Sunriver, OR Oct 8-12, 2001. Abstracts. p38.

McGlynn, B. L. and McDonnell, J. J. 2003. Quantifying the relative contributions of riparian and hillslope zones to catchment runoff. Water Resources Research, 39 (11), SWC2: 1 – 20.

Moussa, R. 1997. Geomorphological transfer function calculated from Digital Elevation Models for distributed hydrological modelling. Hydrological Processes, 11: 429 - 449.

Mualem, Y. 1976. A new model for predicting the hydraulic conductivity of unsaturated porous media. Water Resources Research, 12: 513 – 522.

Newman, B.D., Campbell, A.R. and Wilcox, B.P. 1998. Lateral subsurface flow pathways in a semiarid ponderosa pine hillslope. Water Resources Research, 34(12): 3485 - 3496.

Noguchi, S., Tsuboyama, Y., Sidle, R. C. and Hosoda, I. 1999. Morphological Characteristics of Macropores and the Distribution of Preferential Flow Pathways in a Forested Slope Segment. Soil Science Society of America Journal, 63: 1413 – 1423.

Puigdefabregas, J. G., del Barrio, M. M., Boer, Gutie'rrez, L. and Sole'. A. 1998. Geomorphology, 23: pp 337 – 351.

Rassam, D. W., Šimůnek, J. and van Genuchten, M. Th. 2003. Modelling Variably Saturated Flow with HYDRUS-2D. N. D. Consult, Brisbane, Australia.

Roberts, V., Hensley, M., Smith-Baillie, A. and Paterson, D. 1996. Detailed Soil Survey of the Weatherley Catchment. Institute for Soil, Climate and Water. Report GW/A/93.36, Pretoria, South Africa.

Scanlon, T. M., Raffensperger, J .P., Hornberger, G. M. and Clapp, R. B. 2000. Shallow subsurface storm flow in a forested hedwater

catchment: Observations and modelling using a modified TOPMODEL. Water Resources Research, 36(9): 2575 – 2586.

Schulze, R. E. and Pike, A. 2004. Development and Evaluation of an Installed Hydrological Modelling System. Water Research Commission, Pretoria, Report 1155/1/04, p 48.

Schulze, R. E. 1994. Hydrology and Agrohydrology: A text to Accompany the *ACRU* 3.00 Agrohydrological Modelling System. Water Research Commission, Pretoria, Report TT69/95.

Schulze, R. E. 2005. Hydrological Modelling: Concepts and Practice. School of Bioresources Engineering and Environmental Hydrology, University of KwaZulu-Natal, Pietermaritzburg, South Africa.

Schulze, R. E. 2006. School of Bioresources Engineering and Environmental Hydrology, University of KwaZulu-Natal, Pietermaritzburg, South Africa. Personal Communication.

Seiburt, J., McDonnell, J. J. and Bishop, K. 2001. Conceptually based hydrological and geochemical modelling. AGU Chapman Conference on State-of-the-Art in Hillslope Hydrology. Sunriver, OR Oct 8-12, 2001. Abstracts. P32.

Sidle, R. C., Tsuboyama, Y. and Noguchi, S. 2001. Quantification of the Hydrogeomorpic Concept of Stormflow Generation in Headwater Streams: a First Approximation. AGU Chapman Conference on State-of-the-Art in Hillslope Hydrology. Sunriver, OR Oct 8-12, 2001. Abstracts. P23.

Šimůnek, J., Sejna, M., and van Genuchten, M. Th. 1999. The HYDRUS-2D software package for simulating two-dimensional movement of water heat and multiple solutes in variably saturated media. Version 2.0,

IGWMC – TPS – 53, International Ground Water Modelling Centre, Colorado School of Mines, Golden, Colorado.

Singh, V.P. 1988. Rainfall-runoff modelling. Hydrologic systems, 1. Prentice-Hall, Englewood Cliffs, NJ.

Sklash, M.G., Stewart, M. K. and Pierce, A. J. 1986. Storm Runoff Generation in Humid Headwater Catchments: 2. A Case Study of Hillslope and Low-Order Stream Response, Water Resources Research, 22(8): 1273 – 1282.

Stewart, I. T. and Loague, K. 2000. Uncertainty introduced by upscaling type transfer functions. *in:* Proceedings of Accuracy 2000, edited by G. B. M. Heuvelink and M. P. J. M. Lemmons, pp 617 – 624, Delft University Press, Netherlands.

Stewart, M. and McDonnell, J. J. 1991. Modelling base flow soil water residence times from deuterium concentrations. Water Resources Research, 27(10): 2681 – 2693.

Stieglitz, M., Shaman, J., McNamara, J., Kling, G. W. and Engel, V. 2002. An approach to understanding hydrologic connectivity on the hillslope and the implications for nutrient transport. American Geophysical Union, Fall Meeting 2002, Abstracts.

Troch, P. A., Paniconi, C. and Emiel van Loon, E. 2003. Hillslope storage Boussinesq model for subsurface flow and variable source areas along complex hillslopes: 1. Formulation and characteristic response. Water Resources Research, 39(11), SBH3: 1 – 12.

Uhlenbrook, S. and Leibundgut, C. 2002. Process-orientated catchment modelling and multiple-response validation. Hydrological Processes, 16: 423 – 440.

Uhlenbrook, S. and Hoeg, S. 2003. Quantifying uncertainties in tracer-based hydrograph separations: a case study for two-, three- and five-component hydrograph separations in a mountainous catchment. Hydrological Processes, 17: 431 - 453.

Van Genuchten, M. Th. 1980. A closed form equation for predicting the hydraulic conductivity of unsaturated soils. Soil Science Society of America Journal, 44: 892 – 898.

Van Huyssteen, C. W., Hensley, M., Le Roux, P. A. L., Zere, T. B. and Du Preez, C.C. 2005. The relationship between soil water regime and soil profile morphology in the Weatherley catchment, an afforestation area in the Eastern Cape. Water Research Commission, Pretoria, Report 1317/1/05.

van Zyl, A. J. and Lorentz, S. 2001. Impact of Farming Systems on Sediment Yields in the Context of Integrated Catchment Management. Water Research Commission, Pretoria. Report K5/1059/4.

Vogel, T. and Cislerova, M. 1988. On the reliability of unsaturated hydraulic conductivity calculated from the moisture retention curve. Transport in Porous Media, 3: 1 – 15.

Weiler, M., McGlynn, B.L., McGuire, K.J. and McDonnell, J.J. 2003. How does rainfall become runoff? A combined tracer and runoff transfer function approach. Water Resources Research, 39(11), SWC4: 1 – 13.

Weiler, M., McGuire, K.J., McGlynn, B.L. and McDonnell, J.J. 2003a. A combined tracer and runoff transfer function hydrograph separation model, EGS-AGU-EUG Joint Assembly, Nice, France.

Weiler, M., Naef, F. and Leibundgut, C. 1998. Study of runoff generation on hillslopes using tracer experiments and a physically based numerical hillslope model, *in:* Kovar, K., Tappeiner, U., Peters, N. and Craig, R.

(editors). *Hydrology, Water Resources and Ecology in Headwaters.* IAHS publ. No. 248. Oxfordshire, U. K. pp. 353 - 360.

Weiler, M., Scherrer, S., Naef, F. and Burlando, P. 1999. Hydrograph separation of runoff components based on measuring hydraulic state variables, tracer experiments, and weighting methods. IAHS Publications, 258: 249 - 255.

Weiler, M. 2004. A peferential flow model based on flow variability in macropores. American Geophysical Union, Fall Meeting 2004, Abstracts.

Wenninger, J., Uhlenbrook, S., Tilch, N. and Leibundgut, C. 2004. Experimental evidence of fast groundwater responses in a hillslope / floodplain area in the Black Forest Mountains, Germany. Hydrological Processes. Hydrological Processes, 18(17): 3305 – 3322.

Yue, S. and Hashino, M. 2000. Unit hydrographs to model quick and slow runoff components of streamflow. Journal of Hydrology, 227: 195 - 206.

APPENDIX A

Appendix A contains illustrations of the processs employed in Microsoft Access to combine the input data with the output data in HYDRUS-2D for flux analysis. This includes the HYDRUS-2D input file, one of the HYDRUS-2D output files (Cum_Q.out) and these files being combined so that the timestep of the input data is the same as that of the output data for the comparison of the input and output fluxes for the period, 1 January – 31 October 2001.

Table A1 is an example of HYDRUS-2D input data with the time in hours at breakpoint rainfall intervals, the precipitation of 0.2 mm in one minute converted to hourly intensity (mm/hr), the partitioning of the soil evaporation (rSoil) and the transpiration (rRoot) at breakpoint rainfall intervals, the user defined actual evaporative flux control for very dry conditions, the variable flux (rt) applied and the variable pressure (ht) applied.

Time (hours)	Precipitation	rSoil	rRoot	hCritA	rt	ht
5.95	0	0.000	0.000	8.00E+04	0	0
5.96666667	12	0.000	0.000	8.00E+04	0	0
6	0	0.000	0.000	8.00E+04	0	0
6.53333333	0	0.082	0.109	8.00E+04	0	0
6.55	12	0.000	0.109	8.00E+04	0	0
6.56666667	0	0.082	0.109	8.00E+04	0	0
6.58333333	12	0.000	0.109	8.00E+04	0	0
6.6	12	0.000	0.109	8.00E+04	0	0
6.61666667	12	0.000	0.109	8.00E+04	0	0
6.63333333	0	0.082	0.109	8.00E+04	0	0
6.65	12	0.000	0.109	8.00E+04	0	0
6.66666667	12	0.000	0.109	8.00E+04	0	0
6.75	0	0.082	0.109	8.00E+04	0	0
6.76666667	12	0.000	0.109	8.00E+04	0	0
6.86666667	0	0.082	0.109	8.00E+04	0	0
6.88333333	12	0.000	0.109	8.00E+04	0	0
6.98333333	0	0.082	0.109	8.00E+04	0	0
7	12	0.000	0.109	8.00E+04	0	0

Table A2 is an example extract of the HYDRUS-2D output file (Cum_Q.out), with the time in hours at the model simulation timestep and the various fluxes at those particular timesteps represented within this cross section. The definitions for the various cumulative flows are:

QAP = Cumulative total potential surface flux across the atmospheric boundary (L^2).

QRP = Cumulative total potential transpiration rate (L^2).

QA = Cumulative total actual surface flux across the atmospheric boundary (L^2).

QR = Cumulative total potential transpiration rate (L^2).

QS = Cumulative total seepage rate (L^2).

Time (hours)	CumQAP	CumQRP	CumQA	CumQR	CumQS
5.95	-8.13E+05	0.00E+00	-8.13E+05	0.00E+00	8.61E+04
5.9524	-8.18E+05	0.00E+00	-8.18E+05	0.00E+00	8.61E+04
5.956	-8.26E+05	0.00E+00	-8.26E+05	0.00E+00	8.61E+04
5.9595	-8.34E+05	0.00E+00	-8.34E+05	0.00E+00	8.61E+04
5.9667	-8.50E+05	0.00E+00	-8.50E+05	0.00E+00	8.62E+04
5.9733	-8.50E+05	0.00E+00	-8.50E+05	0.00E+00	8.63E+04
5.9822	-8.50E+05	0.00E+00	-8.50E+05	0.00E+00	8.63E+04
6	-8.50E+05	0.00E+00	-8.50E+05	0.00E+00	8.65E+04
6.0157	-8.49E+05	3.16E+02	-8.49E+05	3.16E+02	8.66E+04
6.0364	-8.49E+05	7.32E+02	-8.49E+05	7.32E+02	8.68E+04
6.0625	-8.49E+05	1.26E+03	-8.49E+05	1.26E+03	8.70E+04
6.0962	-8.48E+05	1.93E+03	-8.48E+05	1.93E+03	8.72E+04
6.1399	-8.47E+05	2.81E+03	-8.47E+05	2.81E+03	8.76E+04
6.1961	-8.47E+05	3.94E+03	-8.47E+05	3.94E+03	8.80E+04
6.2804	-8.45E+05	5.64E+03	-8.45E+05	5.64E+03	8.87E+04
6.3647	-8.44E+05	7.34E+03	-8.44E+05	7.34E+03	8.93E+04
6.5333	-8.41E+05	1.07E+04	-8.41E+05	1.07E+04	9.06E+04
6.5357	-8.47E+05	1.08E+04	-8.47E+05	1.08E+04	9.07E+04
6.5393	-8.55E+05	1.08E+04	-8.55E+05	1.08E+04	9.07E+04
6.5429	-8.63E+05	1.09E+04	-8.63E+05	1.09E+04	9.07E+04
6.55	-8.78E+05	1.11E+04	-8.78E+05	1.11E+04	9.08E+04

Table A3 is an example extract of the combined timestep for the input data and the output data, so that the respective potential and actual fluxes can be compared and checked.

Time (hrs)	Precipitation	Soil	Root
5.95	0	0	0
5.9524	12	0	0
5.956	12	0	0
5.9595	12	0	0
5.9667	12	0	0
5.9733	0	0	0
5.9822	0	0	0
6	0	0	0
6.0157	0	8.20000E-02	0.1089999973
6.0364	0	8.20000E-02	0.1089999973
6.0625	0	8.20000E-02	0.1089999973
6.0962	0	8.20000E-02	0.1089999973
6.1399	0	8.20000E-02	0.1089999973
6.1961	0	8.20000E-02	0.1089999973
6.2804	0	8.20000E-02	0.1089999973
6.3647	0	8.20000E-02	0.1089999973
6.5333	0	8.20000E-02	0.1089999973
6.5357	12	8.20000E-02	0.1089999973
6.5393	12	8.20000E-02	0.1089999973
6.5429	12	8.20000E-02	0.1089999973
6.55	12	8.20000E-02	0.1089999973
6.5524	0	8.20000E-02	0.1089999973
6.556	0	8.20000E-02	0.1089999973
6.5595	0	8.20000E-02	0.1089999973
6.5667	0	8.20000E-02	0.1089999973
6.569	12	8.20000E-02	0.1089999973
6.5726	12	8.20000E-02	0.1089999973
6.5762	12	8.20000E-02	0.1089999973
6.5833	12	8.20000E-02	0.1089999973
6.5917	12	8.20000E-02	0.1089999973
6.6	12	8.20000E-02	0.1089999973

APPENDIX B

Appendix B contains water retention characteristic graphs with van Genuchten (1980) curves fitted to the observed data. From laboratory suction tests that have been performed in the past on the soils from the Weatherley catchment (Lorentz *et al*, 2001), water retention curves have been plotted for the nest sites at different depths along the transects. Thus the observed water retention curve was used to try various combinations of the soil hydraulic properties and finally an adequate simulated fit was found for the water retention curve at each site and depth.

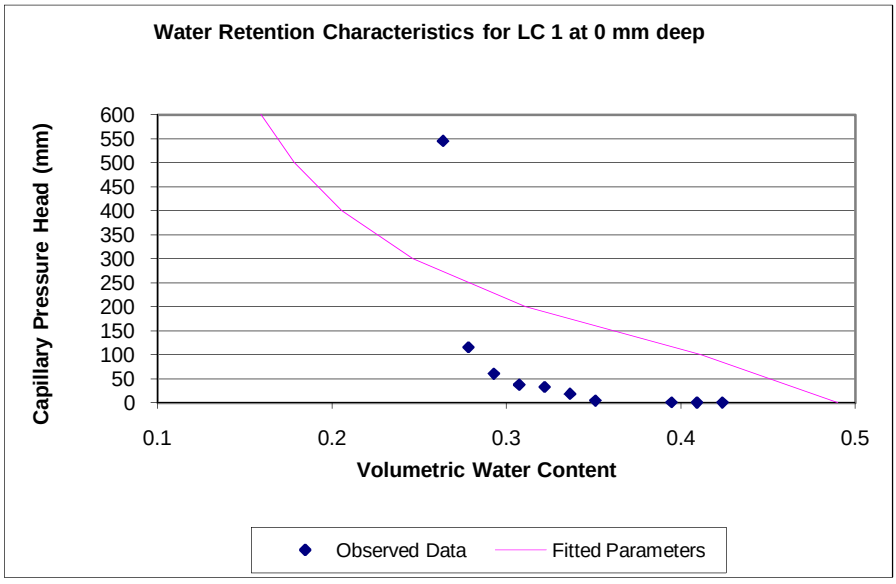

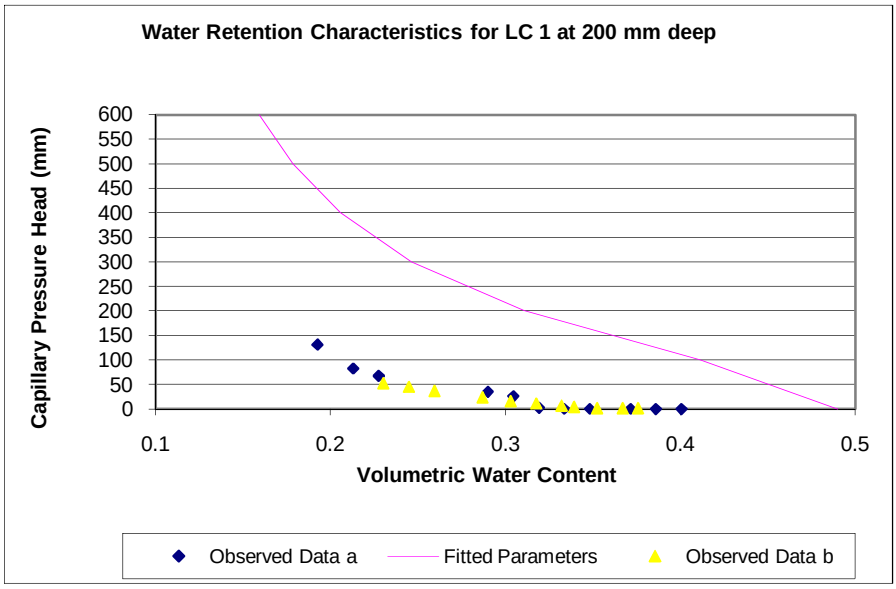

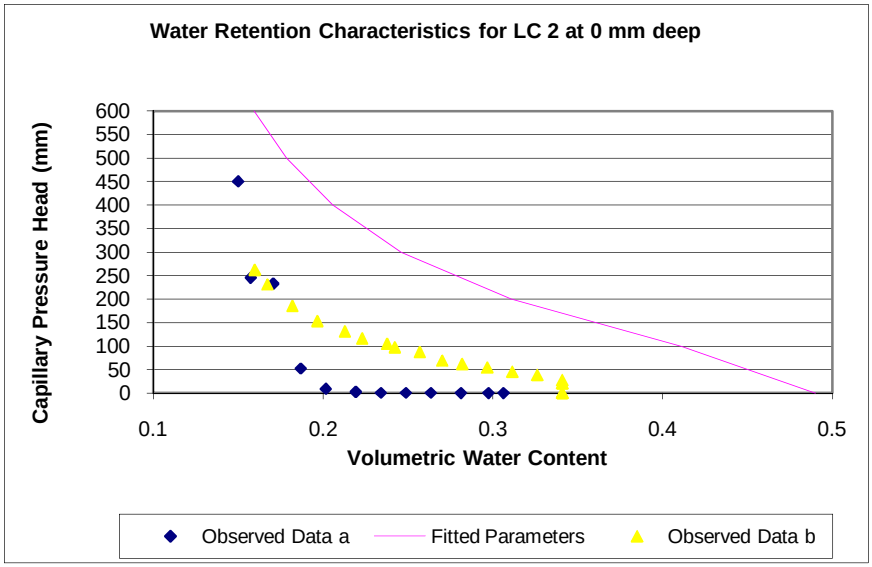
Water Retention Characteristics for LC 2 at 0 mm deep
Capillary Pressure Head (mm)
600
550
500
450
400
350
300
250
200
150
100
50
0
0.1
0.2
0.3
0.4
0.5
Volumetric Water Content
Observed Data a
Fitted Parameters
Observed Data b

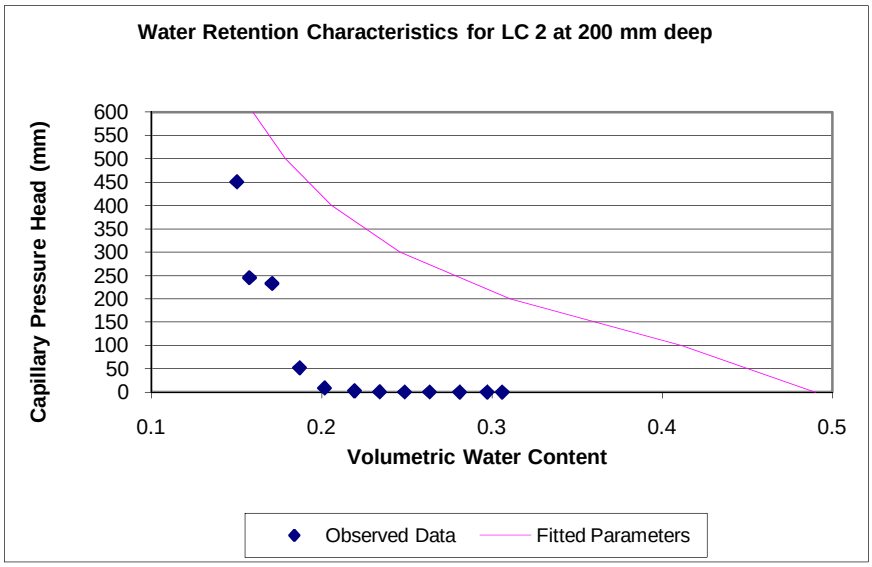
Water Retention Characteristics for LC 2 at 200 mm deep
Capillary Pressure Head (mm)
600
550
500
450
400
350
300
250
200
150
100
50
0
0.1
0.2
0.3
0.4
0.5
Volumetric Water Content
Observed Data
Fitted Parameters

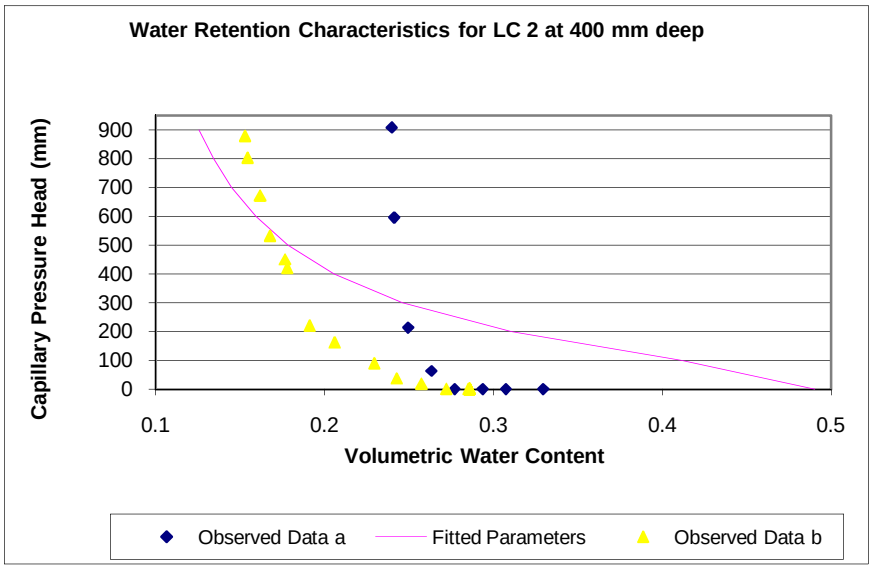
Water Retention Characteristics for LC 2 at 400 mm deep
Capillary Pressure Head (mm)
900
800
700
600
500
400
300
200
100
0
0.1
0.2
0.3
0.4
0.5
Volumetric Water Content
Observed Data a
Fitted Parameters
Observed Data b

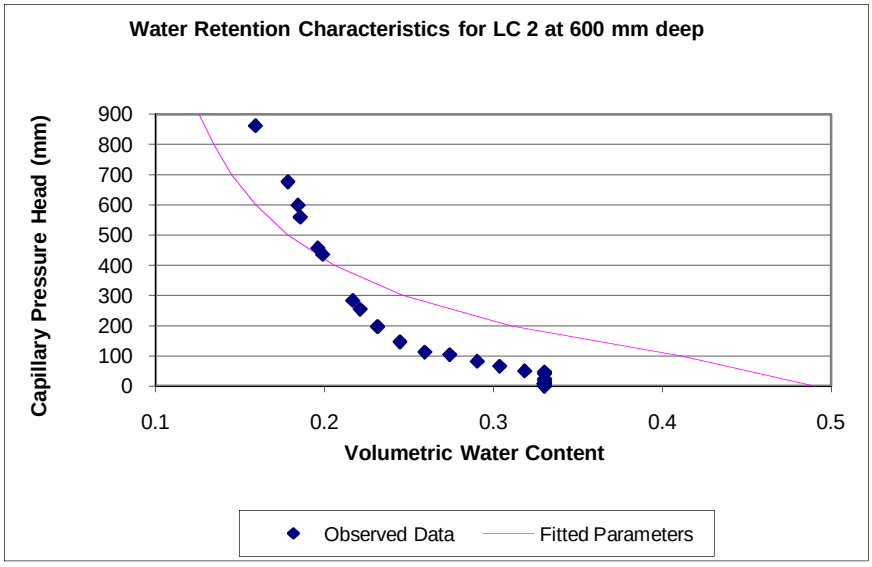
Water Retention Characteristics for LC 2 at 600 mm deep
Capillary Pressure Head (mm)
900
800
700
600
500
400
300
200
100
0
0.1
0.2
0.3
0.4
0.5
Volumetric Water Content
Observed Data
Fitted Parameters

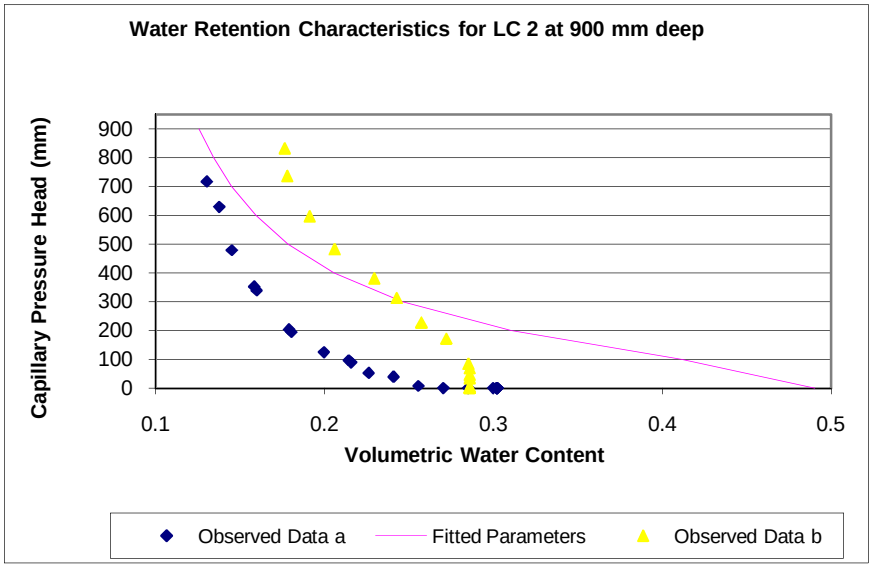
Water Retention Characteristics for LC 2 at 900 mm deep
Capillary Pressure Head (mm)
900
800
700
600
500
400
300
200
100
0
0.1
0.2
0.3
0.4
0.5
Volumetric Water Content
Observed Data a
Fitted Parameters
Observed Data b

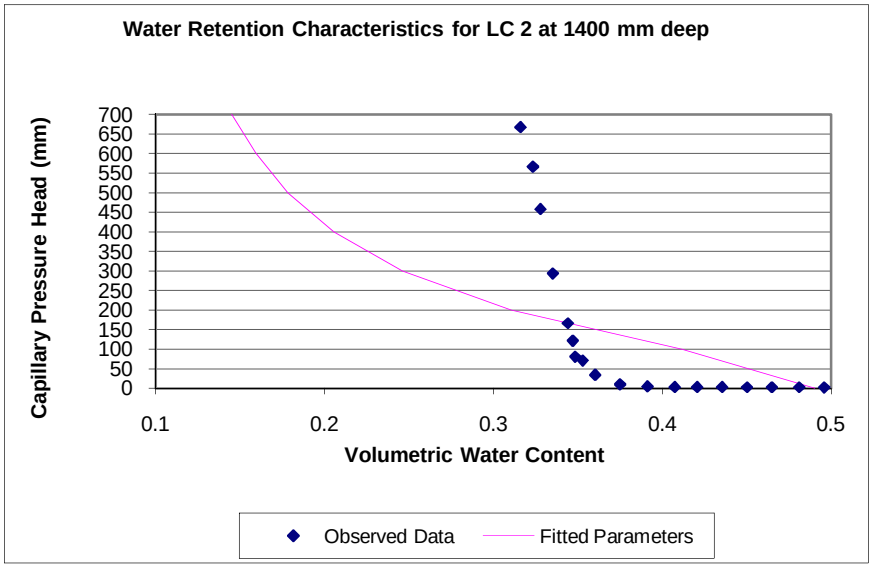
Water Retention Characteristics for LC 2 at 1400 mm deep
Capillary Pressure Head (mm)
700
650
600
550
500
450
400
350
300
250
200
150
100
50
0
0.1
0.2
0.3
0.4
0.5
Volumetric Water Content
Observed Data
Fitted Parameters

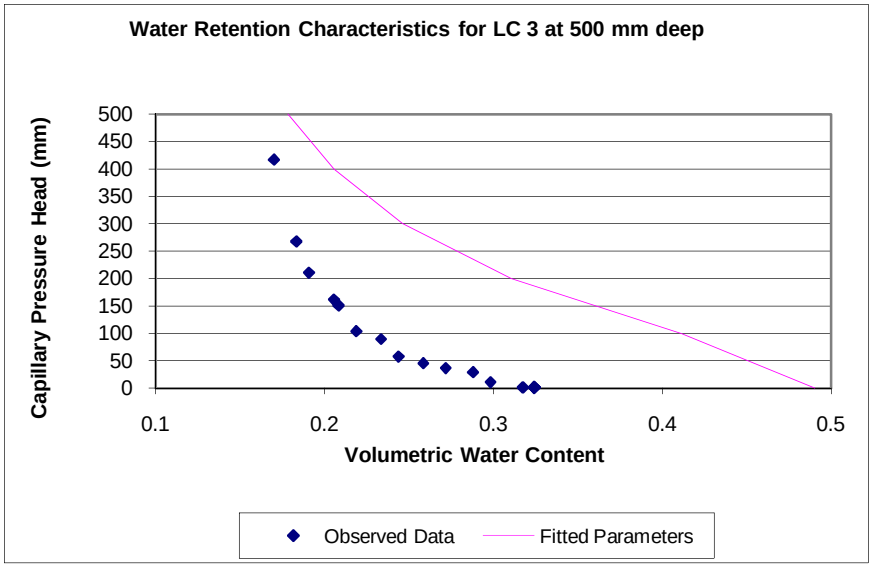
Water Retention Characteristics for LC 3 at 500 mm deep
Capillary Pressure Head (mm)
500
450
400
350
300
250
200
150
100
50
0
0.1
0.2
0.3
0.4
0.5
Volumetric Water Content
Observed Data
Fitted Parameters

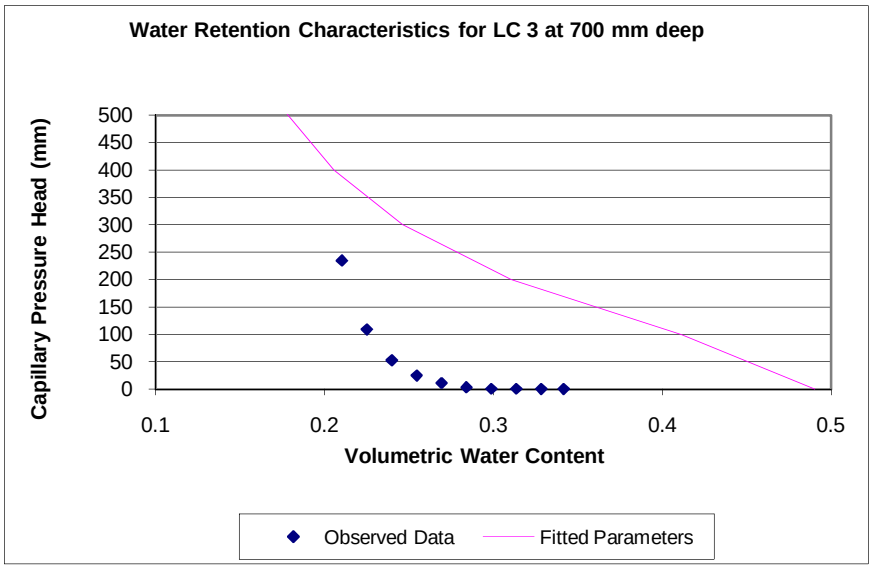
Water Retention Characteristics for LC 3 at 700 mm deep
Capillary Pressure Head (mm)
500
450
400
350
300
250
200
150
100
50
0
0.1
0.2
0.3
0.4
0.5
Volumetric Water Content
Observed Data
Fitted Parameters

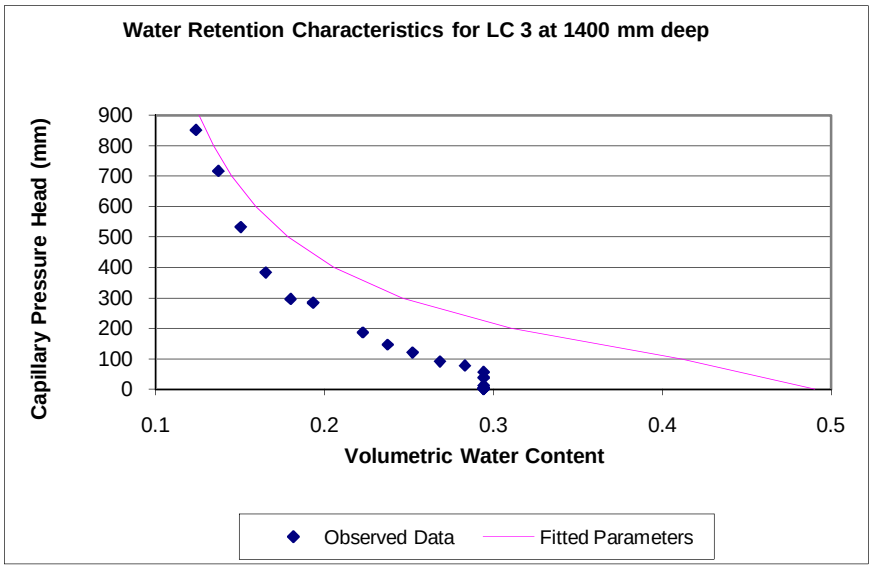
Water Retention Characteristics for LC 3 at 1400 mm deep
Capillary Pressure Head (mm)
900
800
700
600
500
400
300
200
100
0
0.1
0.2
0.3
0.4
0.5
Volumetric Water Content
Observed Data
Fitted Parameters

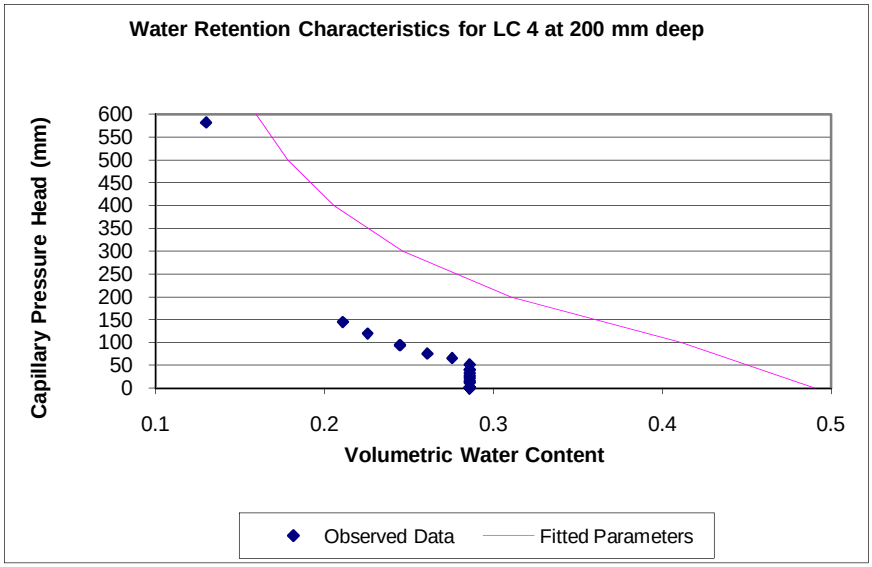
Water Retention Characteristics for LC 4 at 200 mm deep
Capillary Pressure Head (mm)
600
550
500
450
400
350
300
250
200
150
100
50
0
0.1
0.2
0.3
0.4
0.5
Volumetric Water Content
Observed Data
Fitted Parameters

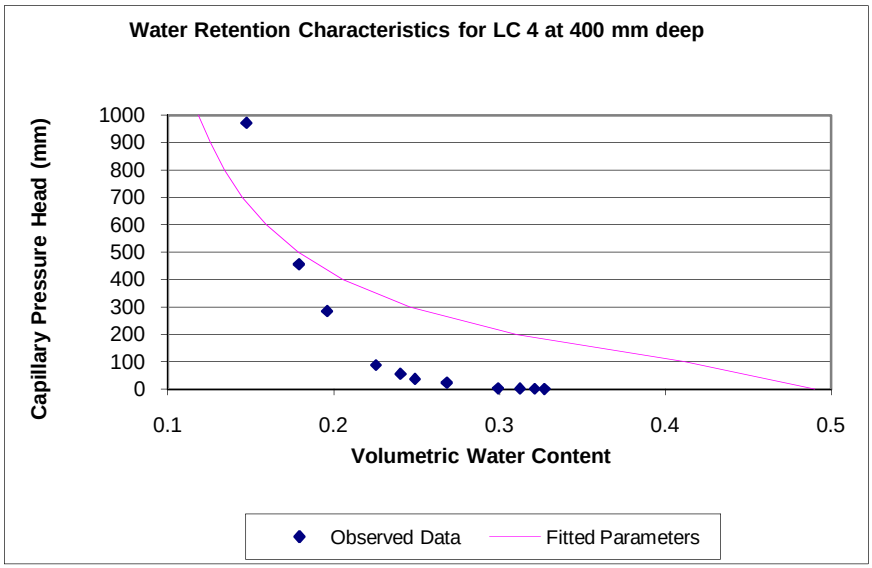
Water Retention Characteristics for LC 4 at 400 mm deep
Capillary Pressure Head (mm)
1000
900
800
700
600
500
400
300
200
100
0
0.1
0.2
0.3
0.4
0.5
Volumetric Water Content
Observed Data
Fitted Parameters

APPENDIX C

Appendix C contains the HYDRUS-2D input menus for each transect and the parameters used in simulating the various transects.

Transect LC 1 – 4:

Latest update: 29 May 2006

```
***             BLOCK             A:             BASIC             INFORMATION
*****************************************
Heading NECF1-4
Ks=50mm/h;Init=@8598hrs; n=1.95;alpha=0.007;ths=0.49;thr=0.05; l=0.6
LUnit  TUnit  MUnit  (indicated units are obligatory for all input data)
mm     hours  mmol
Kat (0:horizontal plane, 1:axisymmetric vertical flow, 2:vertical plane) 2
MaxIt   TolTh   TolH InitH/W  (max. number of iterations and tolerances)
 100    0.001     1       f
lWat lChem lSink Short Flux lScrn AtmIn lTemp lWTDep lEquil lExtGen lInv
 t       f       t       f       t       t       t       f       f       t       t       f
***             BLOCK             B:             MATERIAL             INFORMATION
*****************************************
NMat    NLay    hTab1   hTabN
  1          1     1e-005  100000
   Model   Hysteresis
     0         0
  thr       ths    Alfa       n         Ks      l
  0.05    0.49  0.007   1.95       50      0.6
***             BLOCK             C:             TIME             INFORMATION
*****************************************
      dt       dtMin       dtMax     DMul    DMul2  ItMin ItMax  MPL  tInit     tMax
    0.0025     0.01          5        1.3       0.7       3      7       60       0      7296
TPrint(1),TPrint(2),...,TPrint(MPL)
       100         200         300         400         500         600
       700         800         900        1000        1200        1400
      1600        1800        2000        2200        2400        2600
      2800        3000        3100        3200        3400        3600
      3800        4000        4200        4400        4600        4700
      4800        5000        5200        5400        5600        5700
      5800        5900        6000        6100        6200        6300
      6400        6450        6500        6550        6600        6650
      6700        6750        6800        6850        6900        6950
      7000        7050        7100        7150        7200        7296
***BLOCK          G:ROOT          WATER          UPTAKE          INFORMATION
**********************
    Model  (0 - Feddes, 1 - S shape)
      0
     P0       P2H         P2L       P3          r2H         r2L
```

```
    -10     -2500     -2500    -50000        0.8        0.1
POptm(1),POptm(2),...,POptm(NMat)
    -25
***            END             OF             INPUT             FILE             'SELECTOR.IN'
************************************
```

Transect LC 5 – 7:

Latest update: 21 June 2006

```
*** BLOCK A: BASIC INFORMATION ****************************************
Heading NECF5-7
Ks=44mm/h; Init=@8598hrs; n=1.95;alpha=0.0058;ths=0.43;thr=0.1; l=0.5
LUnit  TUnit  MUnit  (indicated units are obligatory for all input data)
mm    hours   mmol
Kat (0:horizontal plane, 1:axisymmetric vertical flow, 2:vertical plane)
  2
MaxIt   TolTh   TolH InitH/W  (max. number of iterations and tolerances)
 100     0.001      1        f
lWat lChem lSink Short Flux lScrn AtmIn lTemp lWTDep lEquil lExtGen lInv
 t         f        t        f       t       t         t        f         f          t          t        f
*** BLOCK B: MATERIAL INFORMATION ***************************************
NMat    NLay    hTab1   hTabN
  1          1       1e-005  100000
    Model   Hysteresis
      0         0
  thr    ths      Alfa         n         Ks      l
  0.1   0.43  0.0058   1.95       44     0.5
*** BLOCK C: TIME INFORMATION ******************************************
        dt       dtMin       dtMax     DMul    DMul2  ItMin ItMax  MPL
     0.0025    0.025        5          1.3        0.7        3       7       60
      tInit       tMax
         0        7296
TPrint(1),TPrint(2),...,TPrint(MPL)
        100          200          300          400          500          600
        700          800          900         1000         1200         1400
       1600         1800         2000         2200         2400         2600
       2800         3000         3100         3200         3400         3600
       3800         4000         4200         4400         4600         4700
       4800         5000         5200         5400         5600         5700
       5800         5900         6000         6100         6200         6300
       6400         6450         6500         6550         6600         6650
       6700         6750         6800         6850         6900         6950
       7000         7050         7100         7150         7200         7296
*** BLOCK G: ROOT WATER UPTAKE INFORMATION ********************
    Model  (0 - Feddes, 1 - S shape)
       0
      P0       P2H        P2L         P3            r2H        r2L
     -10    -30000    -30000   -100000         0.2         0.1
POptm(1),POptm(2),...,POptm(NMat)
    -25
*** END OF INPUT FILE 'SELECTOR.IN' **********************************
```

Transect LC 8 – 10

Latest update: 9 May 2006

```
*** BLOCK A: BASIC INFORMATION ************************************
Heading NECF 8-10
Ks=35mm/h; Init=@8598hrs; n=1.97;alpha=0.0057;ths=0.5;thr=0.05; l=0.75
LUnit  TUnit  MUnit  (indicated units are obligatory for all input data)
mm     hours  mmol
Kat (0:horizontal plane, 1:axisymmetric vertical flow, 2:vertical plane)
  2
MaxIt   TolTh   TolH InitH/W  (max. number of iterations and tolerances)
 100     0.001     1     f
lWat lChem lSink Short Flux lScrn AtmIn lTemp lWTDep lEquil lExtGen lInv
 t          f       t       f       t      t       t       f       f          t        t       f
*** BLOCK B: MATERIAL INFORMATION ***********************************
NMat    NLay    hTab1   hTabN
  1          1      1e-005  100000
    Model   Hysteresis
      0         0
  thr      ths    Alfa        n          Ks      l
  0.05   0.5  0.0057   1.97       35     0.75
*** BLOCK C: TIME INFORMATION *************************************
       dt       dtMin       dtMax     DMul    DMul2  ItMin ItMax  MPL
    0.0025     0.1          5          1.3        0.7      3       7      60
     tInit       tMax
        0       7296
TPrint(1),TPrint(2),...,TPrint(MPL)
        100         200         300         400         500         600
        700         800         900        1000        1200        1400
       1600        1800        2000        2200        2400        2600
       2800        3000        3100        3200        3400        3600
       3800        4000        4200        4400        4600        4700
       4800        5000        5200        5400        5600        5700
       5800        5900        6000        6100        6200        6300
       6400        6450        6500        6550        6600        6650
       6700        6750        6800        6850        6900        6950
       7000        7050        7100        7150        7200        7296
*** BLOCK G: ROOT WATER UPTAKE INFORMATION **********************
Model  (0 - Feddes, 1 - S shape)
        0
      P0       P2H         P2L         P3          r2H        r2L
     -10    -20000    -20000   -250000         0.5         0.1
POptm(1),POptm(2),...,POptm(NMat)
    -25
*** END OF INPUT FILE 'SELECTOR.IN' *********************************
```

APPENDIX D

Appendix D contains simulations from the HYDRUS-2D modelling exercise, showing the observed versus the simulated tensions and water contents for LC 2, LC 5 and LC 6 as well as LC 8 and LC 9.

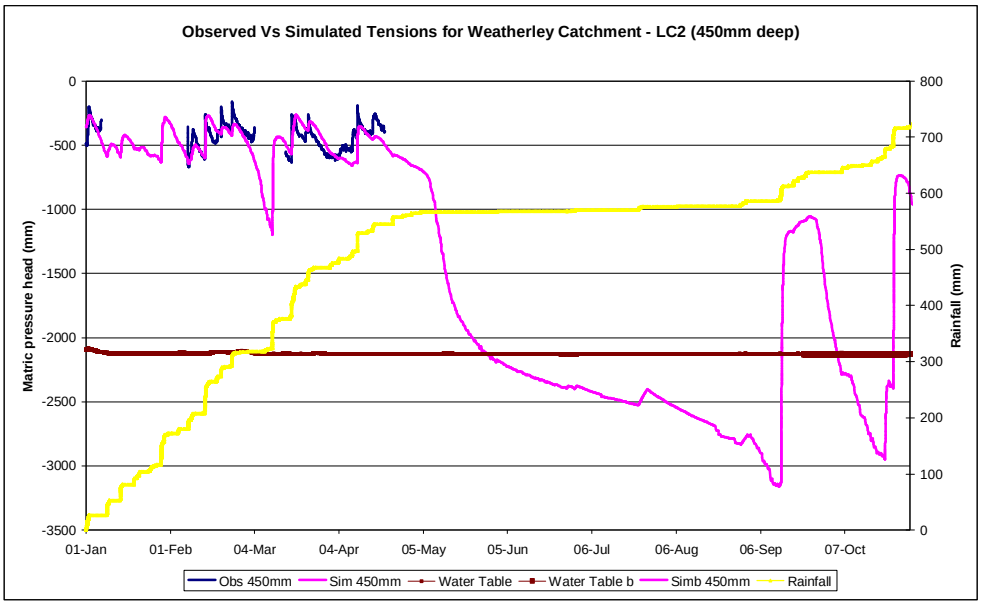

Figure D.1 Observed vs Simulated Tensions from the HYDRUS-2D model for LC 2 at 450 mm deep (Borehole data is reflected as a depth below surface on the matric pressure head axis).

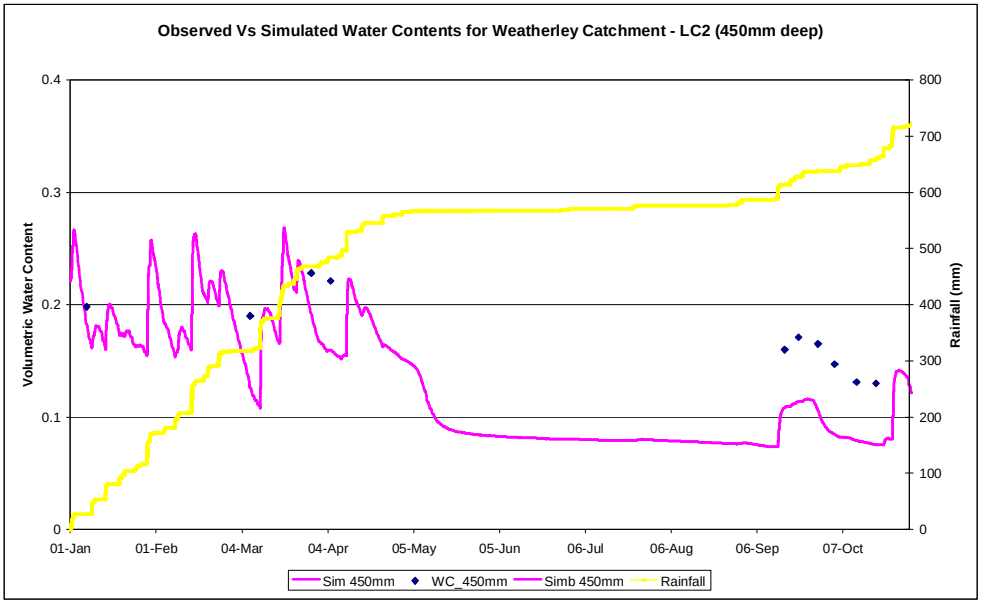

Figure D.2 Observed vs Simulated Water Contents from the HYDRUS-2D model for LC 2 at 450 mm deep.

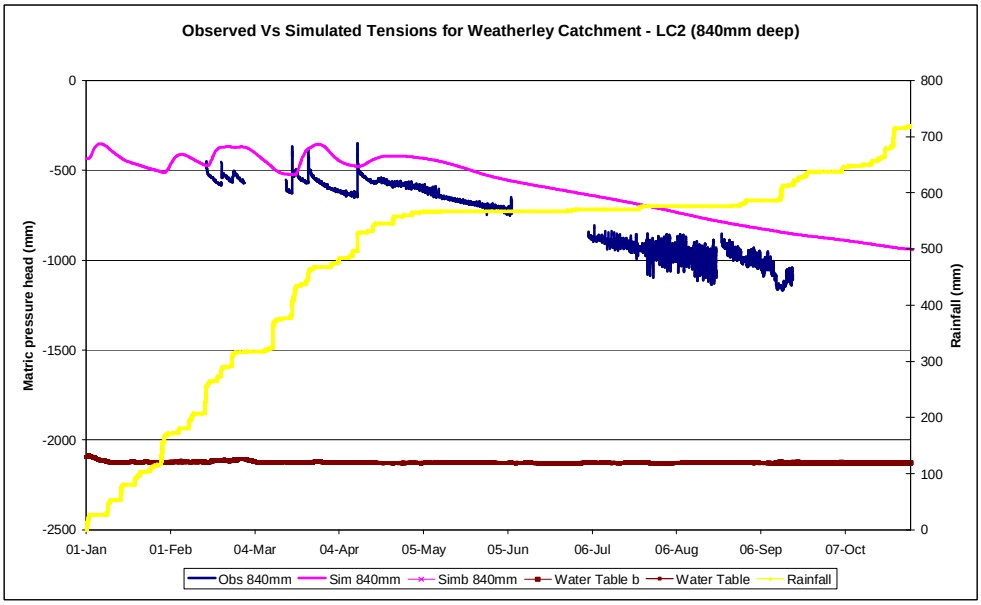

Figure D.3 Observed vs Simulated Tensions from the HYDRUS-2D model for LC 2 at 840 mm deep (Borehole data is reflected as a depth below surface on the matric pressure head axis).

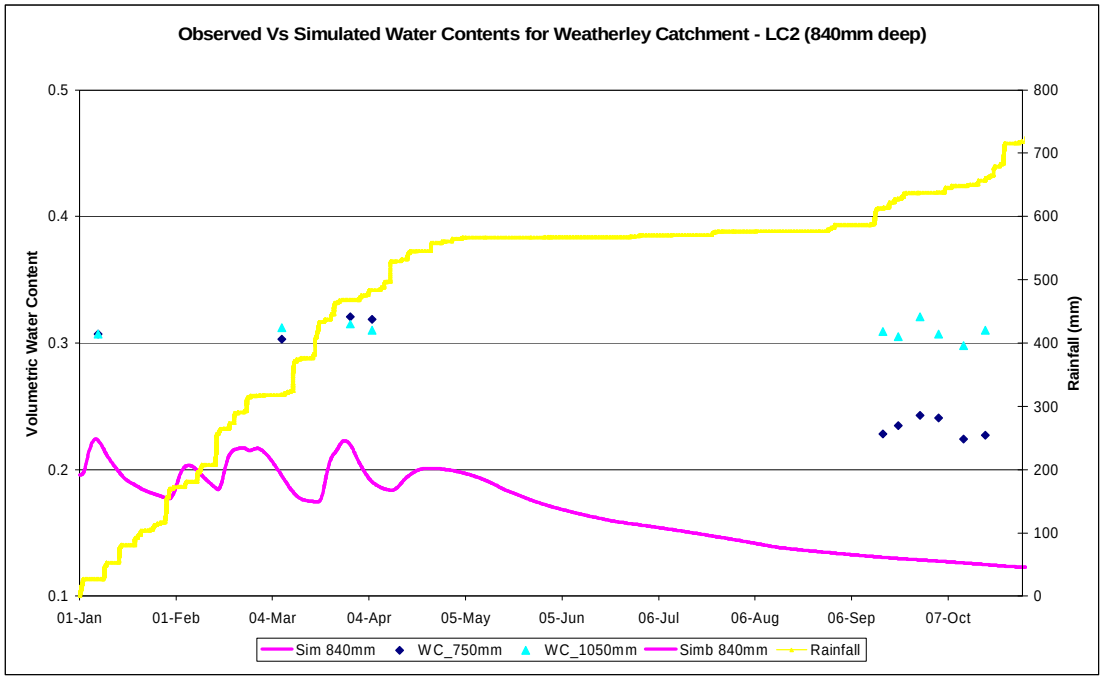

Figure D.4 Observed vs Simulated Water Contents from the HYDRUS-2D model for LC 2 at 840 mm deep.

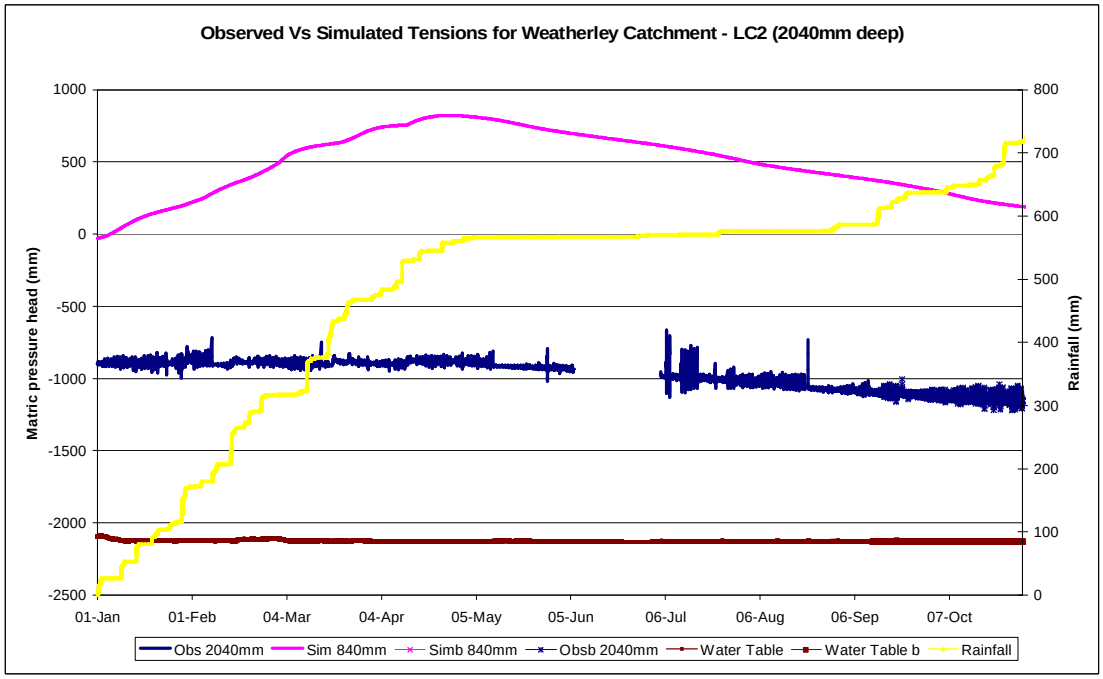

Figure D.5 Observed vs Simulated Tensions from the HYDRUS-2D model for LC 2 at 2040 mm deep (Borehole data is reflected as a depth below surface on the matric pressure head axis).

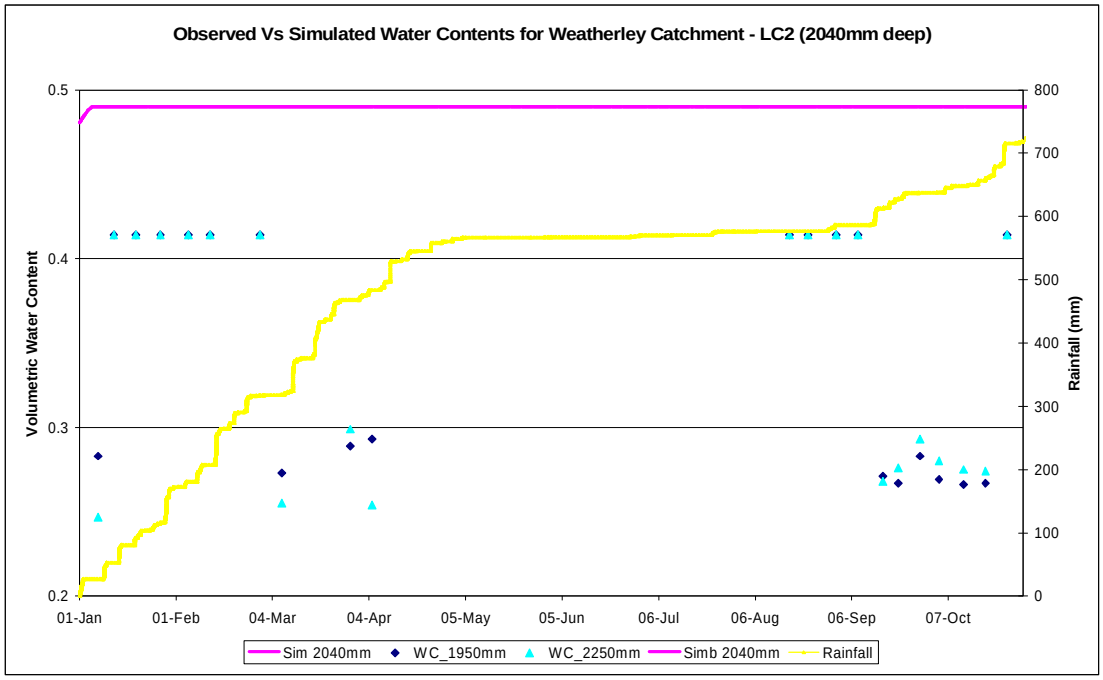

Figure D.6 Observed vs Simulated Tensions from the HYDRUS-2D model for LC 2 at 2040 mm deep.

Comparison of Simulated Results against Observations at Lower Catchment 5 (LC 5)

The simulation of the observed tensions for LC 5 at 740 mm deep was moderate as can be seen in Figure D.7. In the summer months, the simulation tends to dry the soil too much, with the peaks and troughs in the observed data not being mimicked well as can be seen in Figure D.7 from January until April. This was owing to the presence of the variable flux boundary condition dampening the effects of wetting during precipitation events and those of drying in between rainfall events. In the winter recession period, the simulation is good in terms of the shape of the simulated values, but the values are a drier as can be noted in Figure D.7. This is due to the crop factors used in winter being slightly higher than those in the literature for the Highlands Sourveld type of grassland, with some transpiration occurring when then literature indicated none due to the unremitting frost (Schulze, 2006). Also the variable flux boundary condition allows water from the upslope seepage component to enter the wetland area around the LC 5 and LC 6 stations, but the seepage flows were dramatically reduced during winter for the simulation. In the springtime, the simulation is average when compared visually with the observed tension data with

only minor responses to the spring precipitation being noticed in Fig D.7, but the simulation is slightly drier due to the reduced seepage inflow in winter to the wetland area. The observed water table responded well to precipitation in comparison with the observed tension data record as can be seen in Figure D.7 at about 31 January as well as 14 February. Some poor observed data were omitted in summer, during March for this period.

The simulated water contents for LC 5 at 740 mm deep performed poorly compared with the observed data, which showed little response as opposed to the opposite situation being found in the observed data (Figure D.8). This is due to the variable flux boundary condition dampening the effects of wetting during precipitation events and those of the drying cycles in between precipitation events. The simulated water contents in spring are the only ones to perform well, with the simulated values being in close agreement to the observed data, but there was no increase in the simulated water contents as can be seen in Figure D.8 in late September and early October. There were a large amount of poor observed data from the neutron probe at this site and these data was appropriately discarded.

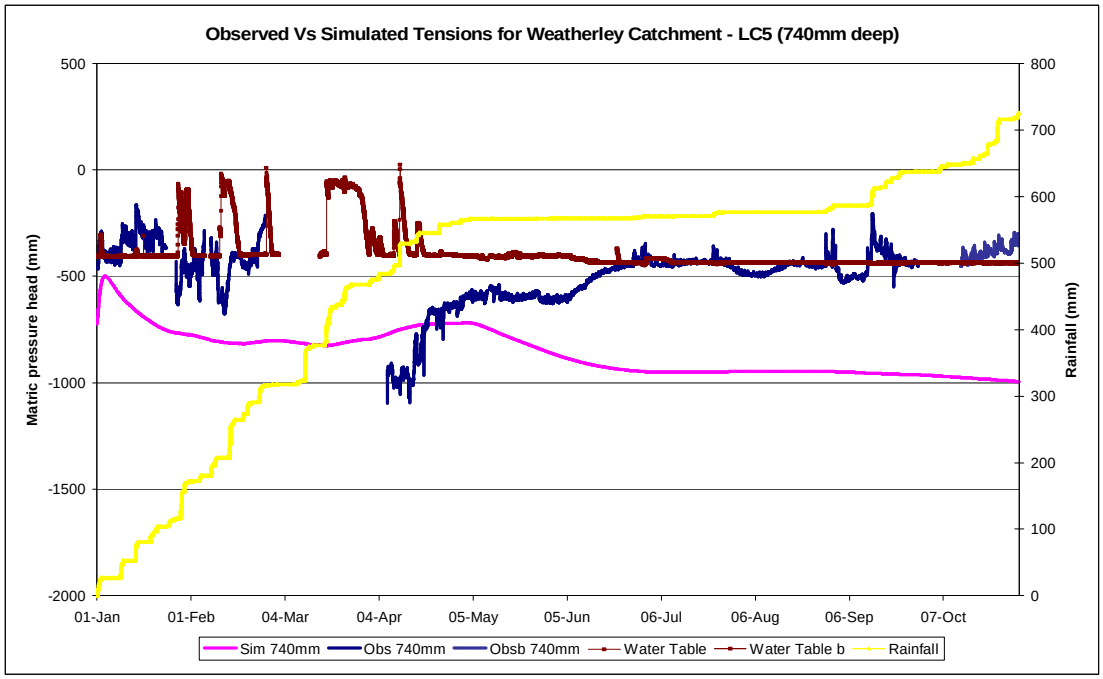

Figure D.7 Observed vs Simulated Tensions from the HYDRUS-2D model for LC 5 at 740 mm deep.

The simulation of the observed tensions for LC 5 at 1280 mm deep was reasonable, with the simulated values remaining close to the observed data record (Figure D.9). The simulated tensions in the summer months were not able to mimic the multifaceted interchanges of the water dynamics satisfactorily, yet the values remained in close agreement of the observed data. The simulated responses to individual rainfall events were lacking as can be seen in Figure D.9 at about 31 January as well as 14 February. The tensions for the winter period were well simulated, with the simulated tension time series recession fitting the observed data closely, but did not dry out enough at the last stages of winter from July onwards as noticed in Figure D.9. This was due to the crop factors only just allowing transpiration to take place owing to the frost throughout these months (Schulze, 2006), as well as the roots not specified to that depth in the soil profile and barely any evaporation thus takes place at this depth as a result. In spring the simulation was poor, with no response being evident from the precipitation events. The observed water table reacted satisfactorily in respect of the timing and magnitude compared with the observed tension data, particularly in summer, as can be seen in Figure D.9 at about 14 February and 15 April. Most of the observed tensiometer data were used at this site.

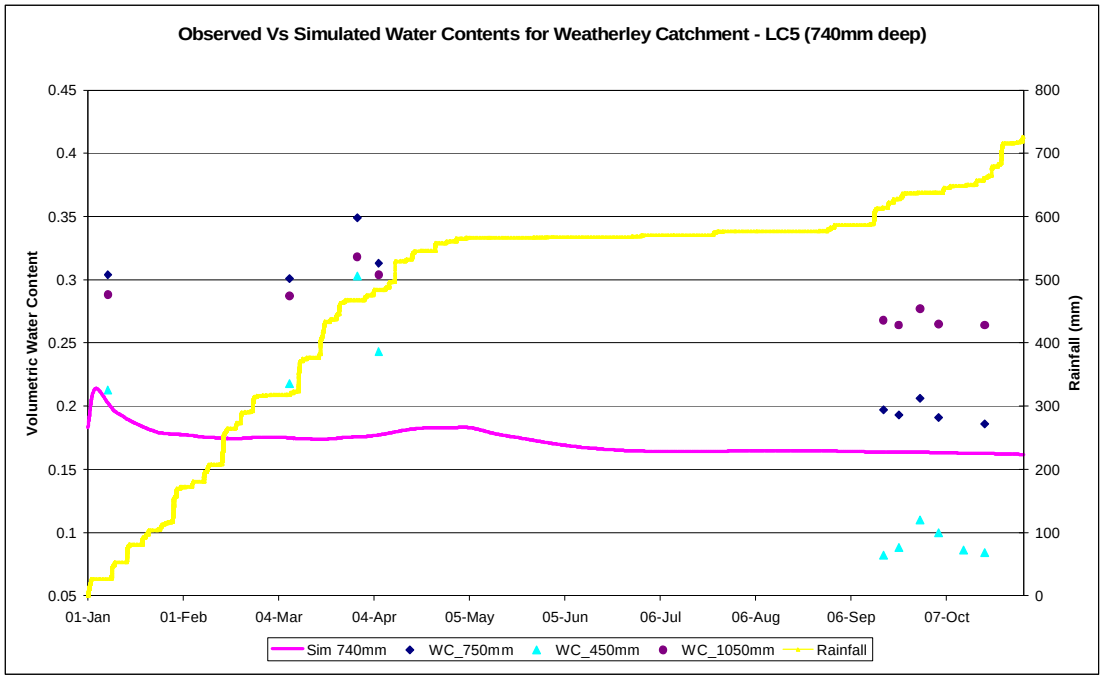

Figure D.8 Observed vs Simulated Water Contents from the HYDRUS-2D model for LC 5 at 740 mm deep.

The simulated water content values were poorly simulated when visually compared with the observed data for LC 5 at 1280 mm deep as can be seen from Figure D.10. The simulated water content values did not respond well to precipitation inputs because of the variable flux boundary condition again, although the simulated values were in close agreement to those of the observed data record in late winter and spring, but the simulated water contents did not increase with the onset of large rainfall events in late September and early October as can be seen in Figure D.10. This is due to the B-horizon being complicated to model with the same parameters used fto model this whole transect, particularly when merely one soil type was specified and no variation was permitted with the increasing depth. A large amount of the observed neutron probe data were omitted at this location as it was decided that it was poor quality data.

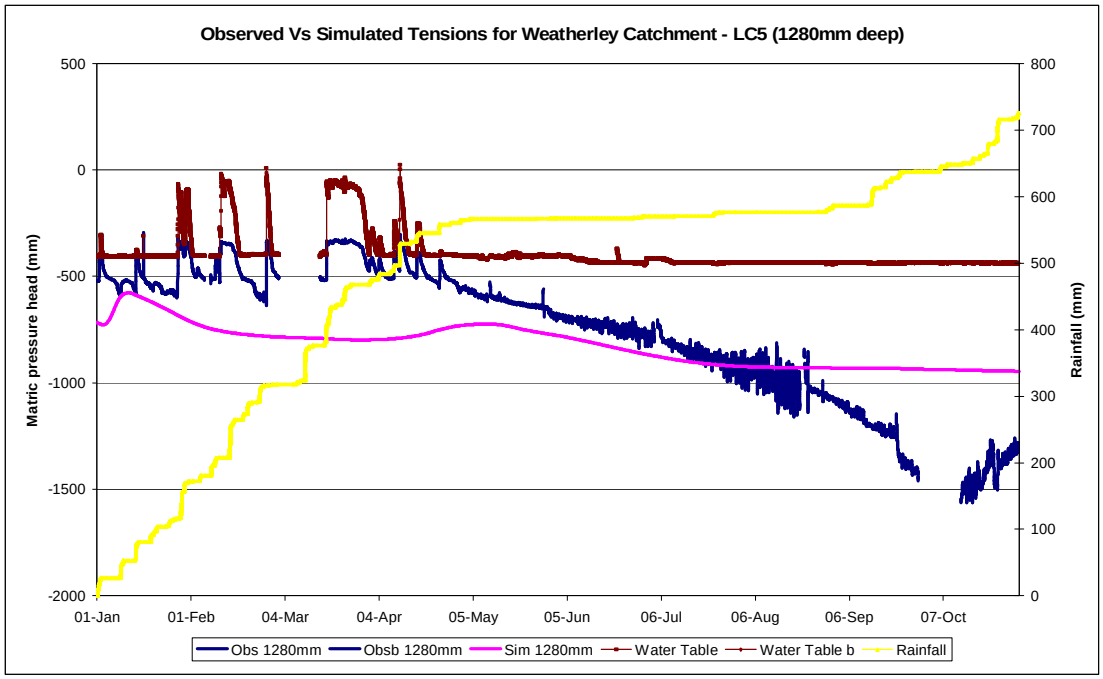

Figure D.9 Observed vs Simulated Tensions from the HYDRUS-2D model for LC 5 at 1280 mm deep.

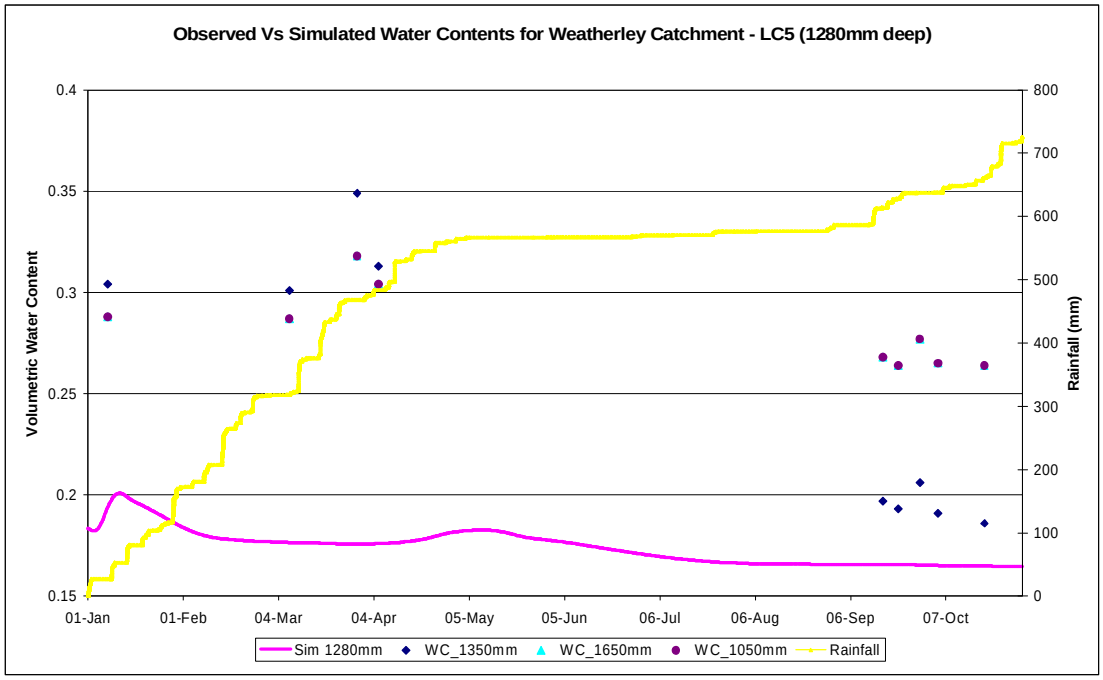

Figure D.10 Observed vs Simulated Water Contents from the HYDRUS-2D model for LC 5 at 1280 mm deep.

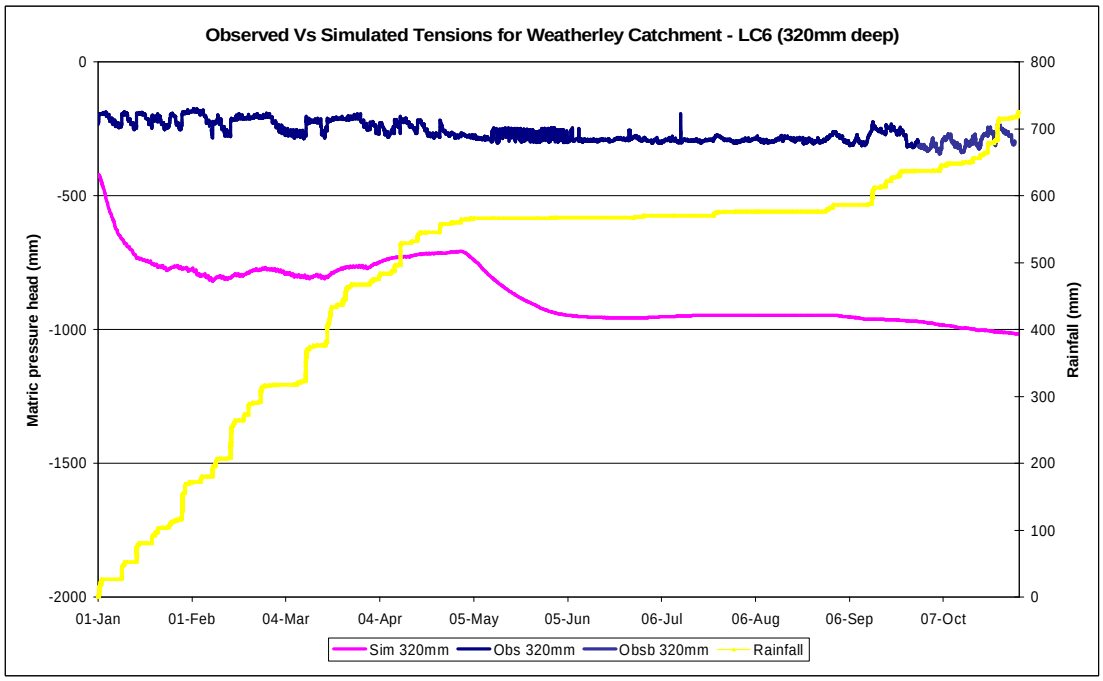

Figure D.11 Observed vs Simulated Tensions from the HYDRUS-2D model for LC 6 at 320 mm deep.

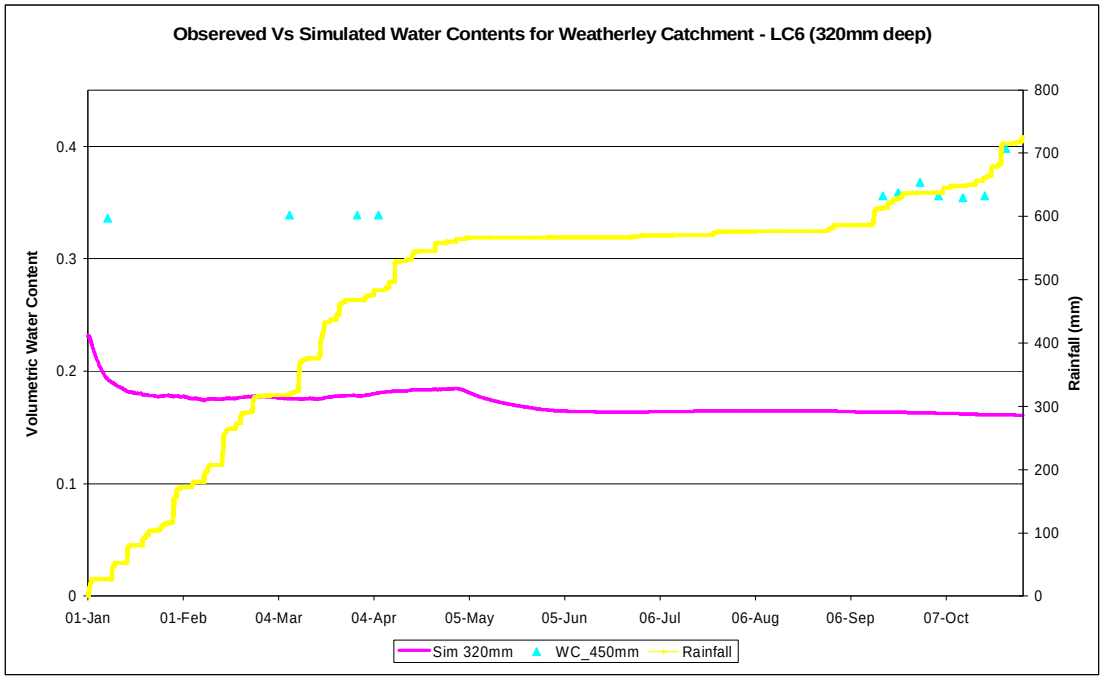

Figure D.12 Observed vs Simulated Water Contents from the HYDRUS-2D model for LC 6 at 320 mm deep.

5.2.2.2 Comparison of Simulated Results against Observations at Lower Catchment 7 (LC 7)

The simulation of the observed tensions and water contents for LC 7 at 460 mm deep was good, with the simulated values following the trends of the observed data well (Figure D.13). The simulated tension values mimic the same trends as the observed data, but never simulate the lesser fluctuations in tensions, especially in summer, even though the overall soil water dynamics are well simulated at the site (Figure D.13). During the summer period, the simulation follows the trends closely with the peaks and troughs not attaining the same frequency detail of the observed data record as can be noted during summer in Figure D.13. The observed water table corresponds well with timing and frequency of the simulated data as well, but is a bit more erratic during summer owing to the upslope groundwater contributions. During the simulated winter tension time series recession period, the simulation dries out well to begin with in May which can be seen in Figure D.13, as according to the observed tension data. Thereafter, the simulated values do not dry out to the extent that the observed record does. Spring precipitation causes wetting of the profile and the tensions respond slowly to rainfall inputs, as can be seen during October in Figure D.13. This slow

response is due to the water table being deeply situated and is yet to rise towards the surface where it will then cause rapid responses with groundwater ridging and groundwater connected macropore type flows. The observed data record is average at this location with almost no data being used from the middle of winter to the end of the simulation as can be noticed in Figure D.13.

The simulated water contents for LC7 at 460 mm deep performed poorly compared with the observed data as can be seen in Figure D.14. There are distinct responses to precipitation, particularly to the larger, more regular rainfall events of the summer months, as can be seen in Figure D.14 at about 12 March as well as 20 March, but the simulated water contents do not exhibit the levels of wetness when compared with the observed data. The winter recession has no observed data to relate to, so little can be interpolated. The simulated responses to the spring rainfall were non-existent except for right at the end of the simulation where a slight increase in water content is noted. Large amounts of neutron probe data were removed from the simulation period for being unreliable data.

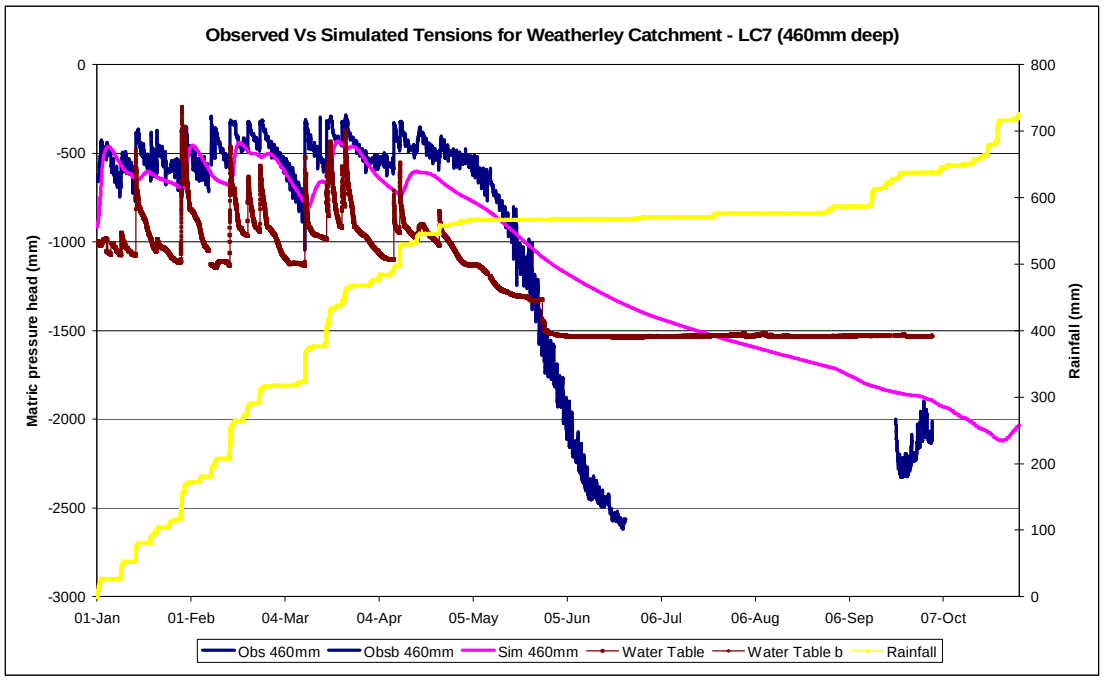

Figure D.13 Observed vs Simulated Tensions from the HYDRUS-2D model for LC 7 at 460 mm deep.

The simulation of the observed tensions for LC 7 at 880 mm deep was satisfactory from visual analysis, with the simulated values continuing in close agreement with the observed data (Figure D.15). The simulated tensions did not demonstrate the finer intricacies of the complex relationships of the soil water dynamics effectively especially during summer, but the values still remained within close proximity of the observed data. The peaks and troughs during summer of the simulated values were out of phase with the observed data as can be seen in Figure D.15 at about 3 March, showing that model was not capable of simulating the transference of deeper soil water downhill and the transference of soil water down the soil profile well. The simulated values being out of phase is also attributed to the B-horizon being difficult to model using the same parameters and the soil type as those used to model this whole transect, with no variation being permitted with increasing depth. The tensions were under simulated, mainly because the crop factors did not permit as much transpiration to take place, because of the frost encountered during the winter months (Schulze, 2006), as well as the roots not being specified to reach to this depth in the soil profile and thus barely any evaporation taking place at this depth. The winter recession was well simulated, but not much of an observed data record is available. There is no simulated tension response to the spring precipitation, probably due to the groundwater remaining disconnected still at this stage of the simulation. The observed water table responded well in respect of the timing and magnitude in comparison with the observed tension data, but the water table responses were more rapid and larger in the summer. A lot of poor observed data were omitted at this site after May.

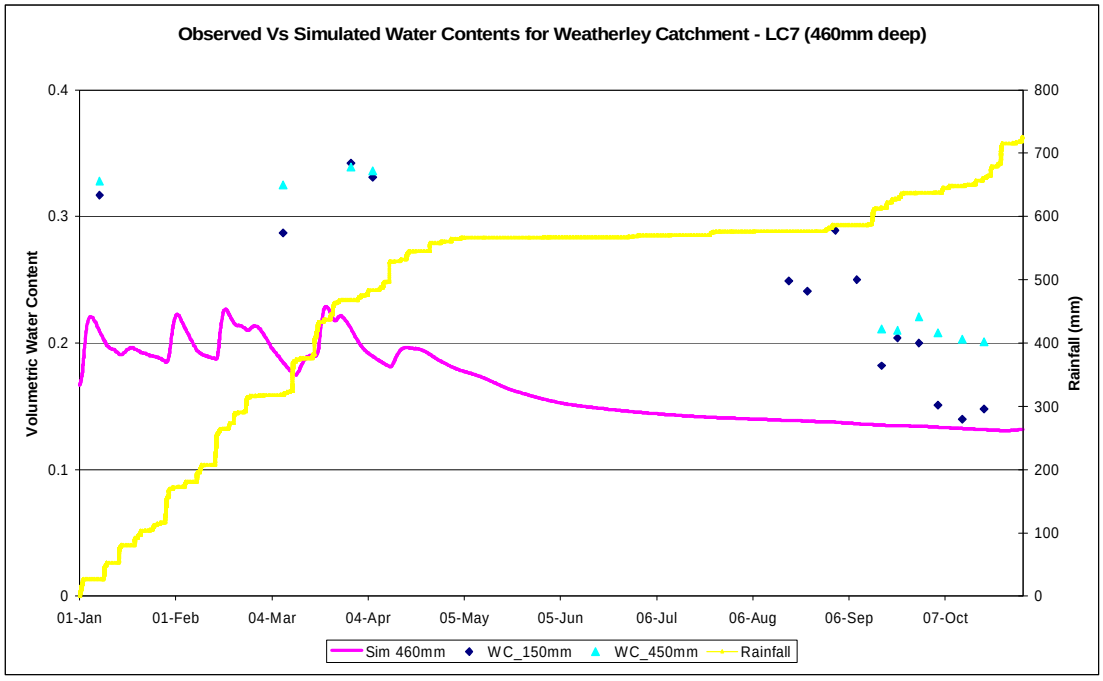

Figure D.14 Observed vs Simulated Water Contents from the HYDRUS-2D model for LC 7 at 460 mm deep.

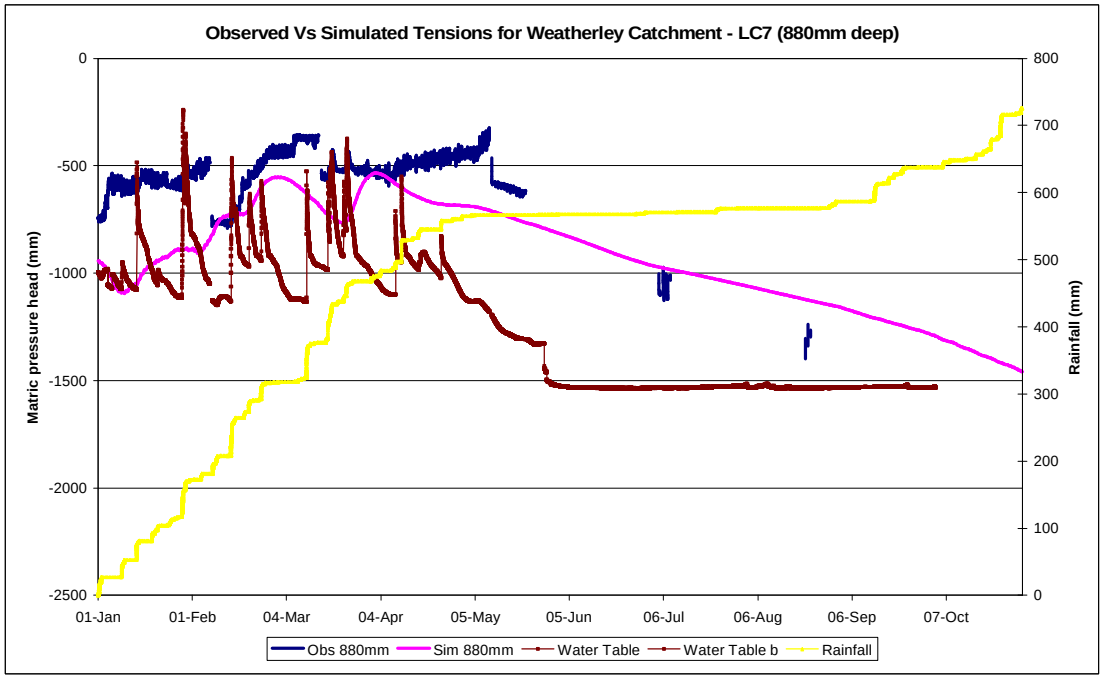

Figure D.15 Observed vs Simulated Tensions from the HYDRUS-2D model for LC 7 at 880 mm deep.

The simulated water content values were poor when visually compared with the observed data for LC 7 at 880 mm deep (Figure D.16). The simulated values

responded well to large summer rainfall inputs and were also preditably lagged as can be seen at about 2 March and 1 April, but were definitely not in proximity with the observed data. This is mainly because the B-horizon is difficult to model using identical parameters as those used for the whole transect, particularly when only one soil type was specified and no variation was considered with the increasing depth. There was no response to the spring precipitation, probably because the water table had not raised enough by this stage in the simulation to cause the groundwater to rise and influence macropore type flow mechanisms. Large amounts of the observed neutron probe data were omitted at this location due to being flagged as poor data.

The simulation of the observed tensions for LC 7 at 1100 mm deep was excellent considering the depth, with the simulated values continuing to be proximal to the observed data (Figure D.17). The simulated tensions did not characterize the complicated interactions of the soil water dynamics capably, but the values still remained within the region of the observed data.

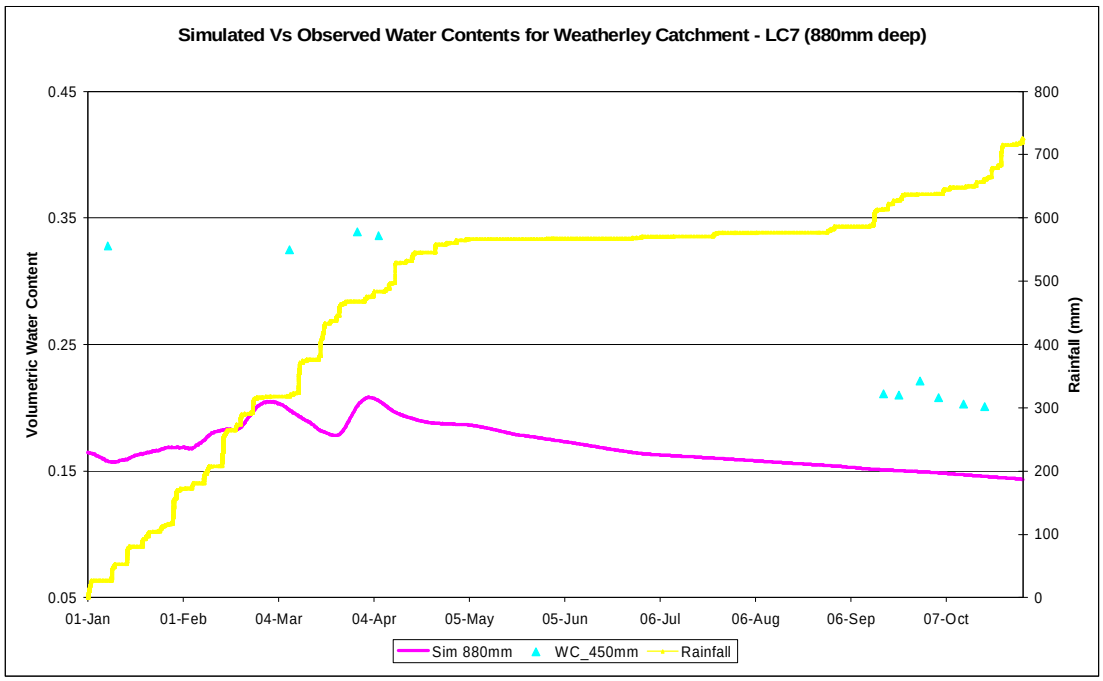

Figure D.16 Observed vs Simulated Water Contents from the HYDRUS-2D model for LC 7 at 880 mm deep.

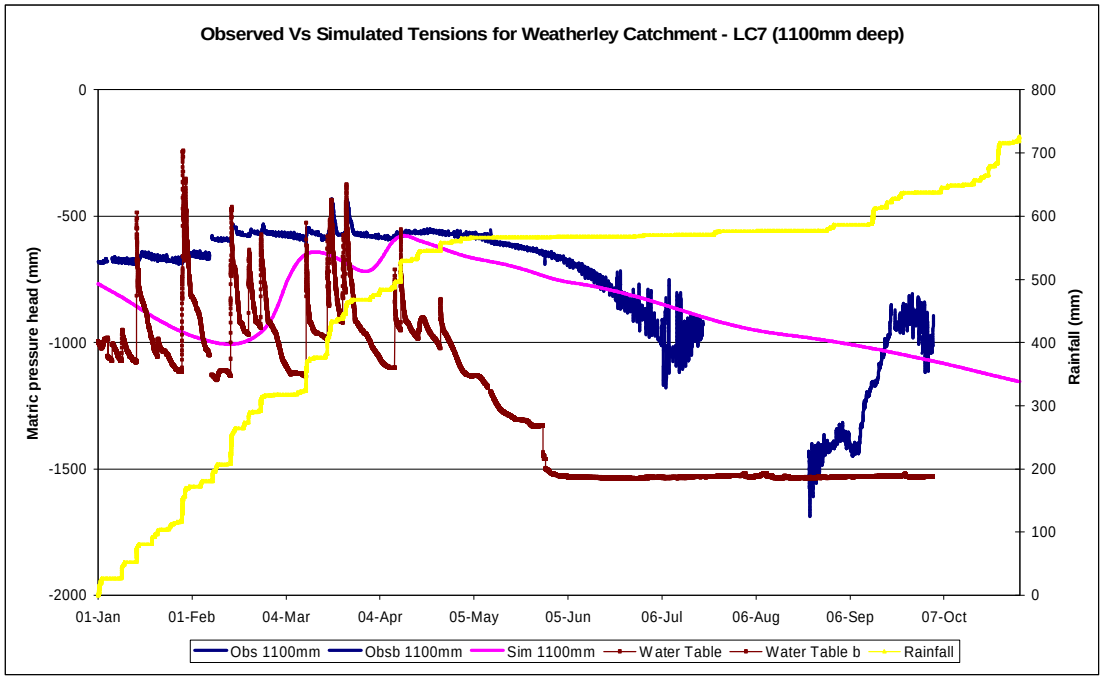

Figure D.17 Observed vs Simulated Tensions from the HYDRUS-2D model for LC 7 at 1100 mm deep.

The peaks and troughs of the simulated values were lagged compared with the observed data, showing that model was not capable of simulating the movement of deeper soil water along and within the wetland segment effectively. The simulated values being lagged is also owing to the C-horizon being complicated to model using the identical parameters for the whole transect, above all when only one soil type was specified and no variation was permitted with the increasing depth. The tensions for the summer months were drier than those of the observed data record (Figure D.17), with responses only showing after large rainfall events occurring when antecedent moisture conditions were high. The tensions for the winter period were well simulated, except for the final section of the winter recession where the simulation remained too wet mainly because the crop factors only allowed a miniscule amount of transpiration to take place, owing to the frost during those months (Schulze, 2006), as well as the roots not being specified to reach to that depth in the soil profile and thus scarcely any evaporation occurring at this depth. The springtime rains did not induce a response at this depth as can be seen in late September and October, due to the water table not being sufficiently high yet. The observed water table responded well to the rainfall events during summer compared to the observed tension data, but the connectivity of the groundwater is periodic, depending on upslope contributions. Most

of the observed tension data record were utilised for this site and depth except for some during the spring period.

5.2.3.1 Comparison of Simulated Results against Observations at Lower Catchment 8 (LC 8)

The simulation of the observed tensions and water contents for LC 8 at 490 mm deep was a decent one from visual examination, with the simulated values following the tendencies of the observed data closely. The simulated tension values follow the similar trends of the observed data without ever encapsulating the less significant fluctuations in tensions, while the simulation mimics the general water dynamics that are present at the site, although there is some under simulation (Figure D.18). In the summer months, the simulation tends to dry the soil out too much as can be seen in Figure D.18 at about 12 January and 15 April, with the peaks never attaining the highs of the observed data which can be seen at about 22 February as well as 24 March. In the simulated winter time series recession period, the simulation dries out well, according to the observed tension data, but the values are all under simulated. This is for the reason that the crop factors used in winter are faintly higher than the ones in the literature for the Highlands Sourveld, with some transpiration happening when the literature specified none due to the unremitting frost (Schulze, 2006). When rainfall takes place again in the spring, the simulation is poor with the observed tension data being well within the proximity, but the response is not forthcoming. There is no observed water table data at this site. Most of the observed data was included at this site and depth.

The simulated water contents for LC8 at 490 mm deep performed poorly compared with the observed data from visual analysis (Figure D.19). The simulation lacked precision during drying phases between the precipitation events, as can be seen in Figure D.19 at about 9 March, with the simulated values showing swift drying and the observed data vice versa. There are distinct simulated water content responses to rainfall inputs, which are more spontaneous during the larger, more regular rainfall events of the summer months showed in Figure D.19 at about 18 February .

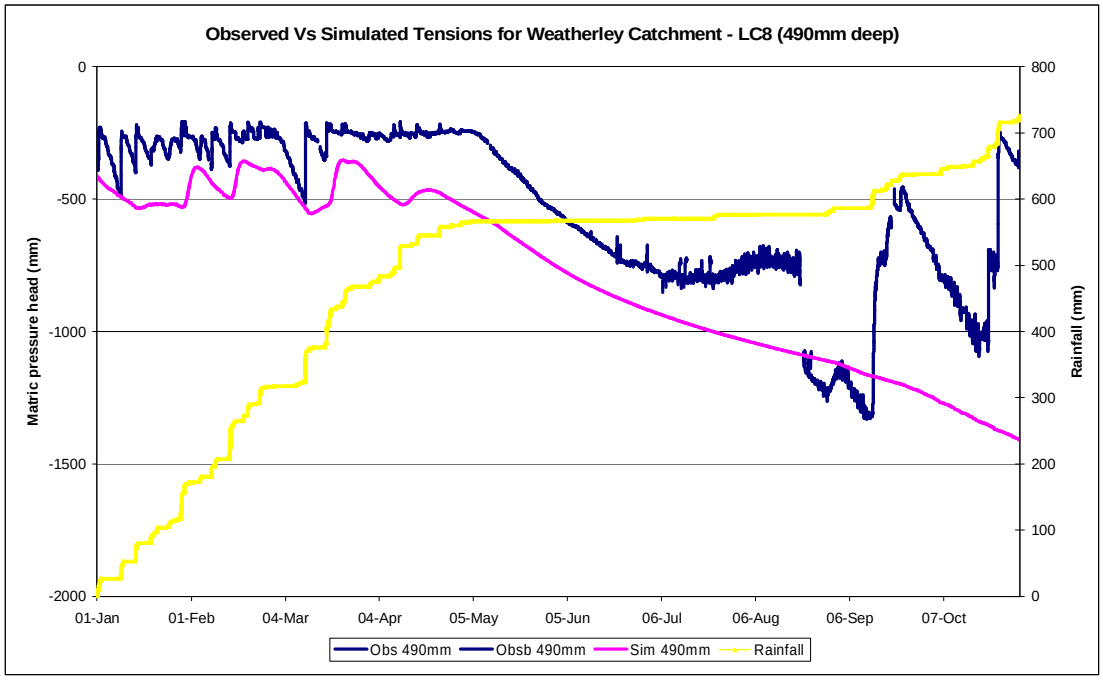

Figure D.18 Observed vs Simulated Tensions from the HYDRUS-2D model for LC 8 at 490 mm deep.

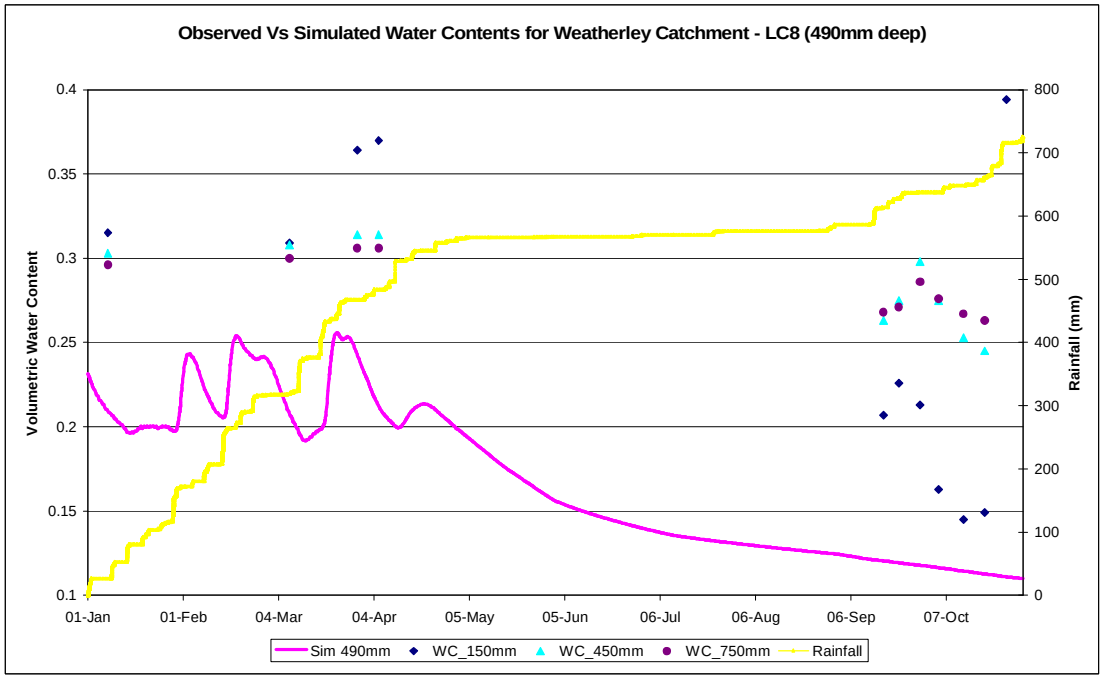

Figure D.19 Observed vs Simulated Water Contents from the HYDRUS-2D model for LC 8 at 490 mm deep.

During the winter recession, the simulation tailed off as expected, but there is no observed data to allow further comment. The response to the spring rainfall was

poorly simulated, with the observed data showing far wetter conditions throughout. This could be due to the soil horizons not having been wet up sufficiently from upslope contributions yet. There was a lot of poor observed data from the neutron probe at this location and thess bad data were duly discarded.

The simulation of the observed tensions for LC 8 at 820 mm deep was acceptable from visual assessment, with the simulated values remaining close to the observed data (Figure D.20), but the simulation tended to under simulate throughout the period. The tensions during the summer months did not capture the intricate interactions of the water dynamics, but the values were still within the general proximity of the observed data. The tensions in early winter were disappointingly simulated, but the tensions in late winter, from July until late September in Figure D.20, were simulated better. This was owing to the crop factors hardly allowing transpiration to occur due to the frost throughout these months (Schulze, 2006), as well as the roots not being able to reach to this depth in the soil profile and barely any evaporation takes place at this depth. In spring the simulated values were disappointing with no response being evident from the precipitation events. The observed water table data was again absent at this site. Hardly any data was omitted from this site.

The simulated water content values were of poor quality compared with the observed data for LC 8 at 820 mm deep (Figure D.21). The simulated values reacted well to precipitation inputs, as can be seen in Figure D.21 at about 10 as well as 28 February, and were adequately lagged, but were never in proximity of the observed data points. This owing to the B-horizon being complex to model using the unchanged parameters as those used for this entire transect, particularly when only one soil type was specified and no variation was allowed with the increasing soil profile depth. Large amounts of the observed neutron probe data were omitted due to being flagged as poor data.

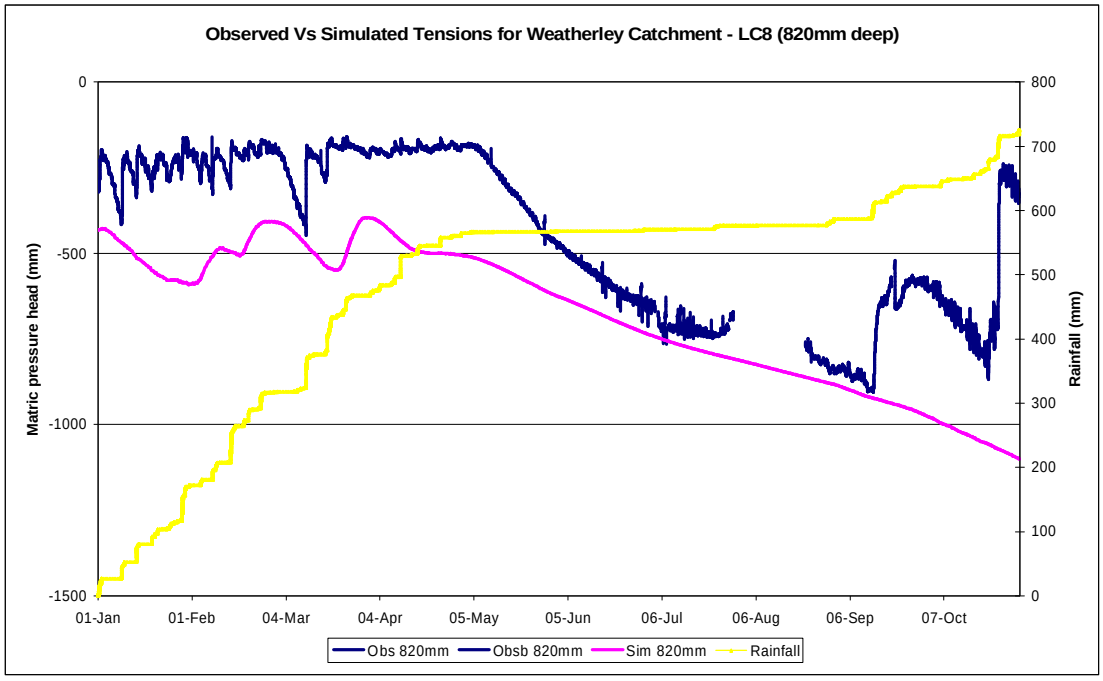

Figure D.20 Observed vs Simulated Tensions from the HYDRUS-2D model for LC 8 at 820 mm deep.

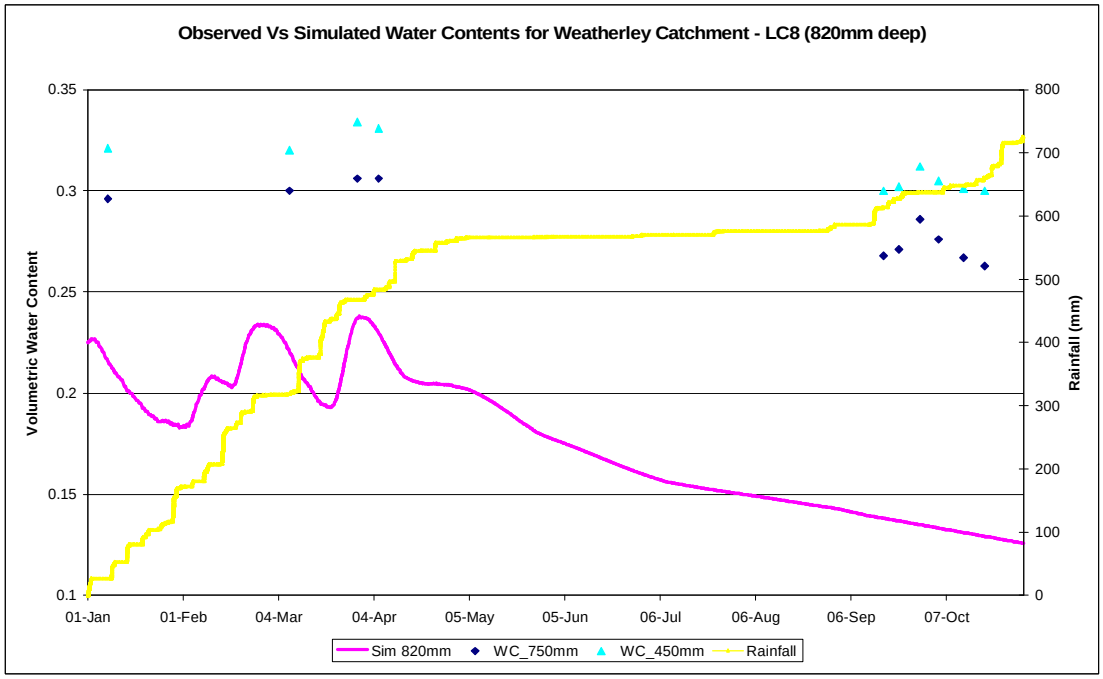

Figure D.21 Observed vs Simulated Water Contents from the HYDRUS-2D model for LC 8 at 820 mm deep.

The simulation of the observed tensions for LC 8 at 1450 mm deep was exceptional considering the depth, with the simulated values continuing to be proximal to the

observed data (Figure D.22). The simulated tensions represent the complex interactions of the soil water dynamics capably. The peaks and troughs of the simulated values were lagged compared with the observed data, showing that model was unable of simulating the slow redistribution of deeper soil water to the bedrock water table downslope along this transect effectively. The simulated values being lagged is also because the C-horizon is complicated to model using the identical parameters as those used for this whole transect, particularly when only one soil type was specified and no variation was allowed with the increasing soil profile depth. The tensions for the summer months were initially drier than those of the observed data record, with responses only being prevalent long after large rainfall events having occurred when antecedent moisture conditions were high as can be seen at about 14 March in Figure D.22. The tensions for the winter period were well simulated. The springtime rains did not invite a response at this depth, due to the water table not being sufficiently high yet. The observed water table data was absent from this location. Most of the observed data was utilised for this site and depth except for some during the late winter period from July to mid August.

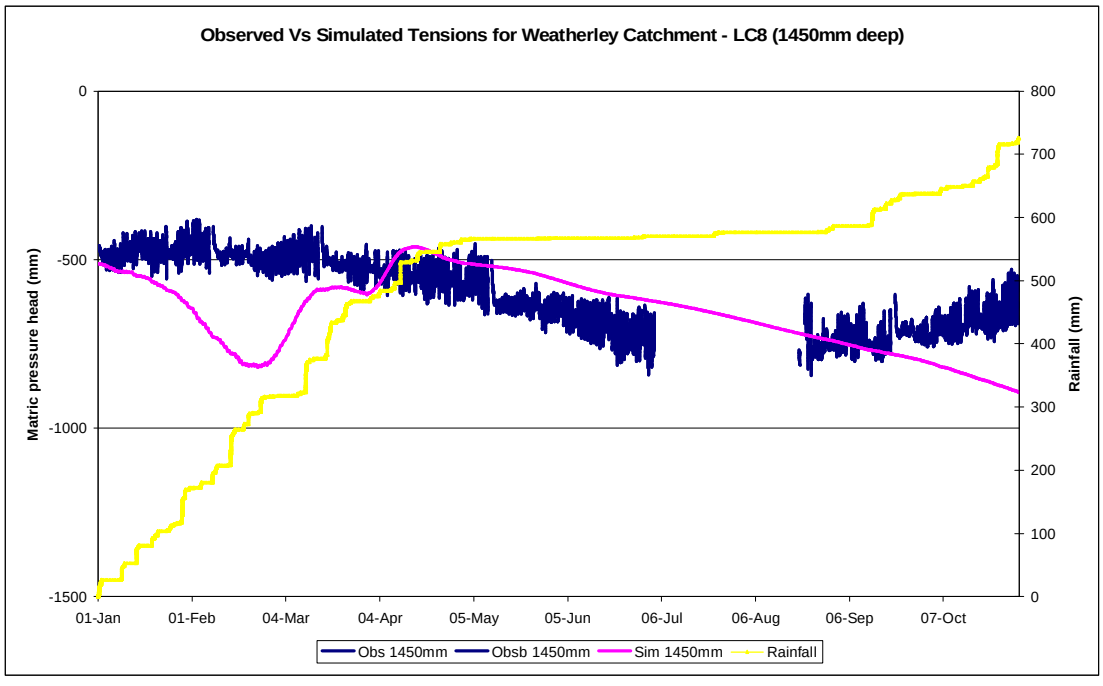

Figure D.22 Observed vs Simulated Tensions from the HYDRUS-2D model for LC 8 at 1450 mm deep.

The simulated water content values were ineffectively modelled when visually compared with the observed data for LC 8 at 1450 mm deep (Figure D.23). The

simulated values responded to the rainfall inputs and were lagged, but were certainly not in close agreement with the observed data points. This is mainly because the C-horizon is difficult to represent using the same parameters as those used for the whole transect, particularly when only one soil type was specified and no variation was allowed with the increasing depth. Large amounts of the observed neutron probe data were not included due to being flagged as poor data.

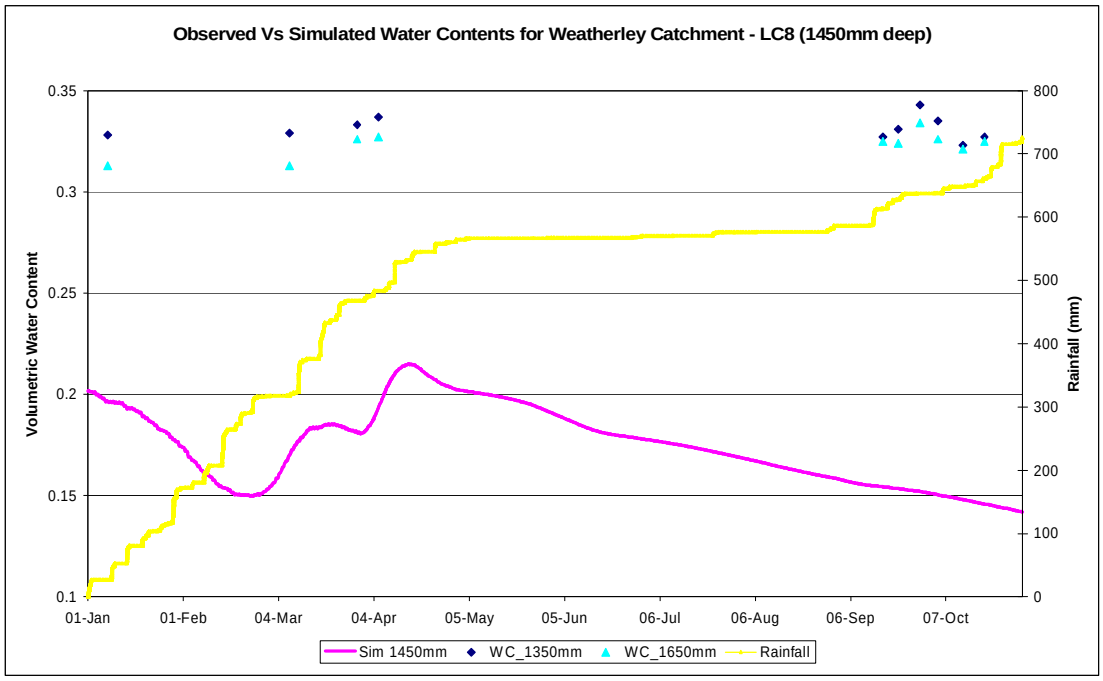

Figure D.23 Observed Vs Simulated Water Contents from the HYDRUS-2D model for LC 8 at 1450 mm deep.

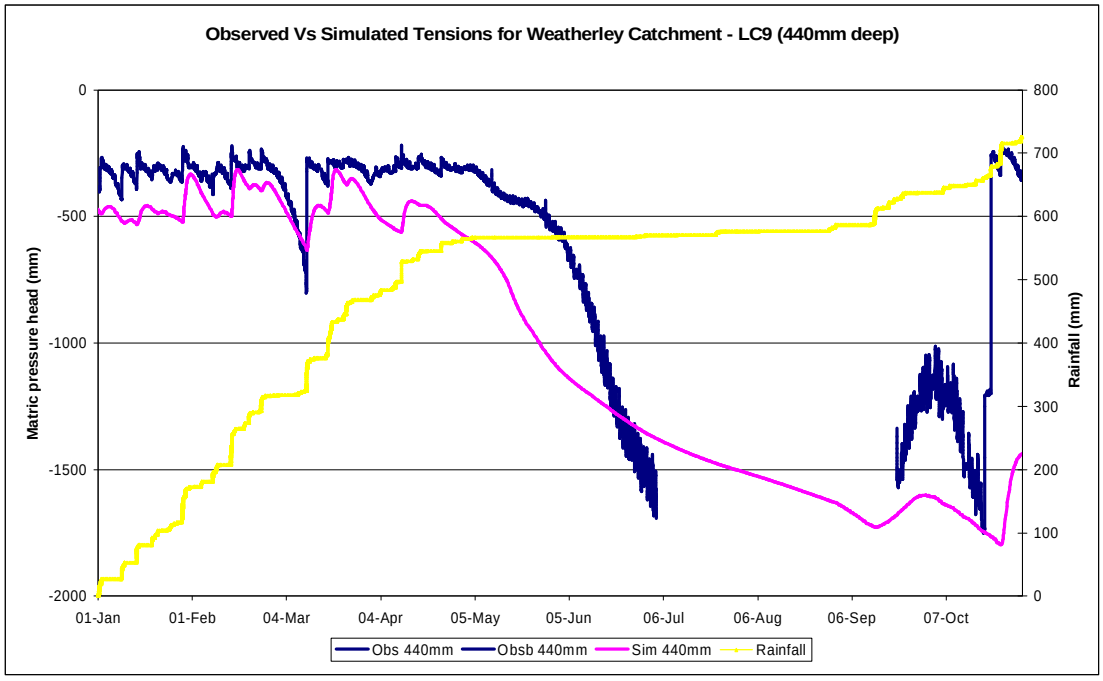

Figure D.24 Observed vs Simulated Tensions from the HYDRUS-2D model for LC 9 at 440 mm deep.

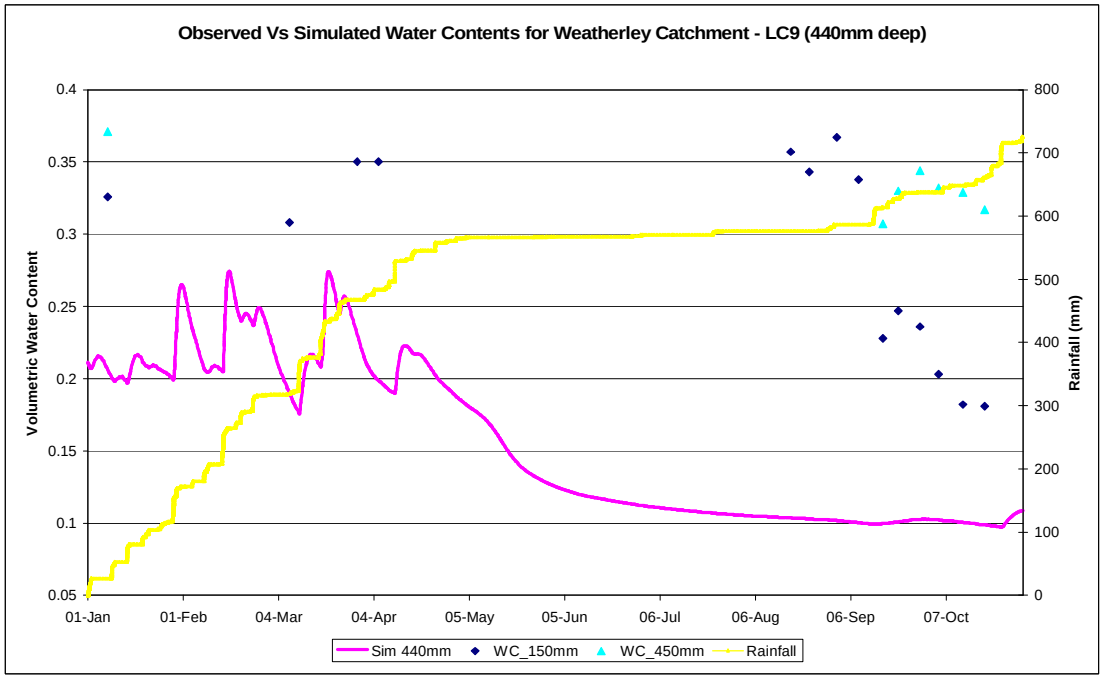

Figure D.25 Observed Vs Simulated Water Contents from the HYDRUS-2D model for LC 9 at 440 mm deep.

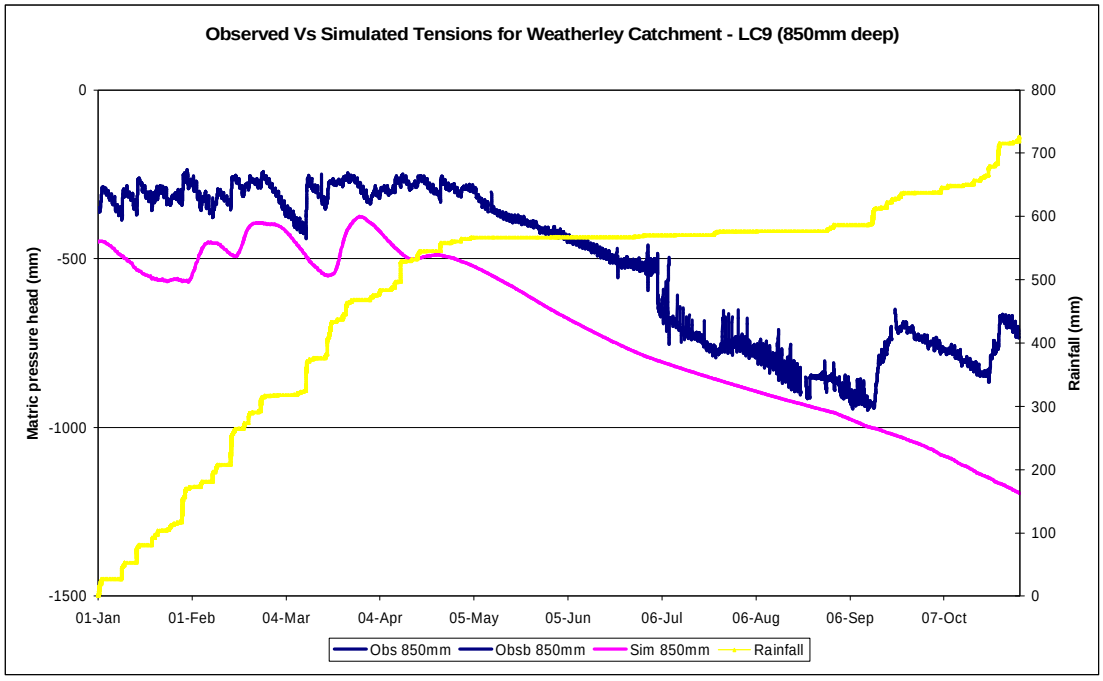

Figure D.26 Observed vs Simulated Tensions from the HYDRUS-2D model for LC 9 at 850 mm deep.

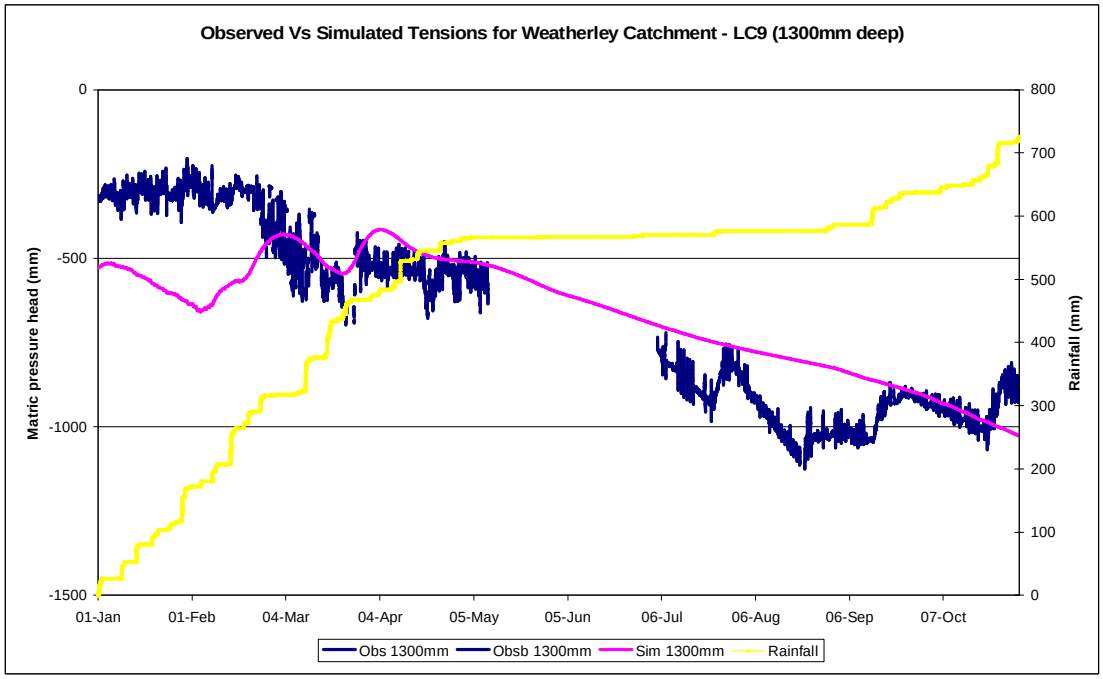

Figure D.27 Observed vs Simulated Tensions from the HYDRUS-2D model for LC 9 at 1300 mm deep.

5.2.3.2 Comparison of Simulated Results against Observations at Lower Catchment 10 (LC 10)

The simulation of the observed tensions for LC 10 at 530 mm deep was good as can be seen in Figure D.28. In the summer months, the simulation tends to be slightly wetter than the observed data, with the peaks (29 January) and troughs (14 February) in the observed data being mimicked well. In the simulated winter time series recession period, the simulation is excellent initially, from May to mid June, and thereafter the simulation does not dry out rapidly enough. In the springtime, the simulation is not good with the observed tension data being badly represented with some late responses to the spring precipitation being achieved at about 28 October in Figure D.28, but the simulation does not respond with the same magnitude and abruptness that the observed data record does. This may be owing to the soil horizons not having been saturated sufficiently to cause an adequate response to the spring precipitation. The observed water table responded well in association with the simulated values as well as the observed tension data record, with the peaks correlating really well. Some bad observed tensiometer data were omitted at this site during the late winter period from mid June to mid September.

The simulated water contents for LC 10 at 530 mm deep performed well when compared visually with the observed data record, but were found to be short of accuracy during the spring precipitations as can be seen in Figure D.29. There are distinctive responses to rainfall inputs, particularly to the larger, more frequent precipitation events of the summer months, as can be seen in Figure D.29 at about 21 February as well as 31 March, and they are well simulated with the values following the trends closely as seen from the observed points. The responses to the spring precipitation were inadequate, with the observed data showing wetter conditions as well as large responses compared with the gradual decline and no response of the simulated values. There was an ample amount of poor observed tensiometer data from the neutron probe that were not included at this location.

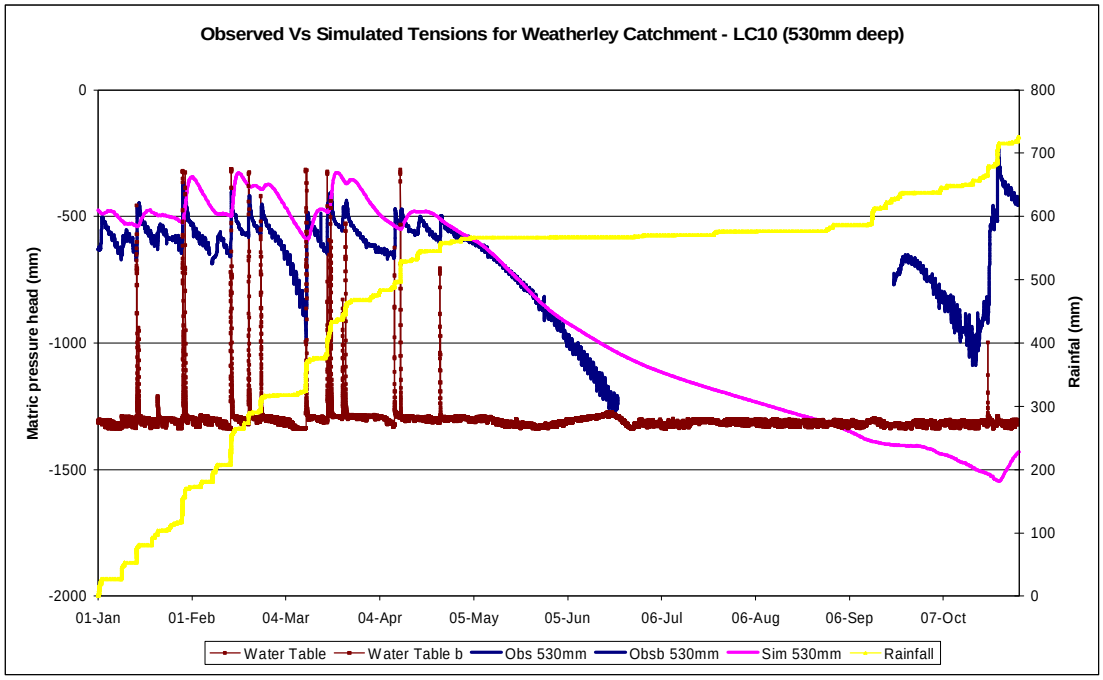

Figure D.28 Observed vs Simulated Tensions from the HYDRUS-2D model for LC 10 at 530 mm deep.

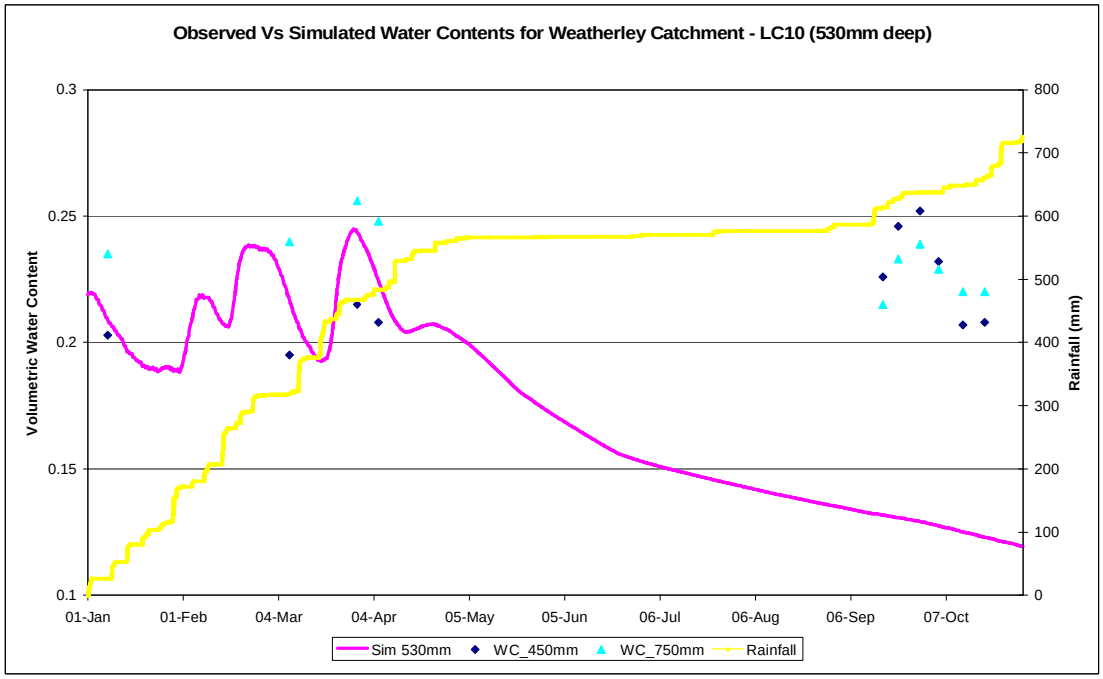

Figure D.29 Observed vs Simulated Water Contents from the HYDRUS-2D model for LC 10 at 530 mm deep.

The simulation of the observed tensions for LC 10 at 830 mm deep was acceptable by visual comparison, with the simulated values continuing in close proximity to the

observed data (Figure D.30). The simulated tensions did not recapitulate the complicated relationships of the soil water dynamics successfully, but the values still remained within the region of the observed data. The peaks (20 February and 24 March) and troughs (14 March and 13 April) of the simulated values were out of phase with the observed data, because there is significant wetting to the B-horizon and the transference is relatively slow. The simulated values being out of phase is also due the B-horizon being complicated to model using the same parameters as those used for this entire transect, especially when only one soil type was specified and no variation was allowed with the increasing depth. The tensions for the entire period were over simulated, but not by a great deal, mainly because the crop factors hardly allowed transpiration to occur, due to the frost throughout those months (Schulze, 2006), as well as the roots being incapable of reaching to this depth in the soil profile and scarcely any evaporation having taking place at this depth. The observed water table responded well in respect of the timing and magnitude in comparison with the observed tensiometer data record. Some bad observed data was omitted during early summer, from January to mid February, and also during late winter (August) at this site.

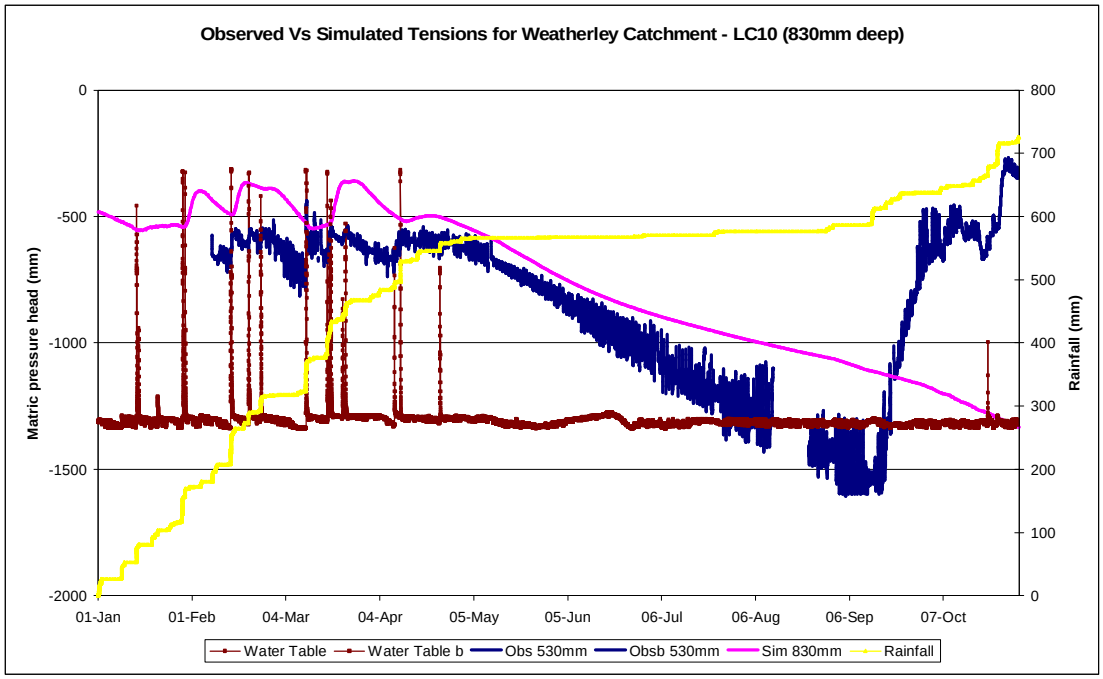

Figure D.30 Observed vs Simulated Tensions from the HYDRUS-2D model for LC 10 at 830 mm deep.

The simulated water content values were adequate when visually compared with the observed data for LC 10 at 830 mm deep (Figure D.31). The simulated values responded well to precipitation inputs in summer, and these were suitably lagged at about 20 February and 26 March in Figure D.31, with the responses following the wetting and drying cycles well in timing but not in magnitude. This is chiefly because the B-horizon is difficult to represent using the identical parameters as those used for the entire transect, particularly when only one soil type was specified and no variation was allowed with the increasing depth. The winter and spring simulated values were ineffectively simulated, with no response being forthcoming with the onset of the spring rains. Large amounts of the observed neutron probe data were omitted due to being flagged as poor data.

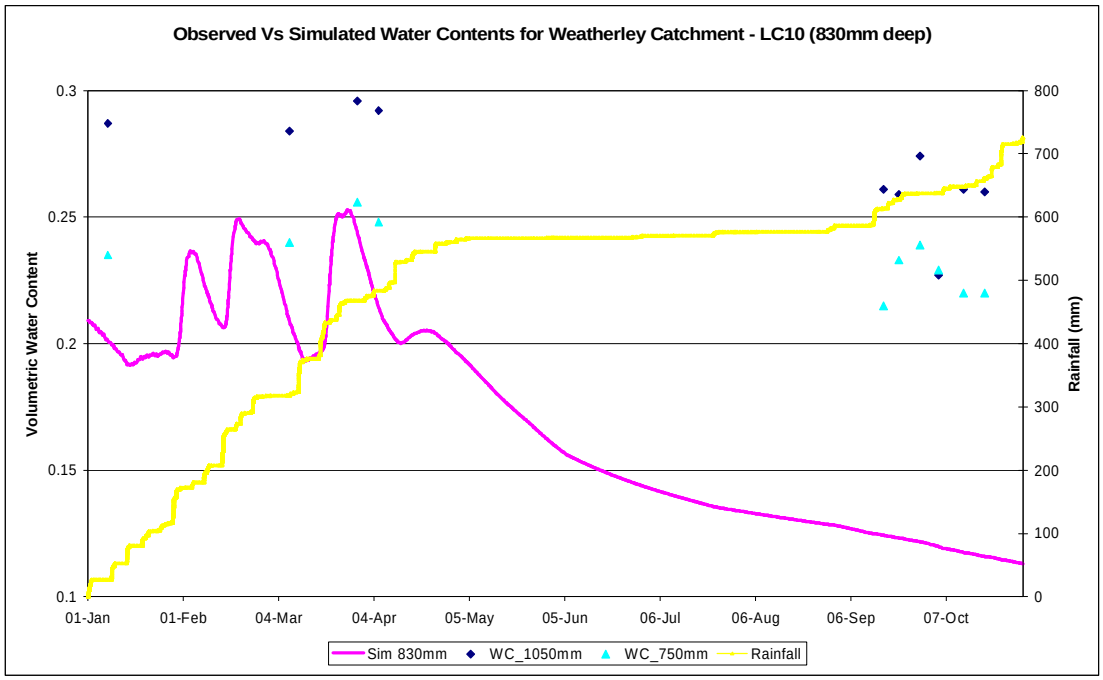

Figure D.31 Observed vs Simulated Water Contents from the HYDRUS-2D model for LC 10 at 830 mm deep.

The simulation of the observed tensions for LC 10 at 1390 mm deep was adequate, especially taking into account the depth, with the simulated values remaining proximal to the observed data when visually compared (Figure D.32). The simulated tensions did not capture the complex relationships of the soil water dynamics competently, but the values remained proximal to the observed data. The peaks (5 March and 6 April) and troughs (21 March) of the simulated values were lagged

compared with the observed data, indicating that the model was incapable of simulating the slow transference of precipitation to deeper soil horizons. The lagging simulated values happens because the C-horizon is problematic to model using the same parameters used for this entire transect, particularly with one soil type and no variation being allowed with the increasing soil depth. The tensions for the summer months were wetter than those of the observed record, with responses being heavily lagged and only subsequent to large precipitation events (5 March and 6 April) taking place when antecedent moisture conditions were high. The tensions for the winter period were ably simulated with the necessary steady decline of the simulated values being witnessed. The springtime rains did not incite a response at this depth, owing to the water table not being sufficiently high yet. The water table responded well to individual precipitation events during summer and late spring, but the connectivity of the groundwater is episodic, depending on upslope contributions. Most of the observed data from tensiometers was used at this location and depth apart from some during the winter period from the end May to early July.

The simulated water content values were tolerably modelled when visually compared with the observed data for LC 10 at 1390 mm deep (Figure D.33). The simulated values responded excellently to precipitation inputs and were suitably lagged in the summer period. The simulated values were however not well modelled in spring, where no responses to rainfall inputs were forthcoming. This is chiefly because the C-horizon is complicated to characterize using the identical parameters as those used for the entire transect, above all when only one soil type was specified and no variation was allowed with the increasing depth. Large quantities of the observed neutron probe data were omitted due to being flagged as poor quality data.

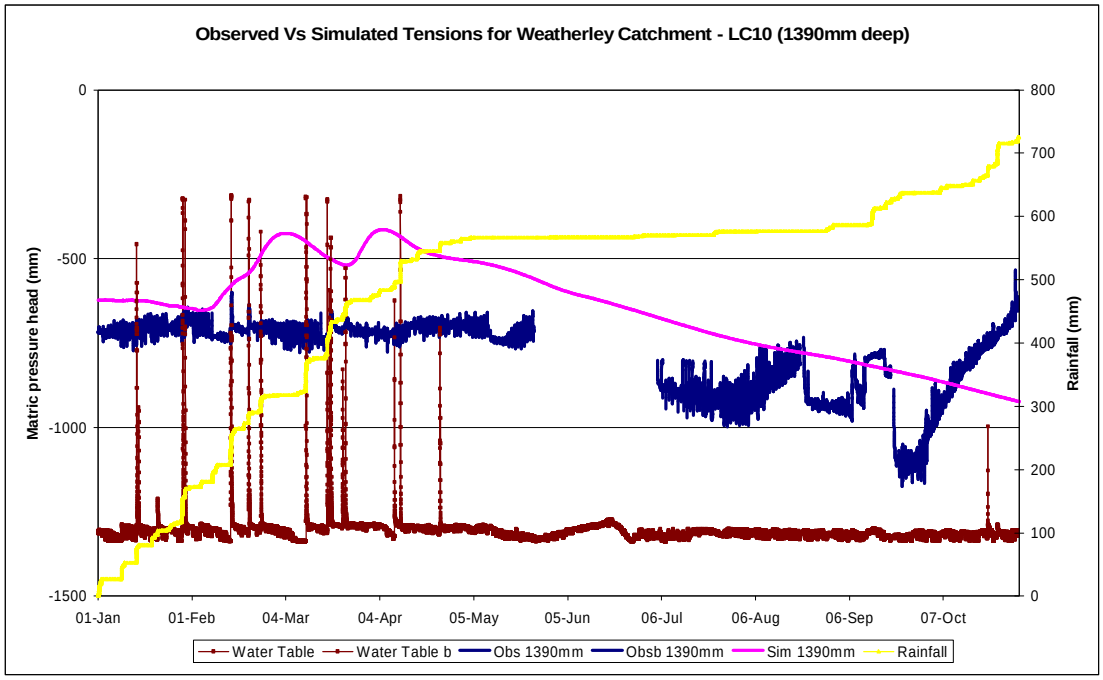

Figure D.32 Observed vs Simulated Tensions from the HYDRUS-2D model for LC 10 at 1390 mm deep.

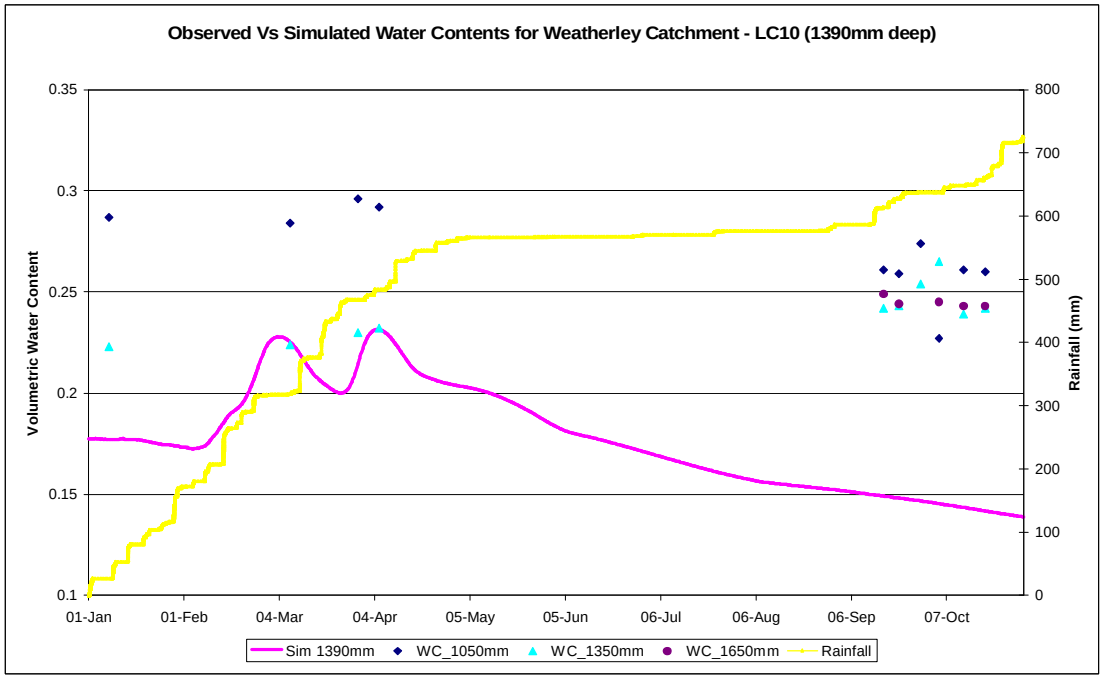

Figure D.33 Observed vs Simulated Water Contents from the HYDRUS-2D model for LC 10 at 1390 mm deep.